SUBMISSION FOR THE DEGREE OF DOCTOR OF SCIENCE

The published works which follow are submitted for the degree of Doctor of Science. They are divided into three groups:-

I. Studies of the ionospheric F region

II. Studies of Aurorae and Airglow

and III. Miscellaneous studies.

The state of knowledge in the field prior to publication of each paper, and the new knowledge which the paper has contributed are detailed in this preface.

I. STUDIES OF THE IONOSPHERIC F REGION

(a) "The equatorial F region of the ionosphere"
Journal of Atmospheric and Terrestrial Physics 18, 89 (1960).

(b) "Universal-time control of the arctic and antarctic F region"
Journal of Geophysical Research 67, 1823 (1962).

(c) "Lunar variations in the ionosphere"
Australian Journal of Physics 9, 112 (1956).

(d) "The behaviour of a Chapman layer in the night F_2 region of the ionosphere"
Australian Journal of Physics 9, 436 (1956).

(e) "Luni-solar variations in the ionosphere"
Australian Journal of Physics, (In print).
Accepted for publication in March 1963 issue.

(f) "Computations of electron density distributions in the ionosphere making full allowance for the geomagnetic field"
Journal of Geophysical Research 63, 491 (1958).

I. Studies of the Ionospheric F Region

(a) "The equatorial F region of the ionosphere"
Journal of Atmospheric and Terrestrial Physics
12, 80 (1960).

(b) "Universal-time control of the arctic and subarctic
F region"
Journal of Geophysical Research 67, 1823 (1962).

(c) "Lunar variations in the ionosphere"
Australian Journal of Physics 9, 112 (1956).

(d) "The behaviour of a Chapman layer in the night F
region of the ionosphere"
Australian Journal of Physics 9, 134 (1956).

(e) "Semi-solar variations in the ionosphere"
Australian Journal of Physics, (In print).

(f) "Comparisons of electron density distributions
in the ionosphere making full allowance for the
geomagnetic field"
Journal of Geophysical Research 67, 491 (1958).

II. STUDIES OF AURORAE AND AIRGLOW

(a) "Photometric observations of subvisual red auroral arcs at middle latitudes"
Australian Journal of Physics 12, 197 (1959).

(b) "Observation of a 6300Å arc in France, the United States and Australia" (with D.Barbier and F.E.Roach)
Annales de Geophysique 18, 390 (1962).

(c) "Simultaneous occurrence of sub-visual aurorae and radio bursts on 4.6 Kc/s"
Nature 183, 1619, (1959).

(d) "Polarisation of the red oxygen line"
Planetary and Space Science 1, 112, (1959).

(e) "Photometric observations of 5577A and 6300A airglow during the I.G.Y."
Australian Journal of Physics 13, 633 (1960).

III. MISCELLANEOUS STUDIES

(a) "The measurement of the drift velocity of electrons through gases by the electron shutter method"
Australian Journal of Physics 10, 54 (1957).

(b) "Some studies of geomagnetic micropulsations"
Journal of Geophysical Research 65, 2087 (1961).

III. MISCELLANEOUS STUDIES

I. STUDIES OF THE IONOSPHERIC F REGION

(a) "The equatorial F region of the ionosphere"

The greatest and most persistent concentration of electrons in the upper atmosphere - the F region - is believed to be generated by ultra-violet sunlight, but it has long been a matter of concern and interest that much of its behaviour cannot be simply explained on this basis. One of the most notable anomalies was discovered during the second world war; electron densities are greatest, not at the geographic equator, but along two belts of magnetic latitude $\pm 20^{\circ}$.

Mitra (1946) suggested that much of the ionization comprising the F region might diffuse down from great heights. Diffusion occurs only along the geomagnetic field lines, so that this ionization would be guided away from the magnetic equator to the two sub-tropical belts. Martyn (1954) renewed Mitra's suggestion but invoked electrodynamic lift at the equator, rather than in situ production, as the source of the high ionization.

The candidate's paper showed that electron densities at the magnetic equator and the sub-tropics are negatively correlated. McNish and Gautier (1949) had mentioned this briefly before, but a detailed study

of the correlation, and its use as evidence in support of Martyn's suggestion of ionisation transport, was new. The paper then calculated, for the first time, the latitudinal redistribution of electron density which would result from Martyn's process, and thus showed that it could account quantitatively for the observed morphology of the equatorial F region.

This paper resulted in the candidate being nominated as the official Australian delegate to the International Symposium on Equatorial Aeronomy, Peru, 1962.

(b) "Universal-time control of the Arctic and Antarctic F Region"

This paper revealed for the first time, and in detail, what is perhaps the most severe case of non-solar control of the F region known to date. It showed that over a large part of the Southern Hemisphere, including Antarctic, Patagonia, and the islands south of Australia, F region electron densities vary, not with local solar hour, but with Greenwich time.

In Winter, electron densities at all stations reach a maximum simultaneously at 07 U.T. In Summer the electron density falls to a diurnal minimum at 10 U.T. at the South Pole and this depression then travels northward

as a wave. At the Equinoxes, and in the Arctic, F behaviour is equally remarkable and is described for the first time in this paper.

(c) "Lunar variations in the ionosphere"

Martyn (1947) pointed out that the newly observed lunar variations of F region height and electron density could hardly be attributed to the simple rise and fall of isobaric surfaces; he outlined an alternative theory in terms of dynamo currents and electric polarization. In 1953 a new theory of ionospheric conductivity (Hirono (1950), Fejer (1953), Martyn and Baker (1953)) made the quantitative development of this theory possible.

The candidates paper undertook this task. The conclusions reached were in good agreement with the observed lunar variations in F_2 parameters. Previously it had been thought (Martyn (1955)) that a drift velocity gradient could be responsible for electron density variations in the F region. The candidates paper showed that, because div(E x H) = 0, drift divergence is always zero if produced by polarization fields alone.

The sentence "At night we may consider the F_2 layer to consist of a relatively thick bank of ionization in the upper region of rapid diffusion and low decay, with a lower boundary whose position is determined by the opposing processes of downward diffusion and gravitat-

ional drift on one hand, and the relatively rapid decay of the lower edge on the other" and other passages accurately state the modern accepted theory of F region formation.

(d) "The behaviour of a Chapman layer in the night F_2 region of the ionosphere"

We have seen that the candidate's lunar tidal paper foreshadowed the modern diffusive theory of the F2 region, but this idea was deduced almost simultaneously by a number of workers in Japan, Australia and England. It thus developed independently in the three countries.

In Australia, Martyn (1956) showed that under the influence of diffusion, gravity, and a height gradient of loss a Chapman distribution of electron density, at a particular height which he deduced, would decay without change of form. He expressed the opinion that any initial distribution of electrons would adopt the Chapman form at this height.

The candidate's paper extended this; it showed that a Chapman distribution at any height would maintain its shape, and at the same time drift bodily towards Martyn's equilibrium height. Besides giving an insight into the behaviour of a layer displaced by tides, this extension represented a solution of the general case; a

thick initial distribution could be considered as the sum of a series of Chapman distributions centred at different heights. Each of these would drift towards the common equilibrium height, and the final condition would therefore be a single Chapman distribution at this height.

(e) "Luni-solar tides in the ionosphere"

Martyn studied the variation with lunar time of the height and electron density of the F region measured at chosen solar hours each day. Such studies should throw light on the daily variation of ionospheric conductivity, but in fact the results were puzzling.

The candidate's paper showed that this was because of statistical conservation. Not all of Martyn's coefficients were statistically significant. Those that were agreed in detail with earlier lunar tidal theory, and demonstrated that the E region near the magnetic equator fails abruptly as a dynamo at sunset, while that above Canberra remains active until midnight.

(f) "Computations of electron density distributions in the ionosphere making full allowance for the geomagnetic field"

This paper supplied an electronic computor programme for calculating electron density - height

distributions from ionosonde records; the programme has been used by Australian research workers. Sample reductions, reported in the paper, confirmed theoretical predictions, that the electron density distribution should be close to a Chapman function.

II. STUDIES OF AIRGLOW AND AURORAE

(a) "Photometric observations of sub-visual red auroral arcs at middle latitudes"

and, with D. Barbier and F. E. Roach,

(b) "Observations of a 6300A arc in France, the United States and Australia"

Before the I.G.Y., it was throught that, except during severe magnetic storms, aurorae were confined to the auroral zones at magnetic latitudes of about 70°. Photometric observations of D. Barbier in France, and independently and a few weeks later the candidate, revealed quiet red auroral arcs at middle latitudes and during periods of only moderate magnetic disturbance. The candidate's paper described the arcs in detail which remains accurate today.

The second paper describes an arc seen on the same day in France, the United States, and Australia.

(c) "Simultaneous observations of sub-visual aurorae and radio noise bursts on 4.6 Kc/s" (with G.R.A. Ellis)

It is now known that radio noise is generated in the upper atmosphere. Discrete emissions such as "dawn chorus" are fairly easily recognised, but the continuous background is masked by the enormously greater radiation from thunderstorms, ever-present at some place on the Earth.

The co-author of this paper (G.R.A.Ellis) devised a method of measuring the "auroral" radio noise during the brief periods between lightning strokes, but many people remained sceptical; it was extremely difficult to be certain that, even during these brief quiet periods, the ambient level was not determined by the integrated effect of very distant electrical storms, or by distant electrical machinery.

The present paper demonstrated closely parallel variations of auroral light, and radio noise measured by Ellis. This placed the auroral nature of Ellis's radio noise beyond doubt. The candidate himself first noticed this co-variation.

(d) "Polarization of the red oxygen auroral line"

Prior to this, substantial polarization had

never been found in auroral light. The candidate's paper described an aurora of 8 July 1958 in which the 6300Å oxygen emission was 30 per cent plane polarized with its magnetic vector N-S. The novelty of this observation was probably a result of latitude; very few observers have studied aurorae at a latitude as low as Sydney.

The paper showed that such polarization would be expected if the aurora was excited by electrons gyrating about the geomagnetic field lines. The contempory discovery of the Van Allen belts supplied a possible source of such gyrating electrons.

(c) "Photometric observations of 5577A and 6300A airglow during the I.G.Y."

This paper, written as a report for the Annals of the I.G.Y., does not contain any radically new material.

III. MISCELLANEOUS STUDIES

(a) "The measurement of the drift velocity of electrons through gases by the electron shutter method"

The drift of electrons under the influence of an electric field is an important quantity in the theory of the electrical conductivity of ionized gases. When this paper was written the authoritative measurements of

electron drift velocity were those of Nielsen and Bradbury.

It is now generally accepted (Phys. Rev. 117, 1411, 1960) that, because of the neglect of electron diffusion, these values were consistly too high. The candidate's paper first demonstrated this, and derived the correction which should be applied.

(b) "Some studies of geomagnetic micropulsations"

Canadian workers had earlier briefly reported success in recording geomagnetic micropulsations on slowly moving magnetic tape. The candidate applied this technique to a comprehensive study of micropulsations.

Commonwealth of Australia
COMMONWEALTH SCIENTIFIC AND INDUSTRIAL RESEARCH ORGANIZATION
Reprinted from Journal of Atmospheric and Terrestrial Physics, Vol. 18, Nos. 2/3, pp. 89–100 (1960)
Pergamon Press Ltd. Printed in Northern Ireland

The equatorial *F*-region of the ionosphere

R. A. Duncan
Upper Atmosphere Section, CSIRO, Camden, Australia

(*Received* 26 *October* 1959)

Abstract—A comparison of data from ionospheric sounders at Chimbote and Panama, shows that afternoon critical frequencies in the equatorial zone are negatively correlated with those on the same meridian in the sub-tropical belts. This supports Martyn's suggestion that ionization is transported from the equatorial zone to the sub-tropics.

The process suggested by Martyn, electrodynamic lift at the equator followed by diffusion under gravity along the geomagnetic field lines to the sub-tropical belts, is investigated quantitatively, and it is shown that the process can account for the high sub-tropical electron densities observed.

It is shown that the diurnal variation of the correlation between Chimbote and Panama critical frequencies, the diurnal variation in the height, thickness and electron density of the equatorial *F*-region, and the diurnal variation of electron density enhancement in the sub-tropics, can all be ascribed to the simple diurnal electrodynamic tide expected from the observed magnetic variations, in conjunction with diffusion along the geomagnetic field lines.

Introduction

During the second world war it was discovered (Appleton, 1946; Bailey, 1948; Rastogi, 1959) that the afternoon *F*-region electron density is less near the magnetic equator than in two sub-tropical belts at magnetic latitudes of $\pm 20°$ (Fig. 1). Mitra (1946) suggested that this might be because much of the ionization

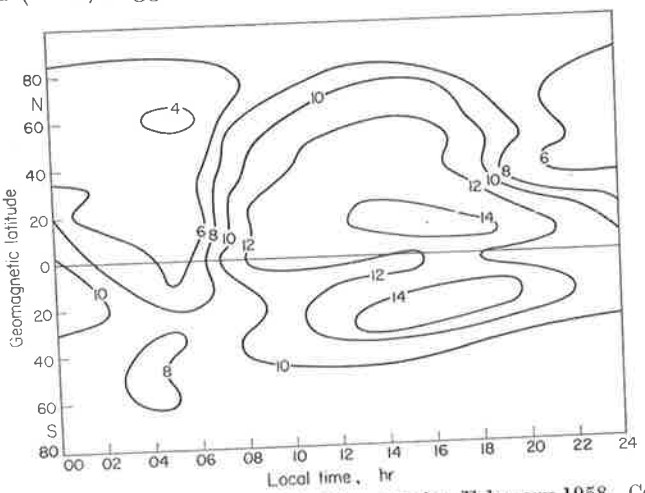

Fig. 1. World contours of *F*-region critical frequencies, February 1958. Contours at 2 Mc intervals (as predicted by the Australian Ionospheric Prediction Service for the west zone).

comprising the *F*-region is produced by ultra-violet light at heights up to 600 km, only subsequently diffusing down under gravity to normal *F*-region heights; diffusion can occur only along the geomagnetic field lines so that the *F*-region at the magnetic equator is robbed of this ionization which is instead guided to the two sub-tropical belts (Fig. 2).

Bailey (1948) (for recent work see Skinner *et al.*, 1954) noticed that the low

equatorial electron densities are associated with high, thick and multiple layer formation (Fig. 3). Martyn (1954) suggested that this feature too, might be due to the inhibition of downward vertical diffusion under gravity. He repeated Mitra's suggestion that diffusion would instead take the ionization via the geomagnetic field lines to the two sub-tropical belts, but invoked electrodynamic

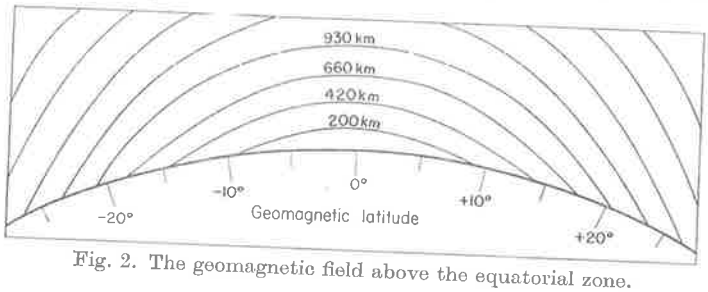

Fig. 2. The geomagnetic field above the equatorial zone.

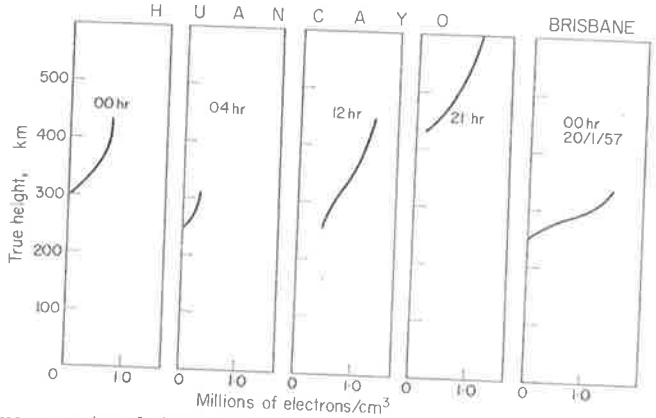

Fig. 3. Huancayo true height—electron density profiles. Mean of five magnetically quiet days, December 1938. A moderate latitude profile is shown for comparison (Huancayo profiles from Schmerling and Thomas, 1955).

lift, rather than *in situ* production by solar radiation, as the source of the high equatorial ionization.

Mitra's and Martyn's explanation of the anomalous equatorial *F*-region has been strengthened by the accumulating evidence that diffusive settling under gravity is indeed a controlling factor at more moderate latitudes. Duncan (1956a) suggested that the opposing forces of downward diffusion under gravity and a negative height gradient of electron decay should combine to stabilize the height of the middle latitude night-time *F2*-region. Yonezawa (1956) developed a similar theory in some detail, for the more involved case of the day-time *F2*. Subsequently Martyn (1956), Duncan (1956b) and Dungey (1956), put the theory for the night-time *F2*-region on a quantitative basis. They showed that under an attachment law of electron decay the electron density will assume a vertical distribution of the Chapman form centred at a height such that

$$\nu = \frac{g \sin^2 \chi}{2 H \beta} \qquad (1)$$

where ν is the positive ion collision frequency;
g is the gravitational field strength;
χ is the geomagnetic dip;
H is the scale height;
β the attachment coefficient.

To account for the observed height of the $F2$-region at middle latitudes this theory requires a neutral particle density of about 10^{10} particles per cm^3 at 300 km (MARTYN, 1956) and this is much higher than the density adopted by the Rocket Panel (1952) and widely accepted at the time.

Recent true height analyses (DUNCAN, 1958) (see also BERKNER, 1940) have shown that the observed night-time electron distribution is indeed close to the Chapman form. Satellites (SCHILLING and STERNE, 1959) have found the high air densities required by the diffusion theory.

The critical frequency at a given hour and station fluctuates irregularly from day to day. WRIGHT *et al.* (1957) have mentioned, without published evidence, that unusually low critical frequencies in the equatorial zone are associated with unusually high critical frequencies in the sub-tropics. This negative correlation was evidently noticed by MCNISH and GAUTIER (1949) during their studies of equatorial lunar tides*. Such an inverse relation supports the idea of ion transport from one place to the other.

In this paper the correlation between critical frequencies at Chimbote near the magnetic equator, and Panama in the sub-tropics will be studied in some detail. It will be shown that the diurnal variation of this correlation, the diurnal variation of the height, thickness and electron density of the equatorial F-region, and the diurnal variation of electron density enhancement in the sub-tropics can all be ascribed to a simple diurnal electrodynamic tide and MARTYN'S ion transport process. It will be suggested, however, that *in situ* ion production at great heights, as suggested by MITRA, may be important in the winter polar region. MARTYN'S process; electrodynamic lift at the equator followed by diffusion under gravity down the geomagnetic field lines to the sub-tropics, will be analysed and it will be shown that it can account quantitatively for the high electron densities observed in the sub-tropical belts.

THE CO-VARIATION OF ELECTRON DENSITY AT THE EQUATOR AND SUB-TROPICS, AND OTHER EVIDENCE FOR ION TRANSPORT

In Fig. 4 we have compared the daily fluctuations of critical frequency at 1500 hours at two stations lying near the 75°W meridian, Chimbote, Peru, near the magnetic equator (magnetic dip 7°N) and Panama in the sub-tropical belt (dip 37°N). It will be seen that they are negatively correlated; above average critical frequencies are observed at Panama on afternoons when below average critical frequencies are observed at Chimbote, and vice versa.

This lends support to the picture of electron transport. We may suppose that the intensity of the electrojet and hence the magnitude of the F-region electrodynamic lift varies from day to day and that this variation in turn results in a variation of the quantity of ionization shifted from Chimbote to Panama.

* Private communication, J. W. WRIGHT.

Part of the variation of the electrojet is no doubt due to the ever-changing phase relationship of the solar and lunar atmospheric tide. This is the connexion between the present study and that of McNish and Gautier (1949).

It might be thought that the ideas advanced above could be best substantiated by a study of the daily values of the magnetic variation and the true height of the F-region. However, daily true $h_{\max}F$ data are not available; magnetic data are available, but it is believed that a great part of the magnetic variation observed

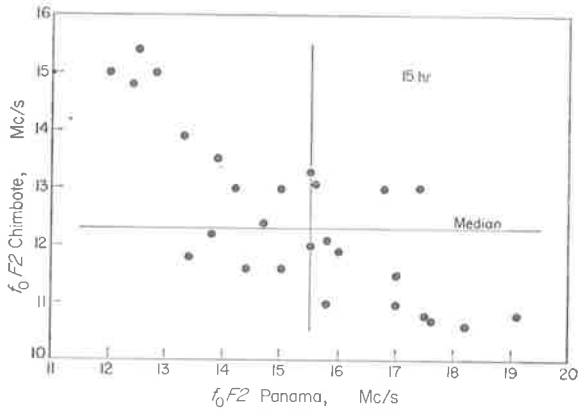

Fig. 4. Critical frequency at 1500 hours at Chimbote against that at Panama, February 1958.

at the ground is not due to ionospheric electric currents, but to something in the nature of Chapman and Ferraro's (1941) ring current much further out.

However, that part of the magnetic variation which shows a diurnal pattern should be of ionospheric origin and we shall see in a later section that this mean diurnal magnetic variation is in accord with the mean diurnal behaviour of the equatorial ionosphere and Martyn's ion transport process.

Another consideration favours Martyn's electrodynamic lift rather than Mitra's *in situ* production as the source of ionization high above the equatorial zone. The moderate latitude F-region rises rapidly after sunset. This suggests that ion production occurs predominantly at low heights.

There is one part of the world where this is not true, the winter polar zone. Here the atmosphere is not illuminated below 450 km and the maintainence of the F-region (Gates, 1959) at about the same height, as the moderate latitude night-time F-region, 350 km, is probably due to diffusion from above.

Transport of Ionization from the Equator to the Sub-tropics

We shall suppose that the ionosphere over a large part of the globe is lifted perpendicularly to the geomagnetic field by an eastward electric field and subsequently gravitates back along the magnetic field lines to normal F-region heights. It can be seen from Fig. 2 that this will cause a shift of ionization away from the equator. We wish to calculate the actual redistribution of ion density with latitude which will result.

We shall assume that the ionization gravitates to the height from which it was originally lifted. This is not quite true. As we have said ionization is produced predominantly at, and thus lifted from, a height of about 250 km, whereas it settles to a height of between 300 and 350 km. This means that from 50 to 100 km more lift will be needed to produce a given result than our theory will indicate. As we shall argue that lifts of the order of 800 km occur this is of little consequence.

Assuming a dipole field the equation of a geomagnetic line of force is

$$\frac{r}{\cos^2 \theta} = K \tag{2}$$

where r is the radial distance from the centre of the earth;
θ is the geomagnetic latitude;
K is the radial distance of the field line at the equator.

Now at $F2$-heights an electric field (E) perpendicular to the geomagnetic field (H), causes a drift normal to the plane of E and H with a velocity

$$v = \frac{E}{H}. \tag{3}$$

That is, for a given electric field the drift velocity is inversely proportional to the geomagnetic field strength. The distance between adjacent geomagnetic field lines is also inversely proportional to the geomagnetic field strength so that an electric field which shifts the ionization from one geomagnetic line to the other at the equator will, in the same time, shift the ionization from one line to the other at any latitude.

Now if ionization on the geomagnetic field line

$$\frac{r_1}{\cos^2 \theta_1} = K_1 \tag{4}$$

is moved electrodynamically onto the geomagnetic field line

$$\frac{r_2}{\cos^2 \theta_2} = K_2 \tag{5}$$

and if it then gravitates along this line until it reaches its original height, we have

$$r_1 = r_2 \tag{6}$$

and hence

$$r \left\{ \frac{1}{\cos^2 \theta_2} - \frac{1}{\cos^2 \theta_1} \right\} = K_2 - K_1 \tag{7}$$

and from (2)

$$K_2 - K_1 = h \tag{8}$$

where h is the height of line (2) above line (1) at the equator. Thus

$$\frac{1}{\cos^2 \theta_2} - \frac{1}{\cos^2 \theta_1} = \frac{h}{r} \tag{9}$$

i.e.

$$\tan^2 \theta_2 - \tan^2 \theta_1 = \frac{h}{r}. \tag{10}$$

This then is the expression giving the change in latitude of the ionization. We now derive the change in ion concentration.

Referring to Fig. 5, suppose that ionization above the element of area dA_1 is carried to the element dA_2, then if n_1 was the number of ions per vertical column

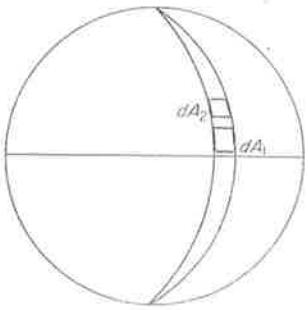

Fig. 5. Geometry of ion transport.

at dA_1 before transport, and n_2 is the corresponding areal density at dA_2 after transport

$$n_1\, dA_1 = n_2\, dA_2. \tag{11}$$

Let r be the radius of the earth, $d\phi$ the element of longitude, and $d\theta$ an element of latitude, then (11) becomes

$$n_1 r\, d\theta_1\, r\cos\theta_1\, d\phi = n_2 r\, d\theta_2 r\cos\theta_2\, d\phi \tag{12}$$

i.e.
$$n_2 = n_1 \frac{\cos\theta_1}{\cos\theta_2}\frac{d\theta_1}{d\theta_2}. \tag{13}$$

Differentiating (10) with respect to θ_2

$$2\tan\theta_2 \sec^2\theta_2 - 2\tan\theta_1 \sec^2\theta_1 \frac{d\theta_1}{d\theta_2} = 0 \tag{14}$$

i.e.
$$\frac{d\theta_1}{d\theta_2} = \frac{\tan\theta_2 \sec^2\theta_2}{\tan\theta_1 \sec^2\theta_1} \tag{15}$$

so that
$$n_2 = n_1 \frac{\tan\theta_2 \cos^3\theta_1}{\tan\theta_1 \cos^3\theta_2}. \tag{16}$$

This is better expressed as a function of θ_2 only.

$$\frac{\cos^2\theta_2}{\cos^2\theta_1} = 1 - \frac{h}{r}\cos^2\theta_2 \tag{17}$$

and
$$\frac{\tan^2\theta_1}{\tan^2\theta_2} = 1 - \frac{h}{r}\cot^2\theta_2. \tag{18}$$

Hence
$$n_2 = \frac{n_1}{(1-(h/r)\cot^2\theta_2)^{1/2}(1-(h/r)\cos^2\theta_2)^{3/2}}. \tag{19}$$

To reiterate; if there were originally n_1 ions per vertical column at a latitude θ_1, an electrodynamic lift equivalent to a lift through a height h at the equator, followed by settling under gravity to the original height, will carry the ions to a

latitude θ_2 determined by equation (10) and the number of ions per vertical column here will now be n_2 as given by equation (19).

It is a property of equations (10) and (19) that m operations with $h = h_1$, $h_2, \ldots . h_i \ldots . h_m$, respectively, produces the same result as a single operation with $h = \sum_{i=1}^{m} h_i$. Two 100 km lifts with settling after each lift produce the same effect as a single 200 km lift followed by settling. Hence lift and settling can occur concurrently without invalidating equations (10) and (19).

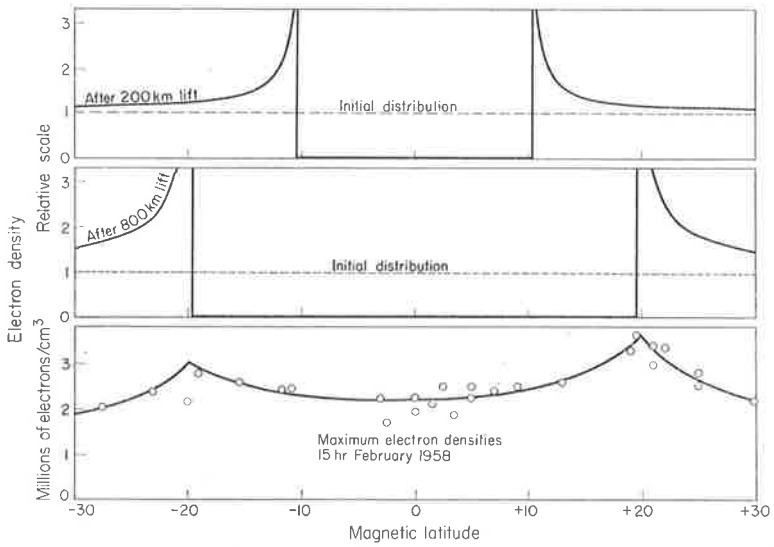

Fig. 6. The latitude distribution of electron content per vertical column, which would be produced from an initially uniform distribution by electrodynamic lift and subsequent settling down the geomagnetic field lines, compared with the mean maximum electron densities observed at 1500 hours during February 1958.

In Fig. 6 we have used equations (19) to determine the latitude redistribution, by lifts of 200 and 800 km, respectively, of an ion density initially uniform with latitude. The observed latitude variation of maximum electron density is shown for comparison. It can be seen that the transfer process can account for the high electron densities observed in the sub-tropics, if lifts as great as 800 km occur.

This is not improbable. The magnetic variations observed at Huancayo (Fig. 7) lead us to expect upward drift during the day and downward drift at night. Calculations analogous to those of DUNCAN (1956a) for the lunar tidal case, suggest velocities of about 85 km/hr. The height of maximum electron density above Huancayo is observed to fall through 300 km during the night (Fig. 8) and the actual downward drift of ionization must be greater, as downward movement of the layer profile is largely countered by preferential decay of the under surface. By day, ion production at a fixed height stabilizes the height of maximum electron density even more strongly, although the expected upward smearing of the layer is observed (Fig. 3). It will not even be the case that individual ions will reach heights of 1000 km because, as we shall show in the next

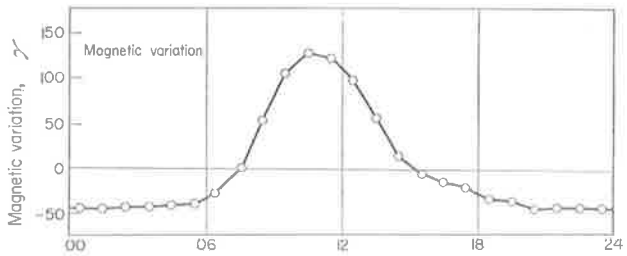

Fig. 7. The diurnal variation of the north–south geomagnetic field at Huancayo. Five quiet days, December 1938 (after JOHNSON *et al.*, 1948).

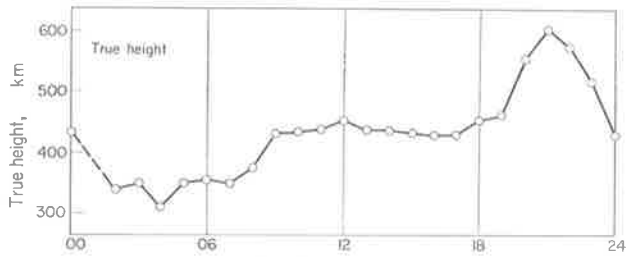

Fig. 8. The diurnal variation of the true height of the ionospheric electron density maximum at Huancayo. Five quiet days, December 1938 (after SCHMERLING and THOMAS, 1955).

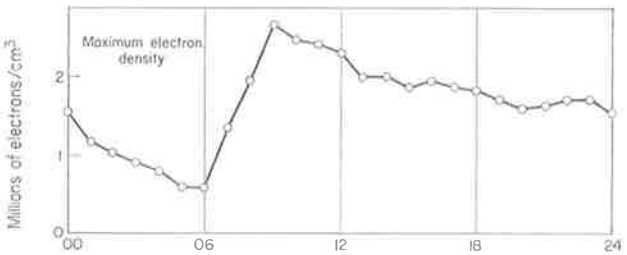

Fig. 9. The diurnal variation of maximum electron density, Chimbote, February 1958.

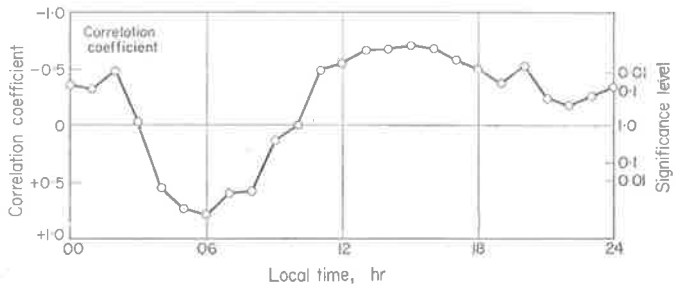

Fig. 10. The diurnal variation of the correlation between f_0F2, at Chimbote and Panama, February 1958. The ordinate has been reversed to bring out the relation of this variation to that of maximum electron density.

section; settling down along the field lines is prompt, and will occur concurrently with electrodynamic lift across them. A drift of 800 km across the geomagnetic field will not, then, result in an 800 km increase in height, but nevertheless there is every reason to believe that it occurs and that it is the cause of the enhanced electron densities observed in the sub-tropics.

The observed distribution of electron density with latitude (Fig. 6) is less extreme than the computed curves, but this is to be expected because of the mollifying effect of continuous ion production and decay.

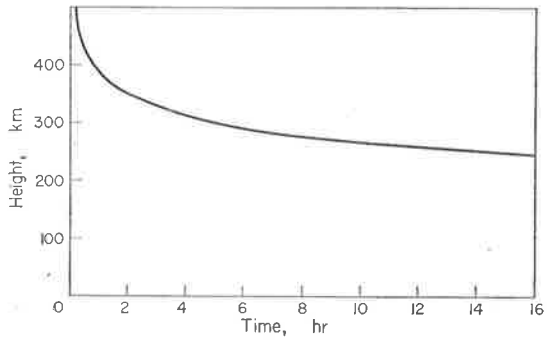

Fig. 11. Time for ionization to diffuse from the equator to various heights at a magnetic latitude of 20°.

Time Required for Ion Transport

It remains to be shown that ionization high above the equatorial zone will gravitate to the sub-tropics in an acceptable time.

The component of gravity along the geomagnetic field lines is $g \sin \chi$, where χ is the dip, and gas theory (Huxley, 1951) indicates that the ionization should gravitate down the field lines with a velocity

$$v = \frac{0{\cdot}85\, g \sin \chi}{\nu} \tag{20}$$

ν being the collision frequency of the positive ions with neutral molecules. The collision frequency term (ν) causes the settling velocity to increase exponentially with height and numerical substitution shows that this factor overwhelms the effect of the great length and low inclination of that part of the geomagnetic field line above the equatorial zone. Almost all the time for the journey is taken over the last hundred or so kilometres. The time for the journey thus depends, not on how far the ionization has travelled, but on the depth to which it settles.

The times needed for ionization at a magnetic latitude of 20° to settle to various heights is shown in Fig. 11. In calculating these Martyn's (1959) estimate of the collision frequency at 300 km, viz. 1·1 sec^{-1}, was adopted and this was assumed to decrease exponentially with altitude with a scale height of 50 km, i.e.

$$\nu = 1{\cdot}1 \exp \frac{300 - h}{50} \text{ sec}^{-1}. \tag{21}$$

It will be seen that ionization settles to 350 km in about 2 hr.

The Mean Diurnal Behaviour of the Equatorial *F*-region

The diurnal variation of the geomagnetic field at Huancayo is shown in Fig. 7. An application of Ampere's law shows that if the currents responsible for this variation flow in the ionosphere they should cause an electrodynamic tide with maximum upward velocity at midday and maximum downward velocity at midnight. Keeping in mind the great resistance to movement of the height of maximum electron density ($h_{\max}F2$) conferred by ion production at a fixed height during the day, it can be seen that the magnetic variation and the observed variation of true $h_{\max}F2$ are in accord (Fig. 8).

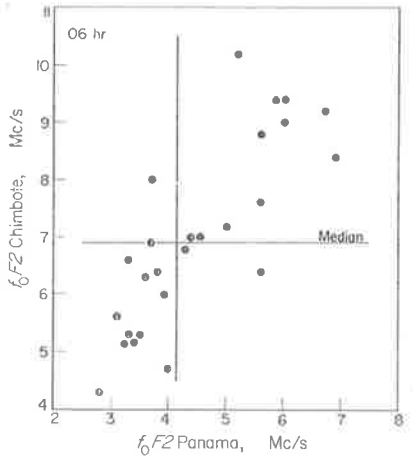

Fig. 12. Critical frequency at 0600 hours at Chimbote against that at Panama, February 1958.

Minimum $h_{\max}F2$ occurs at 0400 hours, naturally a little after the time of maximum downward velocity. Similarly the maximum effect from the day-time upward drift, which as we have said should be more in the nature of an upward smearing of the region than an outright increase in $h_{\max}F2$, should occur in the mid-afternoon.

Consider now the effect these tidal drifts will have on the critical frequency. The lowering of the ionosphere at 0400 hours should carry it into a region of high neutral particle density and consequent rapid electron decay. The critical frequency should therefore drop rapidly at this time and, as is well known, it does (Fig. 9). There is, naturally, a second time-lag here; minimum f_0F2 occurs at 0600 hours, a couple of hours after the time of most rapid decay.

The process just described will be effective at both Chimbote and Panama, so that if day to day fluctuations in f_0F2 are largely due to fluctuations in the amplitude of the electrodynamic tide, Chimbote and Panama f_0F2 should be positively correlated at dawn. Fig. 12 shows that they are.

Upward drift, occurring as it does during daylight, will also cause a decrease of the maximum electron density by spreading ionization upwards from the height of production. The total electron content of the ionosphere will, however,

be increased as electrons are carried to the high regions of low decay. In the afternoon therefore, when, as we have said, the effects of upward drift will be at their maximum, we should expect the critical frequency in the equatorial zone to be perhaps slightly depressed but the layer should be high and thick. This store of electrons in the high regions of low decay should give it long life, and a relatively high electron density should therefore persist after sunset. The observed equatorial F-region (Fig. 9) has the expected behaviour.

The high ionization in the equatorial zone will tend to gravitate down the geomagnetic field lines to the sub-tropics. In the mid-afternoon therefore we should expect f_0F2 at Chimbote and Panama to be negatively correlated and the phenomena of high critical frequencies in the sub-tropical belts to be most pronounced. Figs. 1 and 10 show that such is the case.

Acknowledgements—This work forms part of the programme of the Upper Atmosphere Section of the Commonwealth Scientific and Industrial Research Organization. I am greatly indebted to Dr. D. F. MARTYN for careful criticism of the paper.

Data studied were circulated by the Cavendish Laboratory, the Carnegie Institution of Washington, the Central Radio Propagation Laboratory of the U.S. National Bureau of Standards, the Indian Council of Scientific and Industrial Research, the Belgian Bureau de Geophysique, and the French Institut pour la Recherche Scientifique en Afrique Centrale.

I am indebted to Dr. B. A. CHARTRES for advice on the use of Sydney University's Silliac computor, on which the correlation coefficients were calculated.

REFERENCES

APPLETON E. V.	1946	*Nature, Lond.* **157,** 691.
BAILEY D. K.	1948	*Terr. Magn. Atmos. Elect.* **53,** 35.
BERKNER L. V.	1940	*International Union of Geodesy and Geophysics, Transactions of Washington Meeting,* 4–15 *September* 1939. Bulletin No 11, p. 417.
CHAPMAN S. and FERRARO V. C. A.	1941	*Terr. Magn. Atmos. Elect.* **46,** 1.
DUNCAN R. A.	1956a	*Aust. J. Phys.* **9,** 112.
DUNCAN R. A.	1956b	*Aust. J. Phys.* **9,** 436.
DUNCAN R. A.	1958	*J. Geophys. Res.* **63,** 491.
DUNGEY J. W.	1956	*J. Atmosph. Terr. Phys.* **9,** 90.
GATES D. M.	1959	*J. Res. Nat. Bur. Stand.* D **63,** 1.
HUXLEY L. G. H.	1951	*Proc. Phys. Soc.* B **64,** 844.
JOHNSTON H. F., MCNISH A. G., THORBUSH S. E., SCOTT W. E., VALSAM E. and LEDIG P. G.	1948	*Magnetic Results from Huancayo Observatory, Peru,* 1936–1944. Carnegie Institution of Washington.
MARTYN D. F.	1954	*The Physics of the Ionosphere,* p. 259. Physical Society, London.
MARTYN D. F.	1956	*Aust. J. Phys.* **9,** 161.
MARTYN D. F.	1959	*Proc. Inst. Radio Engrs, N.Y.* **47,** 147.
MCNISH A. G. and GAUTIER T. N.	1949	*J. Geophys. Res.* **54,** 303.
MITRA S. K.	1946	*Nature, Lond.* **158,** 668.
RASTOGI R.G.	1959	*J. Atmosph. Terr. Phys.* **14,** 31.
ROCKET PANEL	1952	*Phys. Rev.* **88,** 1027.
SCHILLING G. F. and STERNE T. E.	1959	*J. Geophys. Res.* **64,** 1.

Schmerling E. R. and Thomas J. O.	1955	*Tables of* F2*-layer Electron Density on International Quiet Days.* Cavendish Laboratory, Cambridge.
Skinner N. J., Brown R. A. and Wright R. W.	1954	*J. Atmosph. Terr. Phys.* **5,** 92.
Wright J. W., Knecht R. W. and Davies K.	1957	*Annals IGY.* Vol. III, pt. I, p. 50. Pergamon Press, London.
Yonezawa T.	1956	*J. Radio Res. Lab.* **3, 1.**

Commonwealth of Australia

Commonwealth Scientific and Industrial Research Organization

Reprinted from "JOURNAL OF GEOPHYSICAL RESEARCH"

VOL. 67, NO. 5 PAGE NOS. 1823-1830 MAY 1962

Universal-Time Control of the Arctic and Antarctic *F* Region

R. A. DUNCAN[1]

Central Radio Propagation Laboratory, National Bureau of Standards, and High Altitude Observatory, Boulder, Colorado

Abstract. Electron densities in the *F* region above Antarctica vary with universal time. Similar, but weaker, behavior is found above the Arctic. In both hemispheres maximum electron densities occur close to the time of local noon at the geomagnetic pole. Some evidence suggests that during equinox negative ions are produced by proton bombardment and subsequently are detached by sunlight.

INTRODUCTION

In midwinter at the geographic poles darkness prevails from the ground to a height of 575 km, yet, as observers in Antarctica discovered during the International Geophysical Year, *F*-region ionization remains; critical frequencies seldom drop below 5 Mc/s. Furthermore, the poles experience no daily variation of solar zenith angle, yet at the south pole *F*-region critical frequencies (f_0F_2) experience a marked daily

[1] On leave from Upper Atmosphere Section, Commonwealth Scientific and Industrial Research Organization, Camden, N.S.W., Australia.

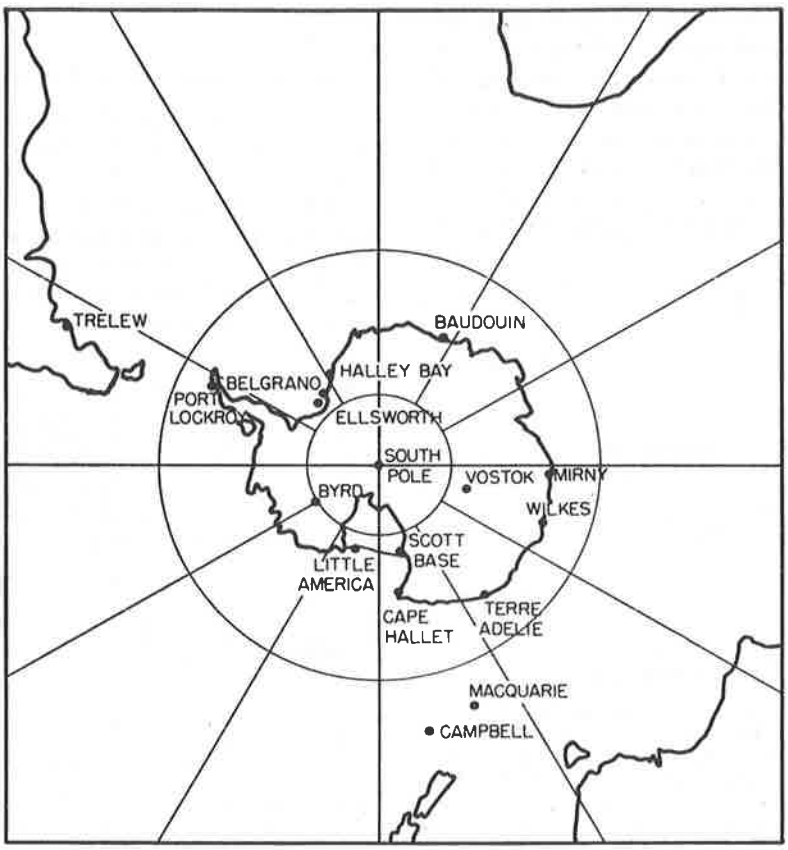

Fig. 1. Map of Antarctica.

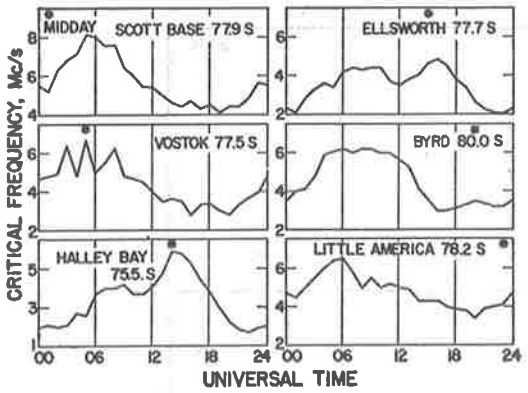

Fig. 2. Universal-time diurnal variation of winter (June 1958) median f_oF_2 at six circumpolar stations. An asterisk marks the time of local noon at each station.

variation [*Knecht*, 1959]. Though their nature is unknown, processes other than electron production by sunlight must be important.

Here we study the diurnal variation of f_oF_2 at those arctic, antarctic, and subantarctic stations for which data are available at the Boulder data center. Arctic and antarctic behavior are compared. The seasonal variation of antarctic f_oF_2 is described. This study shows that universal-time control is more important and widespread than has hitherto been suspected. In the south, it is found at some time of the year at all the stations except Campbell Island (see Fig. 1).

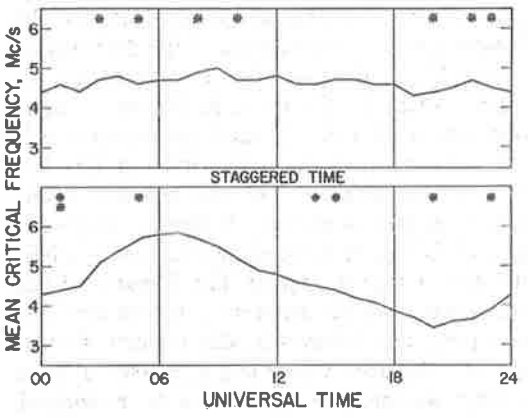

Fig. 3. Lower plot; mean universal-time variation of winter (June 1958) median f_oF_2 at eight antarctic stations: South Pole, Byrd, Little America, Scott Base, Ellsworth, Vostok, Halley Bay, and Cape Hallett. Upper plot; staggered mean for statistical control. An asterisk marks the time of local noon at the various stations.

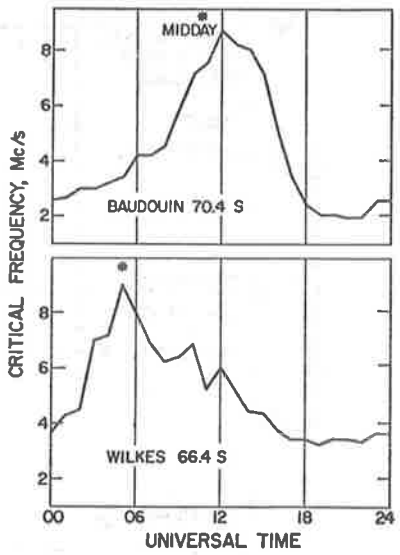

Fig. 4. Universal-time variation of winter (June 1958) median f_oF_2 at Baudouin and Wilkes. Asterisks mark the times of local noon.

We attempt to explain some of the observed phenomena.

Diurnal Variation of Antarctic f_oF_2

Winter. *Knecht* [1959] harmonically analyzed median f_oF_2 from the south pole station for 10 winter months, and for each month found maximum f_oF_2 close to 06 or 07 UT. Figure 2 shows winter f_oF_2 plotted against universal time for six circumpolar stations in Antarctica; on each plot asterisks mark the time of local noon, thus giving an indication of the longitude of the

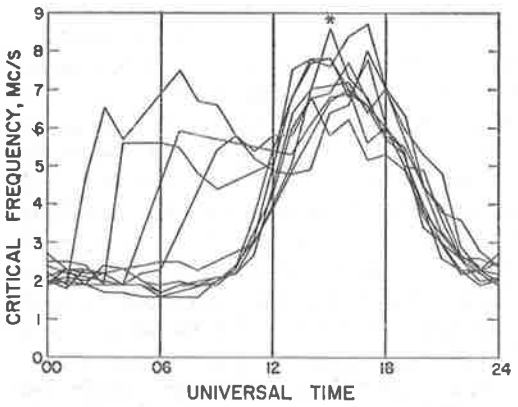

Fig. 5. Superimposed diurnal variations of f_oF_2 at Ellsworth for the first 10 days of August 1958. An asterisk marks the time of local noon.

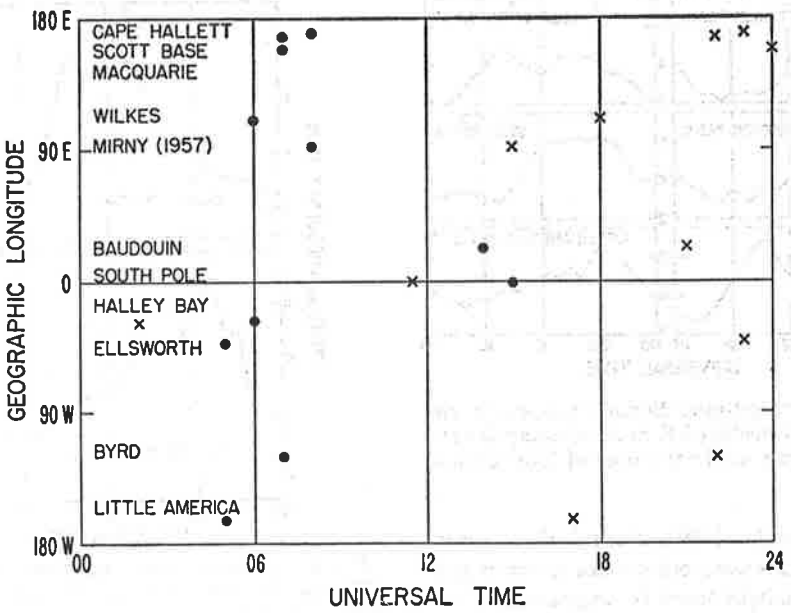

Fig. 6. Universal times of diurnal maxima (dots) and minima (crosses) quartile range of winter (June 1958) f_0F_2 for stations above a geomagnetic latitude of 60°S.

station. At some stations, particularly those at lower latitudes, critical frequencies reach a maximum at local noon, but, in addition, at all stations a maximum occurs near 06 UT.

Figure 3 summarizes the universal-time behavior of winter f_0F_2 at eight antarctic stations above a latitude of 75°, all such stations for which data are available. The top plot is a control recommended by *Bartels* [1948]. Here we have averaged the data in a meaningless manner. Before averaging we arranged the stations in order of geographic latitude and gave each a time advance of 3 hours over the one before it. The resulting variation is featureless, showing that no one station dominates the others. The lower plot is the mean universal-time variation. Asterisks mark the position of local noon at the various stations once more; they are well spaced, so that local time variations should be largely removed. This plot has a peak, much larger than any feature on the control plot, at 07 UT. The 07 UT maximum of winter F-region electron density found by Knecht occurs, not at the pole only, but over the whole polar cap.

Below a latitude of 75° electron production by sunlight begins to drown the 07 UT peak. At Baudouin (latitude 70°) we can see an enhancement near 07 UT, but it is overshadowed by a much larger neighboring noon peak (Fig. 4). At Wilkes, at a still lower latitude, and with the added embarrassment that 07 UT and local noon are only 2 hours apart, it is impossible to deduce any universal-time control from the diurnal plot of median critical frequencies (Fig. 4).

Nevertheless, there is a way of demonstrating universal-time control at lower latitudes. In Figure 5 we have superimposed the daily variation of f_0F_2 at Ellsworth for the first 10 days of August 1958. At Ellsworth in August sunlight is important, but 07 UT and local noon are well separated, so that the daily curve of f_0F_2 has two distinct maxima. The two maxima differ. The noon peak is regular; it occurs every day. The 07 UT peak is sporadic; on perhaps half the days it fails to appear. The F region of the ionosphere over all Antarctica, except the Palmer peninsula, behaves in this manner. Consequently, the daily values of f_0F_2 at 06 UT have a large scatter; the scatter can be recognized even at latitudes, and during months, where local sunlight controls the median values. Figure 6 shows this; it shows the times of maximum (dots) and minimum (crosses) scatter of f_0F_2, measured by the quartile range, for antarctic and subantarctic stations during June 1958.

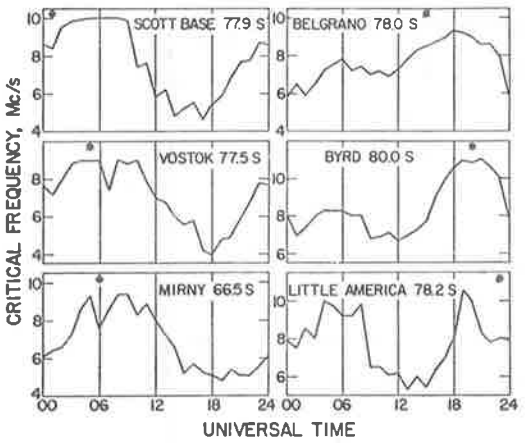

Fig. 7. Universal-time variation of equinox (September 1958) median f_0F_2 at six circumpolar stations. Asterisks mark the times of local noon.

Irrespective of longitude, with only two exceptions, maximum scatter occurs at about 06 UT.

South of Australia (see Fig. 1) sporadic enhancement of f_0F_2 at 06 UT is found north to Macquarie Island, at a geographic latitude of 54.5° south. South of South America the phenomenon ends closer to the pole, somewhere between Halley Bay (75.5°S) and Port Lockroy (64.8°S). This suggests that geomagnetic latitude is involved; the magnetic pole is skewed toward Australia. Figure 6 contains points for all stations within a circle of 60° geomagnetic latitude; sporadic enhancement of F-region electron densities at about 06 UT seems to occur within this boundary.

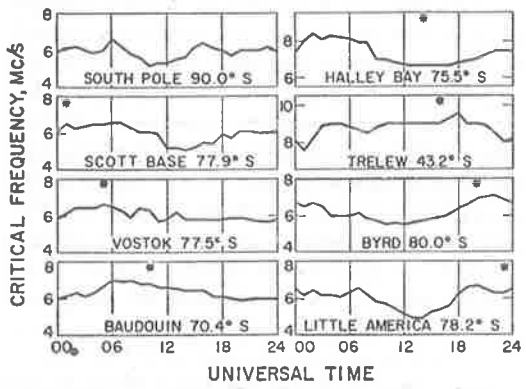

Fig. 8. Universal-time variation of summer (December 1958) median f_0F_2 at seven antarctic and one mid-latitude station. Asterisks mark the times of local noon.

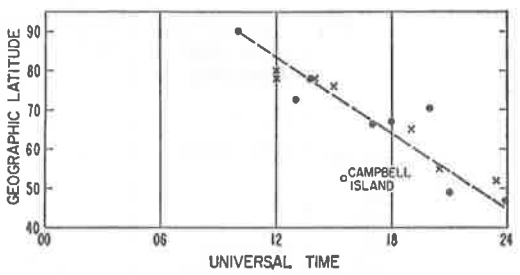

Fig. 9. Universal times of diurnal minima of antarctic summer (December 1958) median f_0F_2 plotted against geographic latitude. Crosses, western; dots, eastern stations. Vostok is omitted, as it showed multiple weak minima (Fig. 8).

Equinox. The maximum of antarctic F-region electron densities near 07 UT, found during winter, is found again during equinox (Fig. 7). In addition, in the western hemisphere at the equinoxes, a second and larger maximum occurs near 19 UT. This increase of electron density occurs only in sunlight; it is not found in the eastern hemisphere, where it is dark at 19 UT during equinox. It is not found at any longitude during winter. The 07 UT peak, also, is enhanced by sunlight; it is larger in the eastern hemisphere, which is sunlit at this time. At the south pole sunlight is continuous during equinox, and there both maxima are large [*Knecht*, 1959].

Summer. The daily variations of antarctic F-region electron densities are small during

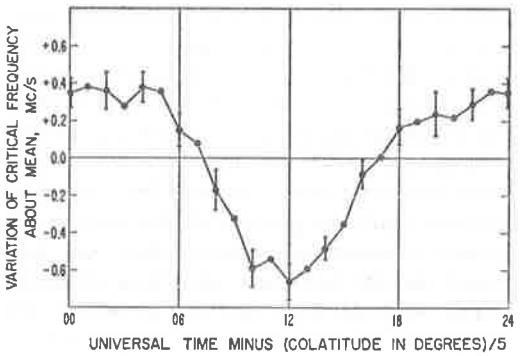

Fig. 10. Diurnal oscillation of summer median f_0F_2 about 24-hour mean, averaged for twelve antarctic stations: South Pole, Byrd, Little America, Scott Base, Ellsworth, Vostok, Halley Bay, Cape Hallett, Baudouin, Terre Adelie, Wilkes, all December 1958; Mirny, December 1957. A latitude adjustment was applied to universal time before averaging.

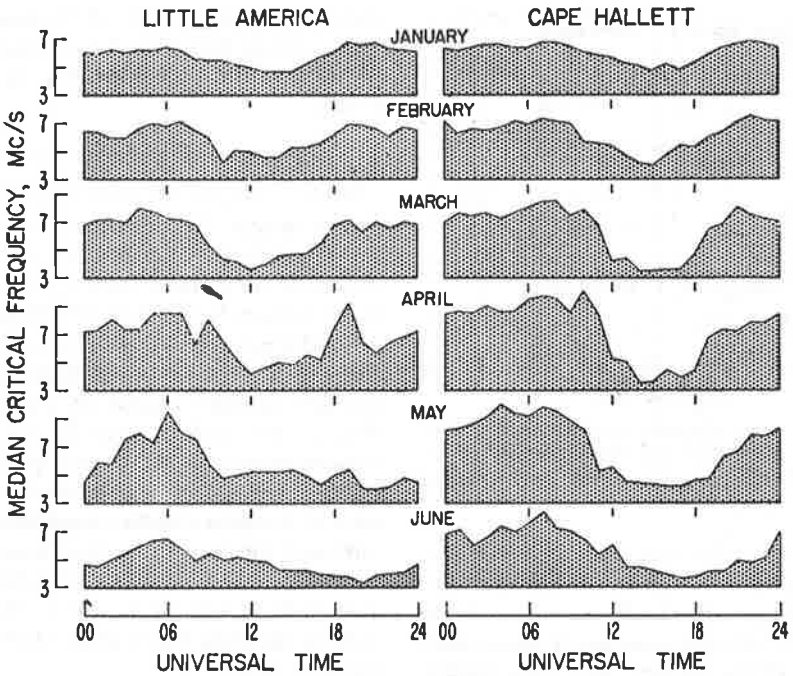

Fig. 11. Universal-time variation of median f_0F_2 at Little America and Cape Hallett for each month from January to June 1958.

summer, but the plots for most stations (Fig. 8) show a broad maximum and a slightly narrower minimum. As in winter, the minimum occurs between 12 and 24 UT. The universal time of the minimum is plotted against geographic latitude in Figure 9. Points for western (crosses) and eastern (dots) stations lie together; once more, local hour is unimportant. Universal time controls the incidence of minimum F-region electron density in the summer Antarctic, but not in a simple manner; minimum electron density occurs earliest, 10 UT, at the pole, and progressively later, by about 1 hour per 5° with decreasing latitude.

We have adjusted time by 1 hour per 5° and then averaged the median daily variation of F-region critical frequencies of twelve antarctic polar-cap stations. Figure 10 shows the result. The expected standard deviations of the points are shown too. The mean daily variation has a trough-to-peak amplitude of about 1 Mc/s and is significant.

The point for Campbell Island in Figure 9 does not fit the general trend. Here, as at stations to the north in New Zealand and Tasmania, universal-time control has disappeared; F-region electron densities reach a minimum before dawn, the normal middle-latitude local time behavior. In the Palmer peninsula–South America sector, on the other hand, universal-time control extends north to the middle-latitude station Trelew (43°S). The minimum f_0F_2 at 01 UT at Trelew (Fig. 8), though not plotted in Figure 9, would fit there very well. From a local time viewpoint the Trelew plot (Fig. 8) would be surprising; f_0F_2 is as high at midnight as at midday. Not only this, but the amplitude of the variation over the Palmer peninsula is greater than it is over the antarctic mainland. At Port Lockroy, during December 1958, median critical frequencies ranged from 7 to 11 Mc/s, in a manner even more surprising from a local-time viewpoint [cf. *Rastogi*, 1960]. We see then that in summer, in contrast to winter, the area of universal-time control of the antarctic F region is skewed toward South America.

Seasonal Variation of Antarctic f_0F_2

It remains to describe the manner of transition from summer to winter behavior. *Bellchambers and Piggott* [1958] have reported a sudden, discontinuous change at Halley Bay. They

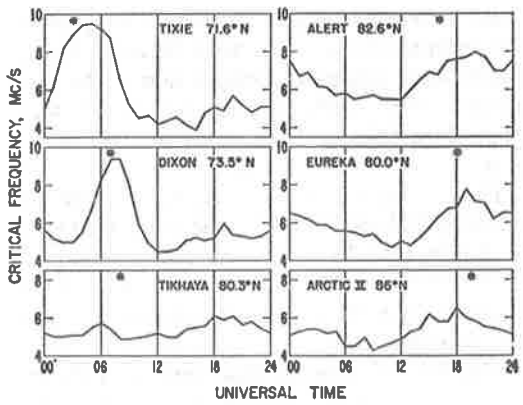

Fig. 12. Universal-time variation of winter (mean of December 1957 and 1958) median f_0F_2 at six arctic stations. Asterisks mark the times of local noon.

may have overemphasized this point. Knecht has given plots of the diurnal variation of south-pole critical frequencies for each month of the year. Figure 11 of the present paper shows similar plots for Little America and Cape Hallett from January to June. The 19 UT peak of the western stations does fade rapidly in May; nevertheless these plots, and similar plots for other stations, including Halley Bay, form a progressive seasonal sequence.

At western stations (Little America, Fig. 11) in summer minor peaks occur near 07 and 19 UT, linked by an appreciable saddle on the 07–19 UT side and a shallow saddle or plateau on the 19–07 UT side. In equinox both saddles deepen, leaving two distinct peaks near 07 and 19 UT. In winter the 19 UT peak falls away, leaving a single peak near 07 UT. The reverse transition occurs from winter to summer. At eastern stations (Cape Hallett, Fig. 11) the behavior is similar but the 19 UT peak is absent. Its place is taken by a less pronounced peak 4 or 5 hours later, sometime between 19 and 24 UT. Little America and Cape Hallett are geographically close together (Fig. 1); the change from western to eastern behavior occurs abruptly. Perhaps this was better shown in Figure 7, where the difference between the behavior of Scott Base and Little America, stations even closer together, is marked.

At all western stations the equinoctial peak near 19 UT is most pronounced not in March and September but in April and September. At Port Lockroy in April 1958 critical frequences slightly exceeded those of September. At all other stations higher median critical frequencies are found in September than in any other month.

Diurnal Variation of Arctic f_0F_2

Winter. Figure 12 shows the diurnal variation of winter f_0F_2 at six arctic stations. We have combined December 1957 and December 1958 data. All stations show a peak near 20 UT. In the western hemisphere 20 UT coincides with local afternoon, but we have chosen western stations at latitudes of, or higher than, 80°N, and here sunlight cannot be important; Byrd (Fig. 2) and Tikhaya (Fig. 12) at similar latitudes show trivial winter noon peaks. The evidence is not strong, but we associate the maximum of F-region electron densities at 20 UT in northern Canada with the maximum at the same universal time in Siberia, and tentatively conclude that in the Arctic, as in the Antarctic, electron densities reach peak values at a fixed universal time.

Equinox. The Arctic experiences nothing like the great enhancement, or the large daily variation, of the antarctic equinoctial F region. In the Arctic electron densities vary from 5 to 7 Mc/s in the course of a day and at most stations are greatest at some time in the local afternoon. Nevertheless, vestiges of universal-time control can be found. As in the Antarctic this seems stronger in April than in March, and so we use

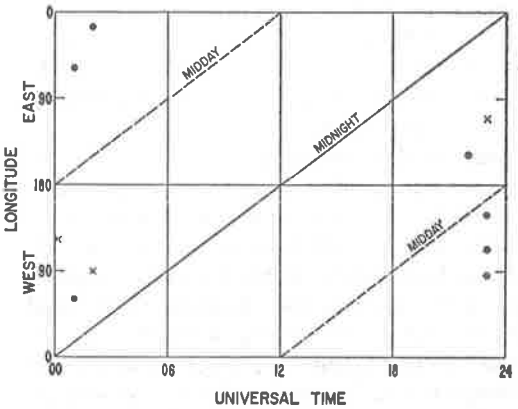

Fig. 13. Universal time of diurnal minimum of arctic f_0F_2 during equinox plotted against geographic longitude. Dots: Fletcher's Ice Is., Arctic 6 Ice Is., Arctic 7 Ice Is., Tikhaya, Eureka, Alert, Svalbard, all April 1958. Crosses: Ice Islands, September 1958.

April 1958 in Figure 13 to represent spring. Figure 13 shows the universal time of minimum f_0F_2 at the seven stations above a latitude of 78°N (dots). In autumn universal-time control is even weaker, but it is still apparent at the high latitudes of the ice islands, and, as by this time these have drifted and become effectively new stations, we also show September 1958 points for them (crosses). At all, effectively ten, stations minimum f_0F_2 occurs within 2 hours of 00 UT. At some stations this is close to local midnight; at others, local midday.

Figure 13 looks convincing, but nevertheless universal-time control is weak in the Arctic during equinox. In Figure 13 we have restricted ourselves to latitudes greater than 78°N, have chosen the most favorable month, April, and have studied only one aspect of the daily variation, the time of minimum f_0F_2. In the Antarctic universal-time control extends to lower latitudes, is found during all months of the year, and during equinox affects the whole pattern of the daily variation.

Summer. Arctic *F*-region electron densities in summer remain almost constant throughout the day [*Coroniti and Penndorf*, 1959]. We have been unable to demonstrate any universal-time control during this season.

5. Some Speculations

Though most noticeable in winter, the maximum of antarctic *F*-region electron density near 07 UT is found in all seasons. Knecht's harmonic analyses imply its presence at the south pole, contributing to either the 24-hour or 12-hour harmonic, in each of the 20 months he studied. An analogous 20 UT peak occurs in the winter arctic *F* region.

Some of the evidence presented suggests that the orientation of the geomagnetic field with respect to the sun is involved. In both hemispheres f_0F_2 reaches a maximum close to the time of local midday at the respective geomagnetic pole. The daily universal-time variation of f_0F_2 is stronger in the Antarctic than in the Arctic; during summer it is absent in the Arctic. Perhaps this is because, on the evidence of the eccentric dipole approximation, the separation of the geomagnetic and geographic poles, and hence the daily universal-time variation of the orientation of the geomagnetic pole with respect to the sun, is greater in the Antarctic than in the Arctic. We might expect the daily transport of the eccentric geomagnetic field through the interplanetary plasma to cause a tide in the geomagnetic field; such an oscillation could cause trapped particles to be dumped into the *F* region.

Though detectable in summer, the peak of antarctic f_0F_2 at 19 UT is enormously greater for a brief period near the equinoxes. Perhaps it is related to the well-known maxima of auroral, blackout, and other corpuscular activity near the equinoxes.

The 19 UT peak occurs only in sunlight. Though not the prime cause, sunlight enhances polar-cap radio-wave absorption too; corpuscular bombardment produces the greatest absorption when it occurs during the day [*Bailey*, 1959; *Hultqvist and Ortner*, 1959]. It is believed that the bombardment produces electrons in the *D* region, and sunlight prevents their subsequent loss by attachment. Attachment is negligible in the *F* region, but *Donahue and Hushfar* [1960] (also *Donahue* [1961]) have predicted that other processes will be important. The charge exchange reactions

$$p + O \rightarrow H + O^+$$

$$H + O \rightarrow p + O^-$$

and others involving molecular oxygen have large cross sections. An incoming proton will thus change back and forth from proton to neutral hydrogen and will leave a trail of positive and negative oxygen ions behind it. The formation of negative ions by proton bombardment and the subsequent detachment of electrons from the negative ions could explain the observed increases of antarctic *F*-region electron densities at 19 UT in the sunlit western hemisphere.

Acknowledgments. My work has been supported at the Boulder World Data Center by a grant from the U. S. National Academy of Sciences, and I have had the use of facilities at both the High Altitude Observatory and the National Bureau of Standards. A study of the antarctic *F* region was suggested by J. W. Wright. C. S. Warwick, T. N. Gautier, and D. K. Bailey read the typescript and made many corrections and suggestions. To all these people I am geatly indebted.

References

Bailey, D. K., Abnormal ionization in the lower ionosphere associated with cosmic ray flux enhancements, *Proc., IRE, 47*, 255–266, 1959.

Bartels, J., *Ann. Meteorol., 1,* 106–127, 1948.
Bellchambers, W. H., and W. R. Piggott, Ionospheric measurements made at Halley Bay, *Nature, 182,* 1596–1597, 1958.
Coroniti, S. C., and R. Penndorf, The diurnal and annual variations of f_0F_2 over the polar regions, *J. Geophys. Research, 64,* 5–18, 1959.
Donahue, T. M., A note on polar blackouts, *J. Atmospheric and Terrest. Phys., 20,* 76–79, 1961.
Donahue, T. M., and F. Hushfar, Detection of negative ions formed by charge transfer, *Nature, 186,* 1038–1039, 1960.
Hultqvist, B., and J. Ortner, Strongly absorbing layers below 50 km., *Planetary and Space Sci., 1,* 193–204, 1959.
Knecht, R. W., Observations of the ionosphere over the south geographic pole, *J. Geophys. Research, 64,* 1243–1250, 1959.
Rastogi, R. G., Abnormal features of the F_2 region at some southern high latitude stations, *J. Geophys. Research, 65,* 585–592, 1960.

(Manuscript received February 28, 1962.)

Reprinted from the
AUSTRALIAN JOURNAL OF PHYSICS
VOLUME 9, NUMBER 1, PAGES 112-132, 1956

LUNAR VARIATIONS IN THE IONOSPHERE

By R. A. DUNCAN

Reprinted from the Australian Journal of Physics, Volume 9, Number 1, pp. 112–132, 1956

LUNAR VARIATIONS IN THE IONOSPHERE

By R. A. DUNCAN*

[*Manuscript received October* 20, 1955]

Summary

The global pattern of the observed lunar variations of the height and electron density of the F_2 region is briefly summarized, new analyses being presented for Canberra (f_0F_2), Brisbane ($h'F_2$), and Washington (h' and f_0F_2). It is concluded that the height variation has an amplitude of from 1 to 3 km and a phase giving maximum height at 06 lunar hours at moderate latitudes and at 09 lunar hours at the geomagnetic equator. The critical frequency variation has an amplitude of from 2 to 4 per cent., maximum critical frequency occurring at about 09 lunar hours at moderate geomagnetic latitudes and 04 lunar hours at equatorial geomagnetic latitudes.

A theory of lunar ionospheric variations is then presented. The current system which Chapman has shown could be responsible for the observed lunar geomagnetic field variations is taken as a starting point: it is considered that this current must flow at a height of about 100 km. The tidal winds needed to drive the current, the potential distribution which will be set up in the dynamo layer, and the resulting periodic vertical drifts of ionization in the higher layers are calculated. It is shown that the divergence of drift velocity is too small to account for the lunar variations in f_0F_2. These are calculated taking into account the probable height variations of recombination coefficient and ionization production rate.

The conclusions thus reached are in good agreement with the observed variations in the F_2. It is concluded that the amplitude of the lunar tidal wind near the E layer is about 45 times greater than that observed on the ground.

I. INTRODUCTION

In recent years periodic atmospheric phenomena have been intensively studied. These phenomena include variations, in both solar and lunar time, of barometric pressure, of geomagnetic field, and of the maximum electron density in the ionosphere; and the horizontal and vertical movements of electron density peaks. The lunar variations can be safely ascribed to a single cause, the Moon's gravitational field, and in this paper an attempt will be made to relate ionospheric phenomena of lunar periodicity to this field.

In 1882 Balfour Stewart suggested that the daily magnetic variations were due to electric currents generated in the upper atmosphere by the daily convective movement of ionized air across the Earth's magnetic field. Subsequently Schuster (1908) and Chapman (1919) developed this "dynamo" theory quantitatively. Two unknowns were in the theory: the tidal velocity and the conductivity in the upper atmosphere.

* Radio Research Board, C.S.I.R.O., Electrical Engineering Department, University of Sydney.

From the study of barometric pressure oscillations, the lunar atmospheric tidal movements on the ground are fairly well understood, but there is no direct information about the corresponding movements in the upper atmosphere. The early workers, Laplace and Lamb, considering perfect isothermal and adiabatic atmospheres respectively, concluded that the tidal velocity at higher levels would be the same as at the ground, which is much too small for the purposes of the dynamo theory ; however, Pekeris (1937) showed that for other cases it was usual for the amplitude to increase with height. From a study of the vertical oscillation of the E layer, Martyn (1947) concluded that the amplification was probably about 200. A new estimate of the tidal velocity in the dynamo layer will be made in this paper.

Pedersen (1927) pointed out that the Earth's magnetic field impedes the movement of ions across it, and for this reason it has been difficult to find enough conductivity to account for the observed magnetic variations. However, Martyn (1948*b*) suggested that because of Hall current and consequent polarization the conductivity would not be as low as Pedersen had suggested, and later Baker and Martyn (1952, 1953) and, independently, Hirono (1950) and Fejer (1953) studied the problem of the conductivity of a thin layer of ionization in a magnetic field in detail and showed that, because of the form of the global wind pattern and the consequent inhibition of Hall current, vertical and horizontal polarization fields are set up, which increase the effective conductivity to about six times the Pedersen value over most of the Earth and to even higher values in a narrow strip over the geomagnetic equator. This removed the last objection to the dynamo theory.

The oscillations of height and ion density of the ionospheric layers remained to be explained. Martyn (1947) pointed out that these could hardly be attributed to the simple rising and falling of isobaric surfaces, and he suggested that they were due to electrodynamical interaction of the dynamo current with the geomagnetic field.

The revised dynamo theory of Baker and Martyn enables us to say with some certainty that the day-time dynamo layer is near the E region and to calculate the global distribution of electrical potential, which differs radically from that given by the Schuster theory. We shall here bring forward experimental evidence that notable lunar variations in ionospheric layer heights and electron densities occur chiefly in the day-time, when the E layer is present. These facts permit the presentation of a consistent explanation of lunar variations.

We first describe the observed ionospheric lunar variations. Then, taking the current system which Chapman has shown to be consistent with the observed lunar geomagnetic field variations, we calculate the necessary tidal winds, the potential field set up in the dynamo layer, and the periodic movements of ionization and changes in ion density which this field will produce in higher layers. The conclusions thus reached are reconciled with all available measurements of movements and electron density changes in the F_2 region of the ionosphere.

II. The Observed Lunar Variations of Electron Density and Height of the F_2 Region

Martyn (1947, 1948*a*), Appleton and Beynon (1948), Burkard (1948), and Matsushita (1949) have shown that the main lunar periodicity of F_2 electron density and height is semi-diurnal. Maximum heights generally occur at 06 lunar hours at moderate latitudes and at 08 lunar hours above the geomagnetic equator (Table 1), the only serious exceptions to this rule being Ottawa and Watheroo, where the tidal amplitudes are small and the phase determinations therefore not so reliable. Maximum electron densities occur 3–4 hr after maximum height at moderate latitudes, and about 4 hr before maximum height at Huancayo.

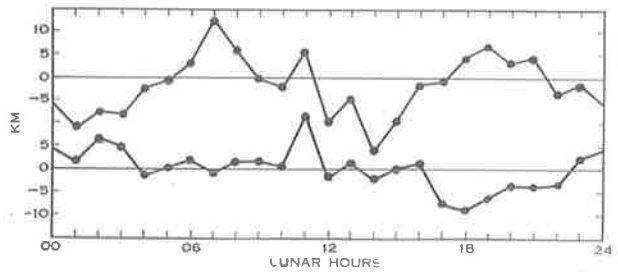

Fig. 1.—The lunar variation of $h^{\max.}F_2$ at 13 (top) and 01 (bottom) solar hours. Huancayo 1942–43–44.

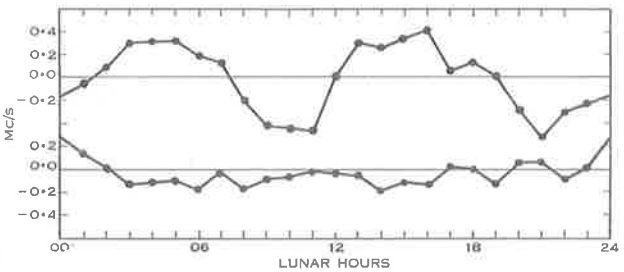

Fig. 2.—The lunar variation of f_0F_2 at 11 (top) and 23 (bottom) solar hours. Huancayo 1942–43–44.

Analyses made by the Radio Research Board, which will be published in detail later, show that large lunar semi-diurnal variations of $h^{\max.}$ and f_0F_2 occur above Huancayo only during the day (Figs. 1 and 2), and above Canberra only during the late afternoon and evening and for a very brief period at dawn.

III. The Theory of Lunar Ionospheric Variations

(*a*) *The Lunar Dynamo Current*

Chapman and Bartels (1940) have calculated the form and magnitude of the currents which must flow in the ionosphere if the observed lunar geomagnetic variations are to be explained in this manner. Figure 3 shows the current at new moon during the equinox ; a similar current system centred near solar noon

TABLE 1

HARMONIC COEFFICIENTS, P_2 AND t_2, OF THE SEMI-DIURNAL LUNAR VARIATIONS OF F_2 REGION DATA

n is the number of months' data examined. Martyn's computations have been re-checked using slightly more accurate procedures, and differences, mostly trivial, will be found between the old values and those given here. Martyn's analyses for f_0F_2 Canberra, $h'F_2$ Brisbane, and f_0 and $h'F_2$ Washington have been extended to cover twice the previous number of months' data

Station	Geomagnetic Latitude	Investigator	$h'F_2$			$h^{max.}F_2$			f_0F_2		
			P_2 (km)	t_2	n	P_2 (km)	t_2	n	P_2 (Mc/s)	t_2	n
Huancayo	− 0·6	Martyn	2·3	9·2	36	5·2	8·4	30	0·14	4·3	48
Cape York	−20·7	Martyn	2·0	6·7	11	2·2	6·3	6	0·12	9·7	10
Kihei	+20·9	Martyn	2·6	7·9	15				0·17	11·4	14
Tokyo	+25·5	Matsushita	3·0	6·6	13						
Durbanville	−32·6	Martyn							0·05	11·6	8
Brisbane	−35·7	Martyn	1·3	6·4	82	2·0	6·0	33	0·08	9·3	31
Watheroo	−41·7	Martyn	0·3	5·9	85	0·6	8·0	73	0·03	9·9	112
Canberra	−44·0	Martyn	1·6	5·6	48	1·7	5·6	36	0·06	9·0	72
Christchurch	−48·0	Martyn	0·8	5·2	28				0·05	8·5	28
Washington	+50·3	Martyn	1·4	5·8	77				0·04	10·2	77
Washington	+50·3	Burkard							0·09	11·0	12
Hobart	−51·6	Martyn	2·0	4·6	10	1·1	5·6	9	0·04	9·3	10
Slough	+54·3	Appleton & Beynon				2·0	6·0		0·05	11·0	12
Ottawa	+56·9	Martyn	0·6	3·0	24				0·01	11·2	30
Burghead	+59·4	Martyn							0·02	8·3	48

in each case flows at first quarter, full moon, and last quarter. At intermediate lunar ages, there is slight distortion of this picture, the day-night boundary cutting across the current loops. As a result of more recent geomagnetic analyses, it is known that an anomalously large current of about twice the intensity shown in Figure 3 flows above the geomagnetic equator.

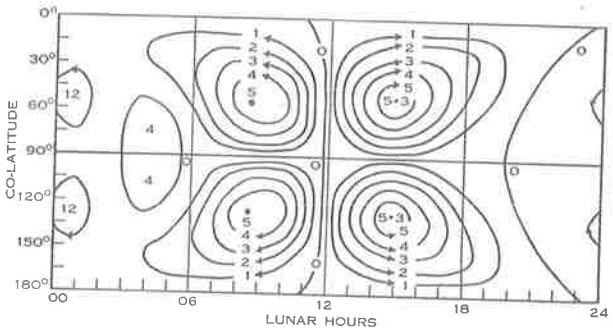

Fig. 3.—The system of ionospheric currents which could cause the lunar geomagnetic variations observed at new moon during the equinoxes. Contours 1000 A apart (after Bartels).

If we ignore the difference between the day and night intensities and the equatorial anomaly, the current system of Figure 3 is well described by the function:

$$R=2\cdot 60J \sin^2\theta \cos\theta \sin 2\varphi \text{ e.m.u.,} \quad \ldots\ldots\ldots (1)$$

$$j_\theta=\frac{\partial R}{r\sin\theta\partial\varphi},\ j_\varphi=-\frac{\partial R}{r\partial\theta},$$

where θ is the co-latitude.

φ is the longitude measured from the Moon,
r is the radius of the Earth,
j_θ is the southward current density,
j_φ is the eastward current density.

This function represents a current system with vortex centres at $\varphi=45°\pm m90°$ and $\theta=54\cdot 7°$ and $125\cdot 3°$, and with a circulation per vortex of J. A clockwise vortex with a day-time circulation of 500 e.m.u. flows in the first octant (Fig. 3) so that J has a day-time value of -500. We shall take the equatorial eastward current j_e to be double that given by (1), so that

$$j_e=(5\cdot 20/r)J \sin 2\varphi. \quad \ldots\ldots\ldots\ldots\ldots (2)$$

The E region must carry the substantial part of this current during the day and early evening, and, as detectable lunar variations in the F_2 are almost entirely confined to these hours, we shall not concern ourselves with the problem of the height distribution of the relatively small night-time dynamo currents.

(*b*) *Lunar Tidal Winds in the Dynamo Layer*

Barometric observations show a lunar pressure variation (p) on the ground of the form

$$p = \sin^3\theta \cos 2\varphi. \quad \ldots\ldots\ldots\ldots\ldots\ldots \quad (3)$$

Fejer (1953) was the first to point out that the Earth's rotation enhances the electromotive effect of the tidal winds, as Coriolis deflection induces east-west air motion, i.e. air motion normal to the geomagnetic field, at higher latitudes. Taking account of the Earth's rotation, then, southward and eastward wind components

$$\left.\begin{aligned} v_\theta &= -\cos\theta \sin 2\varphi, \\ v_\varphi &= -(1 - 0{\cdot}59 \sin^2\theta) \cos 2\varphi \end{aligned}\right\} \quad \ldots\ldots\ldots \quad (4)$$

may be expected (Gold 1910). We are free to choose a suitable phase and amplitude for these winds in the dynamo layer.

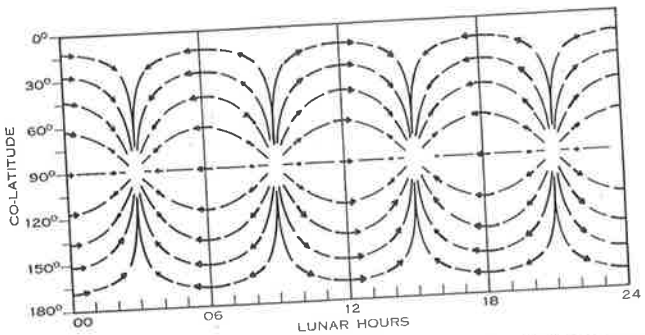

Fig. 4.—The global distribution of the lunar gravitational tidal winds in the dynamo region. An arrow one division long represents a velocity of 100 cm/sec.

Although the conduction of the ionosphere depends on the formation of Hall polarization, Baker and Martyn have shown that the dynamo current at high latitudes is parallel to the dynamo electromotive force, and maximum eastward wind must therefore occur at the time of maximum poleward current, that is at 00 and 12 lunar hours. The phase of the winds in the E layer must therefore be opposite to that on the ground with components of the form

$$\left.\begin{aligned} v_\theta &= v_{\max.} \cos\theta \sin 2\varphi, \\ v_\varphi &= v_{\max.} (1 - 0{\cdot}59 \sin^2\theta) \cos 2\varphi. \end{aligned}\right\} \quad \ldots\ldots\ldots \quad (5)$$

The wind velocities may be estimated by equating the dynamo electromotive force to the ohmic potential drop around a circuit which runs along the meridian $\varphi = 0$ from the equator to the pole, back to the equator along the meridian $\varphi = \frac{1}{2}\pi$, and then along the equator to the starting point: this corresponds very closely to the circuit of maximum dynamo voltages and currents. The dynamo field E_θ along the meridians is

$$E_\theta = H_r v_\varphi, \quad \ldots\ldots\ldots\ldots\ldots\ldots \quad (6)$$

where H_r, the vertical component of the geomagnetic field, equals $-0\cdot622\cos\theta$. No dynamo field is generated along the equator and the total e.m.f. around the circuit is therefore

$$\text{e.m.f.} = 2\int_0^{\frac{1}{2}\pi} -0\cdot622\cos\theta\, v_{\max.}\,(1-0\cdot59\sin^2\theta) r\,d\theta$$
$$= 1\cdot00 r v_{\max.}. \qquad \ldots\ldots\ldots\ldots\ldots\ldots\ldots\ldots\ldots\ldots \quad (7)$$

We shall accept Martyn and Baker's value of $3\cdot5\times10^{-8}$ e.m.u. for the conductivity in the non-equatorial region so that the ohmic drop along the meridians is

$$\frac{2}{3\cdot5\times10^{-8}}\int_0^{\frac{1}{2}\pi} j_\theta r\,d\theta,$$

i.e. from (1), equal to $(1\cdot49\times10^8)J$. Along the equator the conductivity is $1\cdot64\times10^{-7}$, so that from (2) the potential drop is

$$\frac{5\cdot20J}{r(1\cdot64\times10^{-7})}\int_{\frac{1}{2}\pi}^{0} r\sin 2\varphi\,d\varphi = (1\cdot58\times10^7)J.$$

Hence the total potential drop around the circuit is

$$1\cdot65\times10^8 J. \qquad \ldots\ldots\ldots\ldots\ldots\ldots\ldots\ldots \quad (8)$$

Equating (7) and (8), we find

$$v_{\max.} = 130 \text{ cm/sec.} \qquad \ldots\ldots\ldots\ldots\ldots\ldots\ldots \quad (9)$$

This is about 45 times as great as the lunar tidal wind observed on the ground. The E region winds are shown in Figure 4.

(c) Polarization and Electric Fields in the Ionosphere

The E-layer dynamo current will induce polarization, the horizontal distribution of which can be most easily described by dividing it into two parts, an equatorial Schuster polarization and a Hall polarization at the centre of each current loop.

The intensity of this polarization is independent of the diurnal variations of conductivity, as the dynamo current is proportional to the ion density and the induced polarization is proportional to this current divided by the ion density. We may therefore use noon values of current and conductivity in our computations without loss of generality.

The latitude variation of conductivity arising from the variation of solar zenith angle and magnetic dip is important. Although a more precise investigation is by no means intractable, we shall adopt the simplified picture of Baker and Martyn (1953): a region lying within 7° of the geomagnetic equator is taken to have a height integrated direct east-west noon conductivity $\Sigma_y = 1\cdot64\times10^{-7}$ e.m.u. Above the rest of the Earth, a direct conductivity $\Sigma_1 = 6\cdot4\times10^{-9}$ e.m.u., a Hall conductivity $\Sigma_2 = +1\cdot36\times10^{-8}$ e.m.u. in the northern and $-1\cdot36\times10^{-8}$ e.m.u. in the southern hemisphere, and an effective

conductivity $\Sigma_3=\Sigma_1+\Sigma_2^2/\Sigma_1=3\cdot5\times10^{-8}$ e.m.u. will be assumed. The meaning of these four conductivities has already been described by Baker and Martyn and will be clear from the context.

The dynamo electromotive forces (Fig. 5) do not form closed circuits but converge on, or diverge from, four points spaced around the equator so causing "Schuster" polarization, the geographical distribution of which may be described approximately by the expression

$$V_s=V_s^{\max.}\sin^2\theta\cos 2\varphi. \quad \ldots\ldots\ldots\ldots \quad (10)$$

It is this polarization which closes the current loops by producing flow along the equatorial parallels of latitude so that

$$j_e=E_\varphi\Sigma_y, \quad \ldots\ldots\ldots\ldots\ldots\ldots \quad (11)$$

where E_φ, the eastward field, equals

$$-\frac{\partial V_s}{r\sin\theta\partial\varphi}=2V_s^{\max.}\frac{\sin\theta}{r}\sin 2\varphi.$$

Therefore, from (2)

$$\frac{5\cdot20J}{r}=\frac{2V_s^{\max.}\Sigma_y}{r}, \quad \ldots\ldots\ldots\ldots\ldots \quad (12)$$

i.e. $V_s^{\max.}=-79\cdot3\times10^8$ e.m.u. and the extreme potentials due to horizontal polarization above the geomagnetic equator are ±80 V.

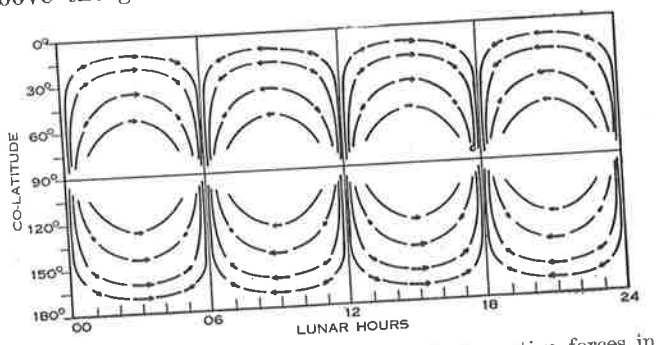

Fig. 5.—The global distribution of the electromotive forces in the dynamo region. An arrow one division long represents an electromotive field of 100 mV/km.

Because the ionosphere has a Hall conductivity, initially a component of current will flow at right angles to the dynamo electromotive forces, but as such currents all converge (or diverge) from the vortex centres, they will be rapidly countered by the accumulation of Hall polarization. As is explained in Baker and Martyn's papers, this Hall polarization then causes its own Hall current to flow around the current loop, augmenting the dynamo current and raising the effective conductivity from Σ_1 to $\Sigma_1+\Sigma_2^2/\Sigma_1$. Of the observed non-equatorial current, therefore, a part proportional to Σ_1 is due directly to the dynamo voltages, but the major part, proportional to Σ_2^2/Σ_1 (and thus a

fraction $\Sigma_2^2/(\Sigma_1^2+\Sigma_2^2)=0\cdot83$ of the whole) is caused indirectly by the Hall polarization. The Hall current function R_H is therefore from (1)

$$\left.\begin{aligned} R_H &= 0\cdot83R, \\ j_{H,\theta} &= 0\cdot83\frac{\partial R}{r\sin\theta\partial\varphi}, \\ j_{H,\varphi} &= -0\cdot83\frac{\partial R}{r\partial\theta}. \end{aligned}\right\} \quad \ldots\ldots\ldots\ldots (13)$$

This current is related to the Hall field E_H and polarization potential V_H by the relations

$$\left.\begin{aligned} j_{H,\theta} &= \Sigma_2 E_{H,\varphi} = -\Sigma_2\frac{\partial V_H}{r\sin\theta\partial\varphi}, \\ j_{H,\varphi} &= -\Sigma_2 E_{H,\theta} = +\Sigma_2\frac{\partial V_H}{r\partial\theta}. \end{aligned}\right\} \quad \ldots\ldots (14)$$

Hence V_H varies in the same manner as R, that is,

$$V_H = 2\cdot60\,V_H^{\max.}\sin^2\theta\cos\theta\sin 2\varphi, \quad \ldots\ldots (15)$$

$$V_H^{\max.} = \frac{-0\cdot83J}{\Sigma_2} = \pm3\cdot05\times10^{10} \quad \ldots\ldots\ldots (16)$$

in the northern and southern hemispheres respectively.

The complete expression for the global distribution of polarization potential V in the dynamo layer is therefore

$$V=[\pm300\times2\cdot60\sin^2\theta\cos\theta\sin2\varphi-80\sin^2\theta\cos2\varphi]\times10^8 \text{ e.m.u.}$$

This is shown in Figure 6. $\ldots\ldots\ldots\ldots\ldots (17)$

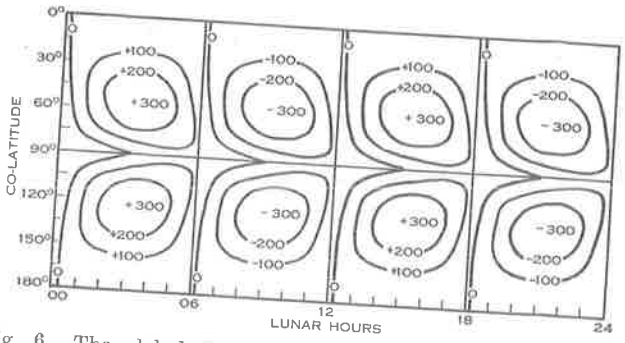

Fig. 6.—The global distribution of horizontal polarization in the dynamo region. Contours 100 V apart.

The polarization of the E region will be communicated to the higher levels along the highly conducting and thus equipotential geomagnetic field lines. Hence, generally,

$$V=[\pm780\sin^2\theta_E\cos\theta_E\sin2\varphi-80\sin^2\theta_E\cos2\varphi]\times10^8, \quad \ldots\ldots (18)$$

where θ_E is the co-latitude at which the region connects via the geomagnetic field lines with the dynamo layer. From the properties of the geomagnetic field

$$\sin^2\theta_E=(r_E/r)\sin^2\theta, \quad \ldots\ldots\ldots\ldots\ldots (19)$$

so that the potential function for the complete ionosphere is

$$V=[\pm 780(r_e/r)\sin^2\theta\sqrt{\{1-(r_E/r)\sin^2\theta\}}\sin 2\varphi-80(r_E/r)\sin^2\theta\cos 2\varphi]\times 10^8,$$
$$V\simeq[\pm 780\sin^2\theta\sqrt{\{1-(r_E/r)\sin^2\theta\}}\sin 2\varphi-80\sin^2\theta\cos 2\varphi]\times 10^8. \ldots (20)$$

In the E region the total electric field will be the sum of the electromotive and electrostatic fields, but due to the greatly decreased pressure at higher levels, which will entail a much greater reduction of gravitational tidal power per unit volume than of viscous and electrodynamic damping, it is likely that in the F region gravitational tidal winds are negligible and that the electrostatic field is the only one which need be considered. There will be horizontal air movements in the F_2 due to the interaction of the electric currents produced by the electrostatic field and the geomagnetic field, but, as Baker and Martyn (1953) have shown, the e.m.f.'s developed by these will be back e.m.f.'s and will merely reduce the effective electric field. This effect will be discussed later.

(*d*) *Vertical Drift of Ionization in the* F_2 *Region*

Martyn has shown that, because of the geomagnetic field, an electric field in the ionosphere produces a drift of neutral ionization. This drift is the same as that given by Ampere's law ; an eastward current being associated with an upward drift of ionization.

A discussion of ion drift in the E region is difficult because of the very rapid change with height, in this region, of the conductivity per ion pair ; we shall confine ourselves to the very much simpler problem of ion drift in the F_2 region. Here there is no Hall current so that an eastward field will cause an eastward current. Martyn (1953) has derived the relation

$$v_r=\frac{E_\varphi}{H}\cos\psi \quad \ldots\ldots\ldots\ldots\ldots (21)$$

for the upward drift velocity (v_r), where E_φ is the eastward electric field, H the geomagnetic field intensity, and ψ the geomagnetic dip angle.

As has been pointed out (Baker and Martyn 1953), this relation will need modification if the air is set in motion by the drifting ionization. A rough measure of the time which air will take to acquire the velocity of ionization drifting through it is given by $t=\rho/(\sigma H^2)$, where ρ is the air density and σ the conductivity. If we evaluate this for the F_2 region we find that t is of the order of an hour ; independent of the air pressure. Hence some air motion probably occurs. However, vertical air drift will be prevented by the Earth's gravitational field and even horizontal motion will be affected by a redistribution of air pressure because the horizontal component of the ion drift has appreciable divergence. Air motion is therefore probably a second order effect, but it should be remembered that it will reduce the vertical ion drift to some extent, particularly at high latitudes.

Going back to equation (**21**), we have from the properties of the geomagnetic field

$$\frac{\cos\psi}{H}=\frac{\sin\theta}{0\cdot311(1+3\cos^2\theta)},$$

also,

$$E_\varphi=-\frac{\partial V}{r\sin\theta\partial\varphi},$$

so that

$$v_r=-\frac{\partial V}{0\cdot311r(1+3\cos^2\theta)\partial\varphi}. \quad \ldots\ldots\ldots (22)$$

From (**20**), then

$$v_r=80\cdot3\frac{\sin^2\theta\sqrt{(94\cdot5\cos^2\theta_E+1)}}{1+3\cos^2\theta}\left[\cos\left(2\varphi-\arctan\frac{-1}{-9\cdot75\cos\theta_E}\right)\right]. \quad \ldots\ldots\ldots\ldots\ldots (23)$$

Hence maximum upward drift velocity should occur at 06 lunar hours over most of the Earth. The theoretical variation of the amplitude of the drift

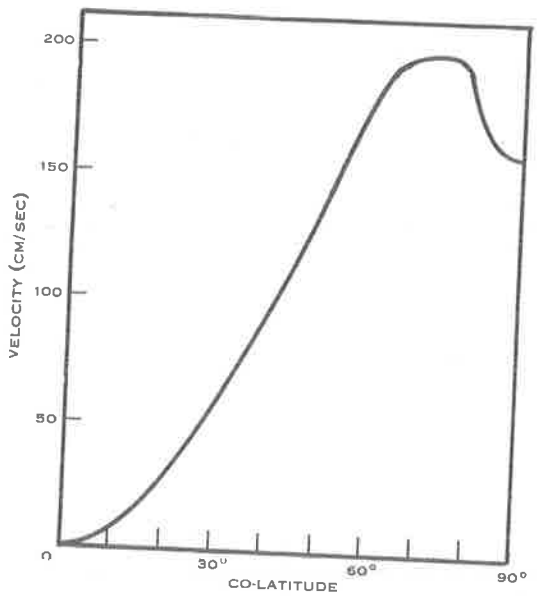

Fig. 7.—The variation with co-latitude of the vertical lunar drift velocity at 300 km.

with latitude is shown in Figure 7. Above the geomagnetic equator the time of greatest upward drift depends on the height, being 09 hours in the dynamo region (100 km), 07 hours at 300 km, and approaching 06 lunar hours at very great heights.

(*e*) *Lunar Periodicity in the Height of the* F *Region*

Integration of equation (**23**) shows that if the *F* region were translated up and down by the drift it would oscillate through about 12 km, maximum

height being reached 3 hr after the time of greatest upward velocity. However, this large movement does not occur because the limited life of electrons (about an hour in the day-time F_2 region) prevents them from being shifted very far from the height at which they are produced. Even at night diffusion and the height gradient of the recombination coefficient tend to stabilize the height of the F_2 layer: if the layer is shifted upwards it tends to diffuse down again: if the layer is shifted downwards the accelerated decay of the lower edge will tend to restore it to its original height. Vertical drift, therefore, will perturb the height of an ionospheric layer rather than shift it bodily.

Suppose that we have in an ionospheric region, ionization, recombination, and a redistribution of electrons by a solar tide. The equation of continuity of the electron density is

$$\frac{\partial N}{\partial t}=I-\alpha N^2-v_r\frac{\partial N}{\partial h}-N\frac{\partial v_r}{\partial h}, \quad \ldots\ldots\ldots\ldots (24)$$

where N is the electron density, t is time, I is the rate of ionization, α is the recombination coefficient, v_r is the velocity of vertical drift, and h is height. In time the electron density will approach a value N_e such that $\partial N_e/\partial t=0$. If the electron density is perturbed from this value by an amount n so that $N=N_e+n$, and the perturbing cause then removed, the equation of continuity becomes

$$\frac{\partial n}{\partial t}=-2\alpha N_e n-n\frac{\partial v_r}{\partial h}-v_r\frac{\partial n}{\partial h}.$$

The only term on the right of this equation which represents a tendency for the perturbation to decay is the first, $-2\alpha N_e n$, the other two terms merely show that the electron density perturbation is redistributed by the solar tide. The electron density perturbation n decays, then, according to the law

$$\partial n/\partial t=-2\alpha N_e n,$$

or

$$n=\exp(-2\alpha N_e t), \quad \ldots\ldots\ldots\ldots (25)$$

so that $\tau=1/2\alpha N$ may be taken as the "relaxation time" of the ionosphere.

If this relaxation time is much shorter than 3 hr, we should expect an ionospheric layer to be displaced a distance $\Delta h=v_r\tau$ by a vertical drift v_r. Of all time intervals τ, that beginning $\frac{1}{2}\tau$ seconds before and ending $\frac{1}{2}\tau$ seconds after the time of maximum upward drift, covers the period of greatest upward drift, and the electrons should be at their greatest height $\frac{1}{2}\tau$ seconds after the time of maximum upward velocity. The following more rigorous treatment shows this picture to be correct.

If $\mathrm{d}N/\mathrm{d}h$ is the height gradient of the electron density, then in the presence of a uniform vertical drift v_r the equation of continuity becomes

$$\frac{\partial N}{\partial t}=I-\alpha N^2-v_r\frac{\partial N}{\partial h},$$

that is,

$$\frac{\partial N}{\partial t}=-2\alpha N n-v_r\frac{\partial N}{\partial h}, \quad \ldots\ldots\ldots\ldots (26)$$

When the relaxation time is short, the layer will reach a new equilibrium state so that $\partial N/\partial t=0$,
and hence

$$n=v_r\tau\frac{\partial N}{\partial h}. \quad \ldots\ldots\ldots\ldots\ldots\ldots \quad (27)$$

This relation implies that to the first order we can consider the ion density perturbation at a given height to be due to the layer being raised undistorted a distance Δh where

$$\Delta h=v_r\tau. \quad \ldots\ldots\ldots\ldots\ldots\ldots \quad (28)$$

(It should perhaps be pointed out that the electron density perturbation at a given height is deduced in (27) merely as a means of obtaining the height perturbation. It is not the observed quantity, the perturbation of the value of the maximum electron density. The latter will be calculated in the next section.)

It is difficult to obtain reliable estimates of τ in the F_2 but if we accept S. K. Mitra's (1952) values of recombination coefficient, we obtain a midday figure of 4000 sec. From this we should expect a day-time lunar height variation of about 6 km, maximum height occurring at 06 lunar hours at moderate latitudes and 07 lunar hours at the geomagnetic equator. Even larger amplitudes and later phases would be expected at night. However, we shall show that at F_2 heights, and particularly at the height of the night F_2 (300 km) diffusion becomes a process important enough to keep the effective relaxation time of the ionosphere short.

The greatest height at which reasonably reliable rocket measurements of temperature and mean free paths have been made is 200 km (Rocket Panel 1952), and on this evidence the coefficient of diffusion of air (K) at this level is roughly $7\cdot5\times10^8$ cm^2/sec. The diffusion coefficient will increase with height due to the increasing temperature and decreasing pressure. Pressure decreases exponentially with height and will have much the greater influence so we shall write

$$K=(7\cdot5\times10^8)e^{h/H}, \quad \ldots\ldots\ldots\ldots\ldots\ldots \quad (29)$$

where h/H is the reduced height above our 200 km datum level.

Huxley (1952) and others before him have shown that the electrons and positive ions in the ionosphere are held together by electrostatic attraction, the electron-positive ion gas diffusing at twice the rate appropriate to the positive ions alone. For our purposes, it will be sufficiently accurate to assume the coefficient of diffusion of the latter equal to that of neutral molecules, so that the coefficient of diffusion of the electron-positive ion gas (K_i) is

$$K_i=(1\cdot5\times10^9)e^{h/H}. \quad \ldots\ldots\ldots\ldots\ldots\ldots \quad (30)$$

The equation of continuity for the electron-positive ion gas is

$$\frac{\partial N}{\partial t}=\text{div}\left[K_i\frac{\partial N}{\partial h}-WN\right], \quad \ldots\ldots\ldots\ldots\ldots\ldots \quad (31)$$

where W is the drift velocity of the ions under gravity. It may be shown from kinetic theory that

$$W=-\frac{K_i mg}{kT}=-\frac{K_i}{H_i}, \quad \ldots\ldots\ldots\ldots\ldots (32)$$

so that, as is well known, diffusion and gravitational drift are in equilibrium when

$$N=N_0 \exp(-h/H_i), \quad \ldots\ldots\ldots\ldots\ldots (33)$$

where H_i, the scale height for the electron-positive ion gas, will be twice that for the neutral molecules (H).

It is clear, however, that in an ionospheric layer gravitational drift and diffusion will not generally balance one another; indeed, on the under side of the layer, the side observed, they both cause a downward flux of ionization. The total effective velocity of this flux (U) is

$$U=-K_i\frac{\partial N}{N\partial h}+W,$$

or

$$U=-K_i\left(\frac{\partial N}{N\partial h}+\frac{1}{H_i}\right). \quad \ldots\ldots\ldots\ldots\ldots (34)$$

We have not yet considered the effect of the geomagnetic field. Ions can gravitate and diffuse only in the direction of this field. If the dip is ψ the components of ion density gradient and gravitational field in this direction are the corresponding vertical components multiplied by $\sin\psi$. To find the vertical component of velocity we must multiply by $\sin\psi$ once again, so that

$$\left.\begin{aligned} U&=-K_i\left(\frac{\partial N}{N\partial H}+\frac{1}{H_i}\right)\sin^2\psi, \\ \text{that is,}\quad U&=-2K\left(\frac{\partial N}{N\partial h}+\frac{1}{2H}\right)\sin^2\psi. \end{aligned}\right\} \quad \ldots\ldots\ldots (35)$$

At night we may consider the F_2 layer to consist of a relatively thick bank of ionization in the upper region of rapid diffusion and low decay, with a lower boundary whose position is determined by the opposing processes of downward diffusion and gravitational drift on one hand, and the relatively rapid decay of the lower edge on the other. A reasonable value for the scale height of the F_2 region is 30 km. We shall take the semi-thickness of the F_2 to be 60 km so that the mean value of $\partial N/\partial h$ is $N_{\max.}/(6\times10^6)$. The mean value of N may be taken as $\frac{1}{2}N_{\max.}$, so that

$$U=-(1\cdot5\times10^9)\left[\frac{1}{3\times10^6}+\frac{1}{6\times10^6}\right]\sin^2\psi e^{h/H},$$

that is,

$$U=-750\sin^2\psi e^{h/H}, \quad \ldots\ldots\ldots\ldots\ldots (36)$$

and hence

$$\frac{dU}{dh}=-25\times10^{-5}\sin^2\psi e^{h/H}. \quad \ldots\ldots\ldots\ldots\ldots (37)$$

An upward electrodynamic drift (v_r) will push the F_2 layer up until the downward diffusion velocity ($-U$) is increased by an amount equal to v_r. Hence, if in the relation

$$dh=-\frac{10^5}{25}\operatorname{cosec}^2\psi e^{-h/H}dU \quad \ldots\ldots\ldots\ldots\ldots (38)$$

we put $-dU$ equal to the upward drift v_r, dh is the displacement which this drift will cause, that is,

$$\Delta h=\frac{10^5}{25}\operatorname{cosec}^2\psi e^{-h/H}v_r, \quad \ldots\ldots\ldots\ldots\ldots (39)$$

or

$$\Delta h=\frac{10^5}{25}\frac{1+3\cos^2\theta}{4\cos^2\theta}e^{-h/H}v_r. \quad \ldots\ldots\ldots\ldots\ldots (40)$$

The F_2 layer is about two scale heights above the 200 km level. We shall put therefore,

$$h/H=2,$$

and

$$v_r=155 \text{ cm/sec},$$

corresponding to the situation at co-latitude 55°.

This gives $\Delta h=1\cdot26$ km.

This crude argument does not take account of the height gradient of recombination, but it indicates approximately how much diffusion will limit the amplitude of the lunar height variations.

It seems therefore that, at moderate latitudes, the amplitude of both the day and night lunar variation of $h'F_2$ should be about a kilometre, and that maximum h' and $h^{\max.}F_2$ should occur close to the time of maximum upward drift velocity ; 06 lunar hours. Table 1 shows that, at most moderate latitude stations, maximum F_2 heights occur close to 06 lunar hours, and that the amplitude of the variation is from 1 to 3 km, in fair agreement with these arguments.

Above the geomagnetic equator vertical diffusion is inhibited and this will lead to large F_2 height variations. The maximum drift velocity here is 160 cm/sec, so that at midday when the relaxation time is about 4000 sec, a maximum positive height variation of about 6 km should occur close to the time of maximum upward drift ; 07 lunar hours. Towards sunset, when the relaxation time is of the order of hours, even larger amplitudes and a phase of 10 lunar hours can be expected.

Martyn (1947) has shown that the observed variation at Huancayo does in fact exhibit these features.

(f) Lunar Periodicity in the Electron Density of the F_2 *Region*

Periodic drift may result in periodic variations in electron density in two ways :

(i) The drift velocity may have a gradient, resulting in the periodic concentration and rarefaction of the ionosphere.

(ii) The drift may shift the layer to a height where a different ionization and recombination rate prevails.

Let us first consider the effect of drift velocity gradients. The drift velocity $\mathbf{v}$ is given in magnitude and direction by the relation :

$$\mathbf{v}=\frac{1}{H^2}(\mathbf{E}\times\mathbf{H}). \quad \ldots\ldots\ldots\ldots\ldots\ldots\ldots\ldots \quad (41)$$

The divergence of the drift is therefore,

$$\begin{aligned}\text{div } \mathbf{v}&=\nabla.\left[\frac{1}{H^2}(\mathbf{E}\times\mathbf{H})\right]\\&=\frac{1}{H^2}\nabla.(\mathbf{E}\times\mathbf{H})+\nabla\frac{1}{H^2}.(\mathbf{E}\times\mathbf{H})\\&=\frac{1}{H^2}(\text{curl } \mathbf{E}.\mathbf{H}-\mathbf{E}.\text{curl } \mathbf{H})+\left(\text{grad } \frac{1}{H^2}\right).(\mathbf{E}\times\mathbf{H}).\end{aligned}$$

Now the first term is zero as both $\mathbf{E}$ and $\mathbf{H}$ can be derived from scalar potentials so that

$$\text{div } \mathbf{v}=\left(\text{grad } \frac{1}{H^2}\right).(\mathbf{E}\times\mathbf{H}). \quad \ldots\ldots\ldots\ldots\ldots\ldots \quad (42)$$

As both H_φ and $\partial(1/H^2)/\partial\varphi$ are zero, this reduces to

$$\text{div } \mathbf{v}=E_\varphi\left[-\frac{\partial(1/H^2)}{\partial r}H_\theta+\frac{\partial(1/H^2)}{r\partial\theta}H_r\right]. \quad \ldots\ldots\ldots\ldots \quad (43)$$

The geomagnetic field is such that

$$H_r=\frac{2M\cos\theta}{r^3},$$

$$H_\theta=\frac{M\sin\theta}{r^3},$$

$$H^2=\frac{M^2}{r^6}(3\cos^2\theta+1).$$

where M is the Earth's magnetic moment. Hence,

$$\frac{\partial(1/H^2)}{\partial r}=\frac{6r^5}{M^2(3\cos^2\theta+1)},$$

and

$$\frac{\partial(1/H^2)}{r\partial\theta}=\frac{6r^5\cos\theta\sin\theta}{M^2(3\cos^2\theta+1)^2}.$$

Substituting these values in (43) we find that

$$\text{div } \mathbf{v}=-\frac{6r^2\sin\theta(\cos^2\theta+1)}{M(3\cos^2\theta+1)^2}E_\varphi. \quad \ldots\ldots\ldots\ldots \quad (44)$$

It is useful to obtain this expression in terms of the vertical component of drift (v_r). From (21)

$$v_r=-\frac{r^3\sin\theta}{M(3\cos^2\theta+1)}E_\varphi,$$

therefore

$$\text{div } \mathbf{v} = +\frac{6\,(\cos^2\theta+1)}{r\,(3\cos^2\theta+1)}v_r.$$

$(1/N)(\partial N/\partial t) = -\text{div } \mathbf{v}$ and, if the F_2 relaxation time is τ, the critical frequency variation will be

$$\frac{\Delta f_0}{f_0} = -\frac{3(1+\cos^2\theta)}{r(1+3\cos^2\theta)}v_r\tau = -\frac{3(1+\cos^2\theta)}{r(1+3\cos^2\theta)}\Delta h. \quad \ldots\ (45)$$

Thus the critical frequency variation due to drift divergence will be in phase opposition to the height variation.

Martyn (1955) has calculated the vertical gradient of the vertical component of the drift velocity ($\partial v_r/\partial r$) on the assumption that the geomagnetic field intensity is uniform, and he has equated this to $-\partial N/N\partial t$. Clearly, we should

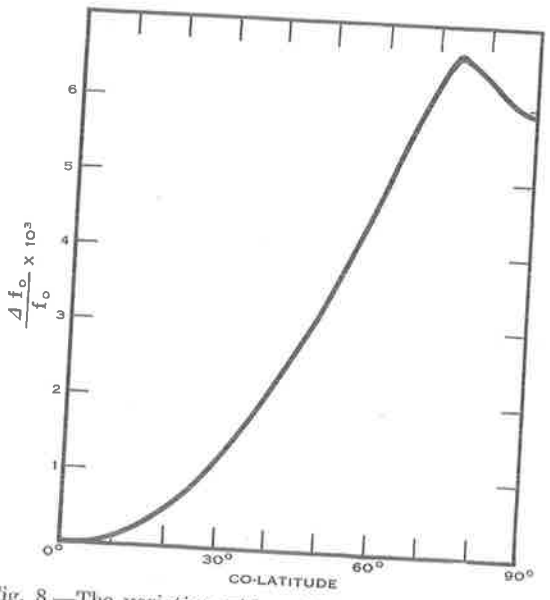

Fig. 8.—The variation with co-latitude of the relative critical frequency changes due to lunar drift velocity divergence at 300 km.

also consider the gradient of the eastward component of drift ($\partial v_\varphi/r \sin\theta\partial\varphi$). The new term is equal and opposite to the old (i.e. $\partial v_r/\partial r = -\partial v_\varphi/r \sin\theta\partial\varphi$) so that the total velocity divergence is zero. The derivation given here [(41)–(45)] shows that this is generally true: the drift divergence due to the electric field gradient is zero because div $(\mathbf{E}\times\mathbf{H})\equiv 0$. The residual velocity divergence is due to the gradient of the geomagnetic field intensity.

The critical frequency variation given by equation (45), for a height of 300 km, τ equal to 4000 sec, and v_r as given in (23), is plotted against geomagnetic latitude in Figure 8. It is seen that a critical frequency variation of about $\frac{1}{2}$ per cent. may result near the geomagnetic equator, but that generally the effect is small.

It seems likely, therefore, that electron density variations at moderate latitudes are principally due to the effect of drift in an ionosphere with a height gradient of electron production and recombination.

Let I be the electron production rate,
α be the recombination coefficient,
N_m be the maximum electron density,
h_m be the height at which this occurs,
$N_{m,0}$ be the maximum electron density which would prevail if there were no drift, and
$h_{m,0}$ be the height at which this would occur, and
$N_{e,0}$ be the equilibrium electron density (i.e. $N_{e,0}=\sqrt{(I_0/\alpha)}$) at the height $h_{m,0}$.

Then let

$$n=N_m-N_{e,0},$$
$$h'=h_m-h_{m,0}.$$

h' is the tidal perturbation of h_m, but n, the perturbation of the maximum electron density, will be due partly to the drift and partly to the natural difference between the actual electron density and the equilibrium value at any time, that is,

$$n=N_m-N_{e,0}=(n_m-N_{m,0})+(N_{m,0}-N_{e,0}).$$

Now,

$$\frac{dN_m}{dt}=I-\alpha N_m^2, \quad \ldots\ldots\ldots\ldots\ldots\ldots\ldots\ldots \quad (46)$$

therefore

$$\frac{dN_{e,0}}{dt}+\frac{dn}{dt}=I_0+\frac{\partial I}{\partial h}h'-\left(\alpha_0+\frac{\partial \alpha}{\partial h}h'\right)(N_{e,0}+n)^2$$

and

$$\frac{dn}{dt}=-\alpha_0(N_m-N_{e,0})n+\frac{\partial}{\partial h}(I-\alpha N_m^2)h'.$$

This relation is precise but to the first order we may write

$$\frac{dn}{dt}=-2\alpha N n+\frac{\partial}{\partial h}(I-\alpha N^2)h',$$

that is,

$$\frac{dn}{dt}=-An+Bh'. \quad \ldots\ldots\ldots\ldots\ldots\ldots\ldots \quad (47)$$

If h' varies sinusoidally semi-diurnally, that is,

$$h'=P_2\cos 2\omega t,$$

where ω is the angular velocity of the Earth, (47) has the solution

$$n=n_0e^{-At}+\frac{BP_2}{\sqrt{(4\omega^2+A^2)}}\cos\left(2\omega t-\arctan\frac{2\omega}{A}\right). \quad \ldots\ldots \quad (48)$$

The first term in this expression shows that the electron density recovers exponentially, with a relaxation time $\tau=1/2\alpha N$, from any initially imposed perturbation n_0.

The second term,

$$n=\frac{BP_2}{\sqrt{(4\omega^2+4\alpha^2N^2)}}\cos\left(2\omega t-\arctan\frac{\omega}{\alpha N}\right). \quad \ldots\ (49)$$

gives the tidal perturbation of the electron density.

Now, as in fact equation (49) implies, because of the intrinsic stability of an ionospheric layer in which ionization and recombination processes are rapid, we should expect appreciable lunar perturbation of the F_2 only during the late afternoon and evening when the relaxation time is reasonably long, yet the E region is still the most highly conducting region of the ionosphere. This is in fact the case at Canberra, as will be shown in a later paper, and it seems reasonable to assume that at all moderate latitude stations the lunar variation extracted from data averaged over all solar hours is dominated by the behaviour at these times.

Recombination is then the dominant process so that we may write

$$B=-\frac{\partial}{\partial h}(\alpha N^2). \quad \ldots\ (50)$$

At the height of the F_2 region at moderate latitudes (250–300 km) the recombination coefficient is proportional to the air density, that is,

$$\alpha=\alpha_0 e^{-h/H},$$

where H is the scale height,

$$B=\frac{\alpha}{H}N^2 \quad \left(\frac{\partial N}{\partial h} \text{ is zero at the density maximum}\right),$$

and

$$n=\frac{\alpha N^2P_2}{H\sqrt{(4\omega^2+4\alpha^2N^2)}}\cos\left(2\omega t-\arctan\frac{\omega}{\alpha N}\right). \quad \ldots\ (51)$$

Now at night the relaxation time $(1/2\alpha N)$ of the ionosphere can be considered infinite, as its value at any time t after sunset is always greater than t. Hence the variation of critical frequency should lag that of height by 3 hr.

We may estimate the amplitude of the critical frequency (f_0) variation from (51)

$$\frac{n}{N}=\frac{\alpha NP_2}{2H\sqrt{(\omega^2+\alpha^2N^2)}},$$

therefore

$$\frac{\Delta f_0}{f_0}=\frac{\alpha NP_2}{2H\sqrt{(\omega^2+\alpha^2N^2)}},$$

where Δf_0 is the total variation of critical frequency, i.e. twice the amplitude of the variation.

Put $\alpha = 3 \times 10^{-10}$ cm^3/sec (Mitra),
$N = 2 \cdot 5 \times 10^5$/cm^3,
$P_2 = 1 \cdot 5 \times 10^5$ cm,
$\omega = 2\pi/(24 \times 3600)$ sec^{-1},
$H = 3 \times 10^6$ cm.

Then

$$\Delta f_0/f_0 = 1 \cdot 8 \times 10^{-2}.$$

Martyn found a variation of about 2 per cent. at Canberra, with maximum critical frequency at 09 lunar hours, in good agreement with these results, and other non-equatorial stations show variations of similar amplitude and phase (Table 1).

The arguments above are not applicable to the F_2 region near the magnetic equator, for here, probably as a result of solar tides (Martyn 1955), the day-time F_2 region occurs at the great height of from 350 to 450 km (Maeda 1955). The recombination coefficient at this height is small and thus the electron relaxation time in the F_2 region near the magnetic equator is of the order of hours during the day when the conductivity of the E region is greatest. Vertical diffusion is inhibited by the geomagnetic field. This will lead to large day-time lunar variations of $h^{\max.}F_2$ and f_0F_2, and we should expect these day-time lunar variations to dominate the variations found in data meaned over all 24 solar hours. Figures 1 and 2 show that this is the case.

There is good evidence that at 300 km electron decay is primarily due to attachment and hence proportional to the pressure, but the rate of electron loss cannot fall indefinitely with height as attachment must ultimately cease to be the most important process of electron loss. At 400 km, then, the effective recombination coefficient has probably fallen to a constant low value.

On the other hand 400 km is well above the height of maximum ion production so that the ionization rate will be practically proportional to the pressure, that is,

$$I = I_0 e^{-h/H}. \quad \ldots\ldots\ldots\ldots\ldots\ldots \quad (52)$$

For day-time equatorial conditions, therefore, $\partial(I - \alpha N^2)/\partial h$ becomes $-I/H$, $\partial N/\partial h$ being zero at the electron density maximum. Substituting this value in (49) we obtain

$$n = -\frac{IP_2}{H\sqrt{(4\omega^2 + 4\alpha^2 N^2)}} \cos\left(2\omega t - \arctan\frac{\omega}{\alpha N}\right),$$

hence

$$\frac{\Delta f_0}{f_0} = \frac{IP_2}{2HN\sqrt{(\omega^2 + \alpha^2 N^2)}}. \quad \ldots\ldots\ldots\ldots\ldots\ldots \quad (53)$$

From this we may estimate the expected phase and amplitude of the Huancayo lunar critical frequency variation.

Put $N=10^6$ cm^{-2}, $\alpha=5\times10^{-11}$ cm^3/sec. Then the relaxation time $(1/2\alpha N)$ equals about 2·8 hr. This is much less than the time for which the sun shines (12 hr) so we should expect the electron density to be approximately equal to the equilibrium value and thus

$$I\simeq\alpha N^2=50 \text{ cm}^{-3}\text{sec}^{-1},$$

also, $P_2=5\times10^5$ cm, $H=3\times10^6$ cm, and $\omega=2\pi/(24/3600)$ sec^{-1}.

Substituting these values in (**53**) gives arctan $\omega/\alpha N$ equal to 55°, i.e. 1·9 hr, and $\Delta f_0/f_0$ equal to $4\cdot7\times10^{-2}$.

Thus, we should expect a lunar critical frequency variation of about 5 per cent. at Huancayo, and maximum critical frequency should occur about 4 hr before the time of maximum height. The phases and amplitudes observed by Martyn (Table 1) are in agreement with these conclusions.

IV. Acknowledgments

This work forms part of the programme of the Radio Research Board of the C.S.I.R.O., and is published by permission of the Board. It was undertaken at the suggestion, and under the very helpful guidance, of the Chief Scientific Officer, Dr. D. F. Martyn.

V. References

Appleton, E. V., and Beynon, W. J. G. (1948).—*Nature* **162**: 486.
Baker, W. G. (1953).—*Phil. Trans.* A **246**: 295.
Baker, W. G., and Martyn, D. F. (1952).—*Nature* **170**: 1090.
Baker, W. G., and Martyn, D. F. (1953).—*Phil. Trans.* A **246**: 281.
Burkard, O. (1948).—*Terr. Magn. Atmos. Elect.* **53**: 273.
Chapman, S. (1919).—*Phil. Trans.* A **218**: 1.
Chapman, S., and Bartels, J. (1940).—"Geomagnetism." (Oxford Univ. Press.)
Fejer, J. A. (1953).—*J. Atmos. Terr. Phys.* **4**: 184.
Gold, E. (1910).—*Phil. Mag.* **19**: 26.
Hirono, M. (1950).—*J. Geomagn. Geoelect., Kyoto* **2**: 1.
Huxley, L. G. H. (1952).—*Aust. J. Sci. Res.* A **5**: 10.
Maeda, H. (1955).—*Rep. Ionosphere Res. Japan* **9**: 60.
Martyn, D. F. (1947).—*Proc. Roy. Soc.* A **190**: 273.
Martyn, D. F. (1948*a*).—*Proc. Roy. Soc.* A **194**: 429.
Martyn, D. F. (1948*b*).—*Nature* **162**: 142.
Martyn, D. F. (1953).—*Phil. Trans.* A **246**: 306.
Martyn, D. F. (1955).—"The Physics of the Ionosphere." (The Physical Society: London.)
Matsushita, S. (1949).—*J. Geomagn. Geoelect., Kyoto* **1**: 17.
Mitra, S. K. (1952).—"The Upper Atmosphere." p. 290. (The Asiatic Society: Calcutta.)
Pedersen, P. O. (1927).—"Propagation of Radio Waves etc." (Danmarks Natur Samf.: Copenhagen.)
Pekeris, C. L. (1937).—*Proc. Roy. Soc.* A **158**: 650.
Rocket Panel (1952).—*Phys. Rev.* **88**: 1027.
Schuster, A. (1908).—*Phil. Trans.* A **280**: 163.
Stewart, B. (1882).—Terrestrial magnetism. *In* "Encyclopaedia Britannica." 9th Ed.

AUSTRALASIAN MEDICAL PUBLISHING CO. LTD.
SEAMER AND ARUNDEL STS., GLEBE, SYDNEY

Reprinted from the
AUSTRALIAN JOURNAL OF PHYSICS
VOLUME 9, NUMBER 4, PAGES 436-439, 1956

THE BEHAVIOUR OF A CHAPMAN LAYER IN THE NIGHT F_2 REGION OF THE IONOSPHERE, UNDER THE INFLUENCE OF GRAVITY, DIFFUSION, AND ATTACHMENT

By R. A. Duncan

Reprinted from the Australian Journal of Physics, Volume 9, Number 4, pp. 436–439, 1956

THE BEHAVIOUR OF A CHAPMAN LAYER IN THE NIGHT F_2 REGION OF THE IONOSPHERE, UNDER THE INFLUENCE OF GRAVITY, DIFFUSION, AND ATTACHMENT

By R. A. DUNCAN*

[*Manuscript received July* 11, 1956]

Summary

It is shown that, in the presence of diffusion, gravity, and attachment, a Chapman layer, no matter what its height, maintains its shape, decaying uniformly with an effective attachment coefficient equal to the true attachment coefficient at the height of the electron density maximum ; and that, at the same time, the layer drifts bodily towards an equilibrium height.

It is then shown that a uniform vertical tidal drift will alter the equilibrium height of a Chapman layer.

I. INTRODUCTION

A number of workers (Martyn 1954 ; Duncan 1956 ; Yonezawa 1956) have suggested that the height gradient of electron decay, and diffusion under gravity should combine to stabilize the height of the night-time F_2 region of the ionosphere. If the layer is raised the increased diffusion under gravity should bring it down again, if it is lowered the increased decay of the lower edge should tend to lift the height of the electron density maximum.

Martyn (1956) gave a quantitative basis to these ideas by showing that, under the action of diffusion, gravity, and attachment, a Chapman layer at a reduced height (Z_m) such that

$$\beta = g \frac{\sin^2 \psi}{2H\nu} \quad \ldots\ldots\ldots\ldots\ldots\ldots \quad (1)$$

decays uniformly without change of shape or height.

Here H is the scale height,
g is the gravitational field strength,
ψ is the geomagnetic dip,
ν is the positive ion collisional frequency,
β is the attachment coefficient.

By a Chapman layer is meant a region in which the height distribution of electron density is described by the relation

$$N = N_m \exp \tfrac{1}{2}[1 - (z - z_m) - e^{-(z-z_m)}], \quad \ldots\ldots\ldots \quad (2)$$

* Radio Research Laboratories C.S.I.R.O., Camden, N.S.W.

where N is the electron density,
N_m is the maximum electron density,
z is the reduced height,
z_m is the reduced height of the electron density maximum.

For convenience, we shall take the height such that equation (1) is satisfied as the datum level, $z=0$, and the positive ion collisional frequency and attachment coefficient at this level will be denoted by ν_0 and β_0 respectively.

In this paper the conclusions reached by Martyn will be extended.

It will first be shown that, in the presence of diffusion, gravity, and attachment, a Chapman layer, no matter what its height, maintains its shape, decaying uniformly with an effective attachment coefficient (β') equal to the true attachment coefficient at the height of the electron density maximum (z_m); and that at the same time, the layer drifts bodily towards the equilibrium height ($z=0$) with a velocity

$$v=-\frac{2g\sin^2\psi}{\nu_0}\sinh z_m. \quad \ldots\ldots\ldots\ldots\ldots \quad (3)$$

It will then be shown that, if an ionospheric region, in equilibrium with gravity, diffusion, and attachment, is subjected to a vertical tidal drift W, its height is perturbed by an amount

$$\Delta z_m=\text{arc sinh}\frac{W\nu_0}{2g\sin^2\psi}=\text{arc sinh}\frac{W}{4H\beta_0}. \quad \ldots\ldots\ldots \quad (4)$$

II. Solution of the Equation of Continuity for a Night-time Chapman Layer in the Presence of Gravity, Diffusion, and Attachment

We shall assume the attachment coefficient to be proportional to the pressure, that is,

$$\beta=\beta_0 e^{-z}. \quad \ldots\ldots\ldots\ldots\ldots\ldots \quad (5)$$

The continuity equation then becomes

$$\frac{\partial N}{\partial t}=\frac{2g\sin^2\psi}{H\nu_0}e^z\left(\frac{\partial^2 N}{\partial z^2}+\frac{3}{2}\frac{\partial N}{\partial z}+\frac{N}{2}\right)-\beta_0 N e^{-z}; \quad \ldots\ldots \quad (6)$$

Ferraro (1945); Martyn (1956).

Substituting equation (2) into this we get

$$\frac{\partial N}{N\partial t}=\frac{g\sin^2\psi}{2H\nu_0}e^z(e^{-2z}e^{2z_m}-e^{-z}e^{z_m})-\beta_0 e^{-z}. \quad \ldots\ldots\ldots \quad (7)$$

Now we have chosen our datum level such that

$$g\sin^2\psi/2H\nu_0=\beta_0, \quad \ldots\ldots\ldots\ldots\ldots \quad (8)$$

and (7) becomes therefore

$$\frac{\partial N}{N\partial t}=\beta_0(e^{-z}e^{2z_m}-e^{z_m}-e^{-z}). \quad \ldots\ldots \quad (9)$$

This may be expanded to

$$\frac{\partial N}{N\partial t}=2\beta_0(e^{z_m}-e^{-z_m})\tfrac{1}{2}\{e^{-(z-z_m)}-1\}-\beta_0 e^{-z_m}, \quad \ldots\ldots \quad (10)$$

or from (8) and (2)

$$\frac{\partial N}{\partial t}=\frac{g\sin^2\psi}{H\nu_0}(e^{z_m}-e^{-z_m})\frac{\partial N}{\partial z}-\beta_0 e^{-z_m}N. \quad \ldots\ldots\ldots \quad (11)$$

This equation corresponds to the general form

$$\frac{\partial N}{\partial t}=-v\frac{\partial N}{H\partial z}-\beta' N, \quad \ldots\ldots\ldots\ldots\ldots\ldots \quad (12)$$

where both v and β' are independent of the height z but depend only on the height of the maximum electron density of the layer z_m.

It is evident that the layer decays uniformly with an effective attachment coefficient

$$\beta'=\beta_0 e^{-z_m}, \quad \ldots\ldots\ldots\ldots\ldots \quad (13)$$

and that the electron density maximum moves with a velocity

$$v=-\frac{g\sin^2\psi}{\nu_0}(e^{z_m}-e^{-z_m}) \quad \ldots\ldots\ldots\ldots\ldots \quad (14)$$

towards the height $z_m=0$, i.e. from the way in which we have defined our datum level, towards the height such that $\beta=g\sin^2\psi/2H\nu$.

III. The Behaviour of an Arbitrary Electron Density Distribution under Gravity, Diffusion, and Attachment

Martyn has suggested that, under the influence of gravity, diffusion, and attachment, an ionospheric region with any initial height distribution of electron density, approaches the Chapman form centred at the equilibrium height $z=0$.

Proof of this is still lacking, but we can show that all those height distributions of electron density that can be built up as the sum of a number of Chapman layers of different peak electron densities, and centred at different heights, approach the simple Chapman form. As equation (6) is linear, each of the component layers in such a region can be considered independently of the others and each therefore satisfies equation (12). Each of the component Chapman layers then, approaches the equilibrium height $z=0$, so that the electron distribution as a whole must approach the Chapman form, centred at the height $z=0$.

IV. The Perturbation of a Chapman Region by a Vertical Drift

If a Chapman region in equilibrium with gravity, diffusion, and attachment is subjected to a vertical tidal drift W it will move with the drift until the restoring velocity as given by equation (14) is equal and opposite to the perturbing tidal

drift. It follows from these considerations that the perturbation of the equilibrium height of the layer is

$$\Delta z_m = \text{arc sinh} \frac{W\nu_0}{2g \sin^2 \psi} = \text{arc sinh} \frac{W}{4H\beta_0}, \quad \ldots\ldots \quad (15)$$

where ν_0 is still the positive ion collisional frequency and β_0 the attachment coefficient, at the equilibrium height of the electron density maximum of the unperturbed layer.

V. Conclusions

Martyn's suggestion that the observed adoption of an approximately parabolic form by the night F_2 region is due to the action of gravity, diffusion, and attachment has been put on a firmer basis, although a proof that *any* initial electron distribution will adopt the Chapman form is still lacking.

Equation (**15**) should make possible a more concise formulation of the author's lunar tidal theory (Duncan 1956).

VI. Acknowledgments

The author is indebted to Dr. D. F. Martyn, the Chief Scientific Officer of the Radio Research Board, and to Mr. W. L. Price for helpful discussions.

VII. References

Ferraro, V. C. A. (1945).—*Terr. Magn. Atmos. Elect.* **50**: 215.
Duncan, R. A. (1956).—*Aust. J. Phys.* **9**: 112.
Martyn, D. F. (1954).—" The Physics of the Ionosphere." p. 256. (Phys. Soc.: London.)
Martyn, D. F. (1956).—*Aust. J. Phys.* **9**: 161.
Yonezawa, T. (1955).—*J. Radio Res. Labs. Japan* **3**: 1.

AUSTRALASIAN MEDICAL PUBLISHING CO. LTD.
SEAMER AND ARUNDEL STS., GLEBE, SYDNEY

LUNI-SOLAR VARIATIONS IN THE IONOSPHERE

By R. A. Duncan

Upper Atmosphere Section, C. S. I. R. O., Camden, N.S.W.

Accepted by Australian Journal of Physics for publication in March 1963 issue.

SUMMARY

Martyn's luni-solar analyses of $h^{max} F_2$ and f_0F_2 at Huancayo and Canberra, are restudied; not all the coefficients are found to be significant. The E region near the magnetic equator appears to fail abruptly as a dynamo at sunset; that above Canberra remains active until midnight.

I. INTRODUCTION

It is well known that the electron densities and heights of the ionospheric layers vary slightly with lunar time (Appleton & Weekes (1939), Martyn (1947), Burkard (1948)). Meaned over a month or more, these variations are predominantly semi-diurnal, as is to be expected, because a semi-diurnal lunar variation of barometric pressure is found at the ground, and the ionospheric variations must be caused, ultimately, by a similar gravitational tide in the upper atmosphere.

The ionospheric effect of the lunar tidal motion, however, even the direction of the effect, depends on the morphology of the ionosphere, a thing chiefly under solar

control. This may greatly complicate the actual lunar variation on a given day.

Martyn (1947, 1948) attacked this problem by studying the variation with lunar time of f_oF_2 and $h^{max}F_2$ measured at chosen solar hours each day. Chapman and Bartels (1940) have shown that such studies need interpretation.

In this paper we examine Martyn's, Huancayo and Canberra, $h^{max}F_2$ and f_oF_2, luni-solar coefficients, and find that not all of them are significant. We interpret the significant variations in terms of Martyn's lunar tidal theory (Martyn (1947), Duncan (1956)); that is, in terms of electric currents in the E region setting up polarization which is conducted along the geomagnetic field lines to the F region.

II. GENERAL CONSIDERATIONS

A "semi-diurnal" lunar coefficient determined from observations at a fixed solar hour each day, does not necessarily reflect semi-diurnal behaviour, that is a variation of the form cos 2ℓ , where ℓ is the lunar hour angle. It can be caused by any variation of the form cos $2(\ell - ns)$, where s is the solar hour angle and n an integer. If, however, the lunar coefficient is determined for each solar hour, and the lunar phase is plotted against solar hour, the ambiguity is resolved. If the slope of the phase plot is μ, the variation can be formally described by a function of the form cos $2(\ell - \mu s)$.

However, because of the conservation of geophysical data the lunar phase determinations for each solar hour are not necessarily independent; a non-significant long period variation will similarly influence them all. With "semi-diurnal" luni-solar coefficients it is a non-significant

semi-monthly variation which matters. This, having the form cos 2(ℓ-s) [(ℓ-s) is the lunar phase] produces an upward sloping phase plot. In such a plot it is necessary to test the significance of each point separately; we have applied the criterion that the "semi-diurnal" component must account for at least half of the total variance.

On the other hand, a horizontal phase plot, cos 2ℓ, indicates a true lunar semi-diurnal variation. This cannot be caused by conservation; in this case each point corroborates the evidence of its neighbours.

If we look, not for a semi-diurnal, but for a lunar semi-monthly variation, the situation is reversed. Now it is a semi-monthly variation which has a horizontal, and a semi-monthly lunar variation which has a sloping phase plot with solar hour. Neglect of this consideration caused an apparent disagreement between the results of Martyn (1947), and McNish and Gautier (1949).

III. ANALYSIS

(a) $h^{max}F_2$ Huancayo

The mean (1942-43-44) lunar variations of $h^{max}F_2$ Huancayo at 01 and 13 solar hours are shown in figure 1. Only the 13 solar hour plot shows a lunar effect. Computation shows that none of Martyn's nighttime luni-solar coefficients are significant (Fig. 2), but all those between 07 and 18 solar hours account for well over 50% of the total variance. Furthermore this part of the phase plot (Fig. 2) is substantially horizontal so that the daytime variation is semi-diurnal in the true sense of the word. But the variation ceases abruptly at sunset, and this must mean that near the magnetic equator the E region ceases to support a lunar current system at sunset.

(b) f_0F_2 Huancayo

Luni-solar studies of critical frequency at Huancayo confirm this conclusion. Again midday critical frequencies show a large lunar effect, midnight critical frequencies show none (Fig. 3), and after applying a significance test, we have rejected some of the points in Martyn's phase plot (Fig. 4).

The horizontal part of the phase plot, i.e. between 08 and 17 solar hours, indicates the presence of a simple semi-diurnal tide during the day.

Between 17 and 21 solar hours the phase plot slopes upward at about one lunar hour per solar hour, that is we have a variation of the form cos $2(\ell-s)$, a semi-monthly variation. This implies the following behaviour. Active lunar perturbation of the F_2 at Huancayo ceases at sunset, but the electron density tends to retain, until 21 solar hours, the perturbation with which it was left at sunset. The critical frequency between 18 and 21 hours depends, then, on the lunar hour at sunset, that is, on the lunar age.

There is, as we have said, no evidence of any lunar control of the critical frequency during the middle of the night; the general upward slope is caused by conservation, but at 04 and 05 solar hours significant lunar control appears again, but with a phase, 10 lunar hours, opposite to that observed during the day. This is to be expected. During the day upward lunar drift increases the electron density by lifting electrons to a region of low decay. In the brief dawn period a downward lunar drift favours increases ion density, as it causes the ions to follow the downward dawn movement of the height of maximum ion production.

Luni-solar studies of Huancayo, f_0F_2, then, confirm the conclusion reached from the study of $h^{max}F_2$. Lunar electric currents and polarization are significant only during the day.

(c) Canberra $h^{max}F_2$

Martyn's luni-solar coefficients for Canberra $h^{max}F_2$, 1942-43-44, are shown in figure 5. The coefficients for solar hours 17 to 23 account for from 25% to 55% of the variance at these hours, and, as they have similar phases, they may be accepted as genuine.

The coefficients for other times of the day are not significant, but the amplitudes at these hours are not small. Hence masking by increased random fluctuations, rather than lessening of the lunar effect could be the explanation.

(d) Canberra f_0F_2

The ratio of regular to random variation at Canberra is much smaller than at Huancayo, and only two of Martyn's luni-solar coefficients for Canberra f_0F_2, the ones for 06 and 14 solar hours, account for more than half of the total variance. However there are reasons for considering some of the other coefficients genuine.

The coefficients between 14 and 23 hours have very similar phases, and, although they account, on the average, for only about 40% of the total variance, they can only be due to a genuine semi-diurnal lunar variation.

The coefficients between 07 and 13 solar hours have small amplitudes and scattered phases; five of them account for less than 10%, and the remaining two (07 and 13 solar hours) account for less than 20% of the total variance at each solar hour. There is therefore no

evidence of lunar tidal effects during the early and middle part of the day. This is not likely to result from failure of E region conductivity; it is almost certainly a consequence of the short relaxation time of the F region, during this period of rapid electron production and decay.

The phase progression of the coefficients between 00 and 05 solar hours suggest mere conservation, but the coefficient for 06 solar hours accounts for 60% of the variance at this hour and must be accepted. At Huancayo the dawn luni-solar coefficient had a phase opposite to those during the day; at Canberra, at a middle latitude, the dawn and daytime phases are similar. This is because at non-equatorial latitudes ionization diffuses down the field lines under gravity and is ultimately lost at low heights by rapid decay. At any solar hour upward drift mitigates this process and enhances the electron density; a downward drift never increases the electron density, the electrons diffuse down - too rapidly for their own long-life - without the help of drift.

IV. CONCLUSIONS

Studies of both $h^{max}F_2$ and f_oF_2 at Huancayo suggest that the part of the E region magnetically linked to the equatorial F region, that is the E region at magnetic latitudes $\pm 10^o$, fails as a lunar tidal dynamo at sunset. The E region above the middle - latitude station, Canberra, appears to act as a tidal dynamo until midnight.

V. REFERENCES

Appleton, E.V. and Beynon, W.J.G. (1948). Nature 162: 486.

Burkard, O. (1948). Terr. Mag. & Atmos. Elect. 53: 273.

Chapman, S. and Bartels, J. (1940). "Geomagnetism" (Oxford University Press): p559.

Duncan, R.A. (1956). Aust. J. Phys. 9: 112.

Martyn, D.F. (1947). Proc. Roy. Soc. A. 190: 273.
(1948). Proc. Roy. Soc. A. 194: 429.

McNish, A.G. and Gautier, T.N. (1949). J. Geophys. Res. 54: 181.

CAPTIONS

Figure 1: The lunar variations of the daily values of Huancayo $h^{max}F_2$ at 13 and 01 solar hours respectively; 1942-43-44.

Figure 2: The solar hour variation of the semi-diurnal luni-solar coefficients for Huancayo $h^{max}F_2$; 1942-43-44. Non-significant points are shown as hollow circles.

Figure 3: The lunar variations of the daily values of Huancayo f_oF_2 at 11 and 23 solar hours respectively; 1942-43-44.

Figure 4: The solar hour variation of the semi-diurnal luni-solar coefficients for Huancayo f_oF_2; 1942-43-44. Non-significant points are shown as hollow circles.

Figure 5: The solar hour variation of the semi-diurnal luni-solar coefficients for Canberra $h^{max}F_2$; 1942-43-44. Non-significant points are shown as hollow circles.

Figure 6: The solar hour variation of the semi-diurnal luni-solar coefficients for Canberra f_oF_2; 1942-43-44. Non-significant points are shown as hollow circles.

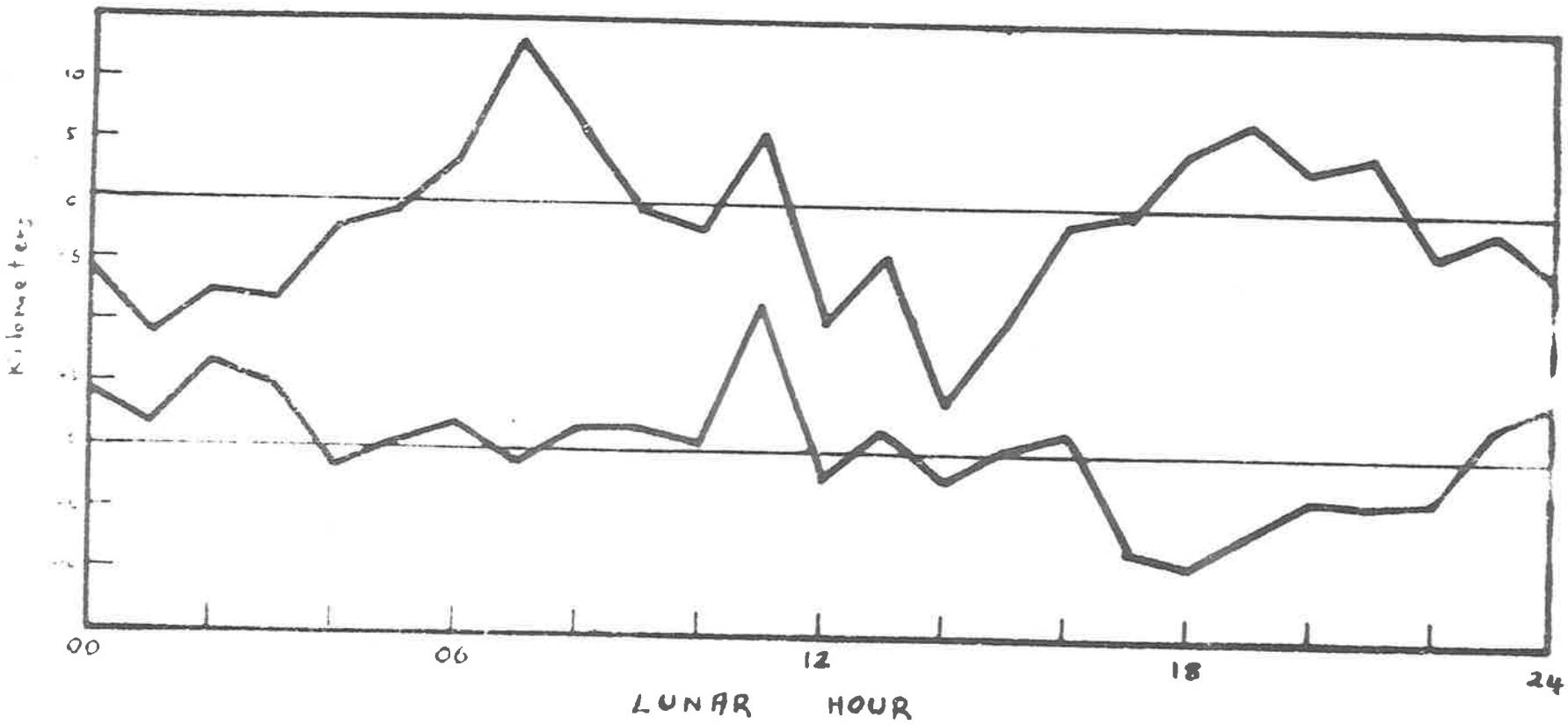

Figure 1

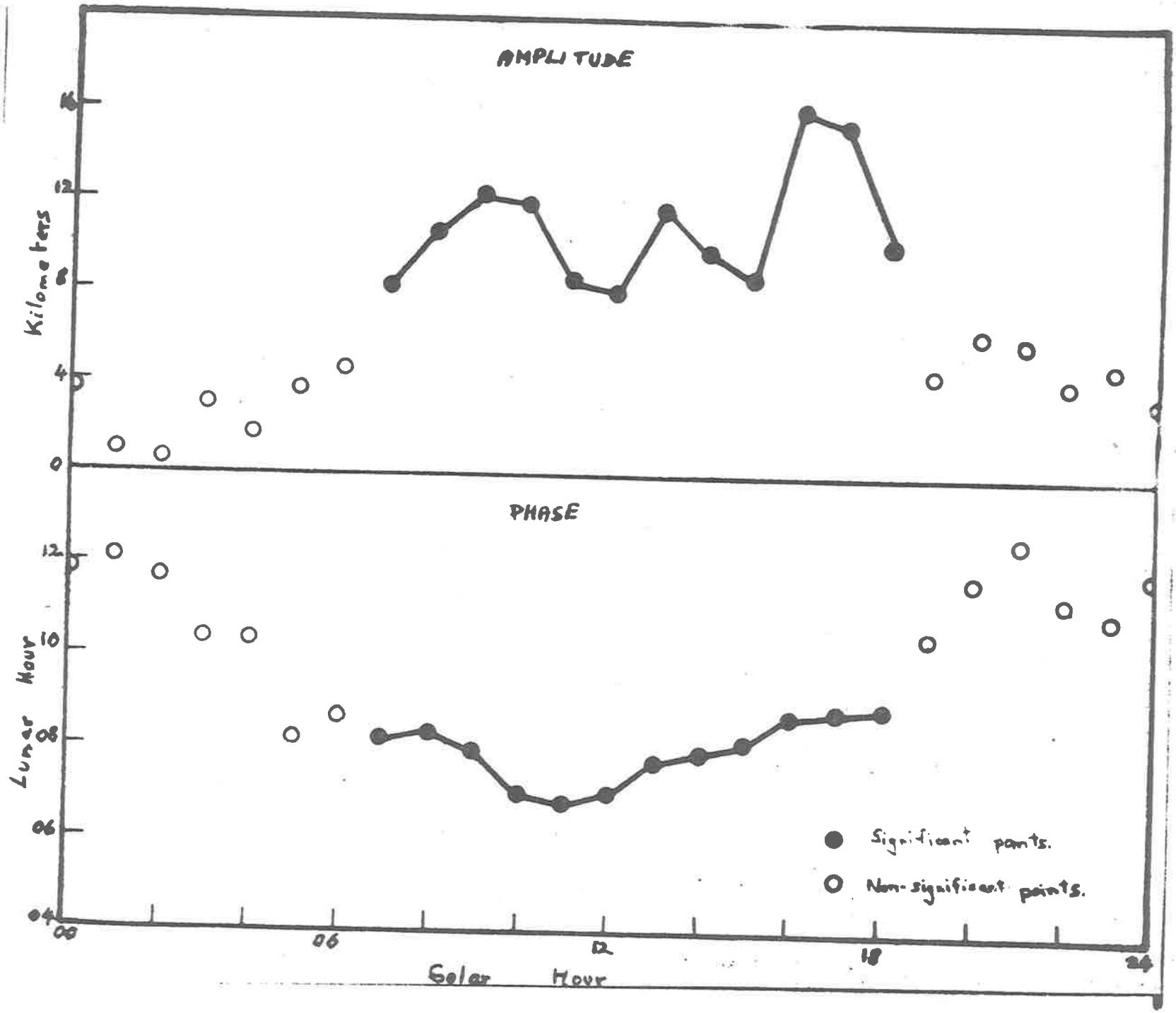
AMPLITUDE
Kilometers
16
12
8
4
0
PHASE
Lunar Hour
12
10
08
06
04
00
06
12
18
24
Solar Hour
Significant points.
Non-significant points.

Figure 2

Figure 3

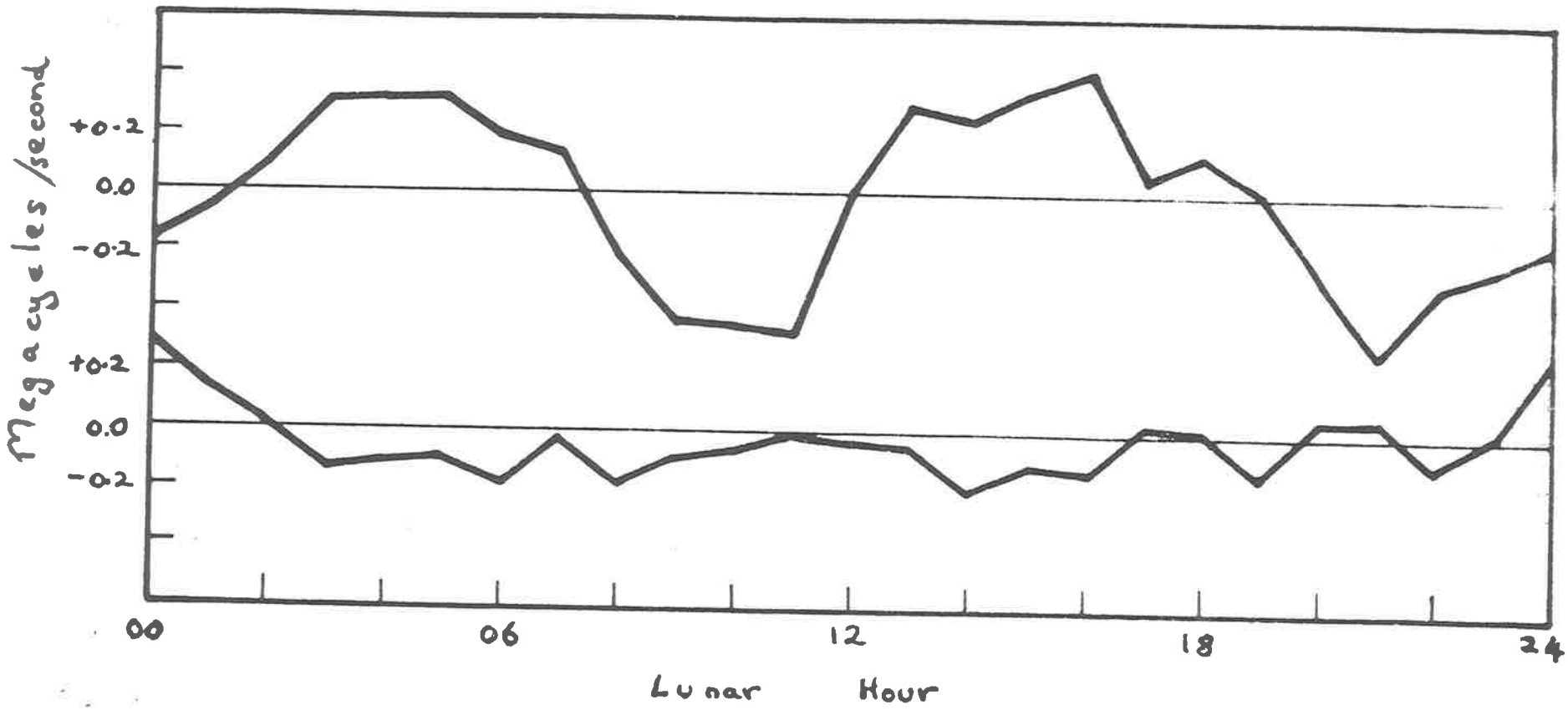

Figure 3

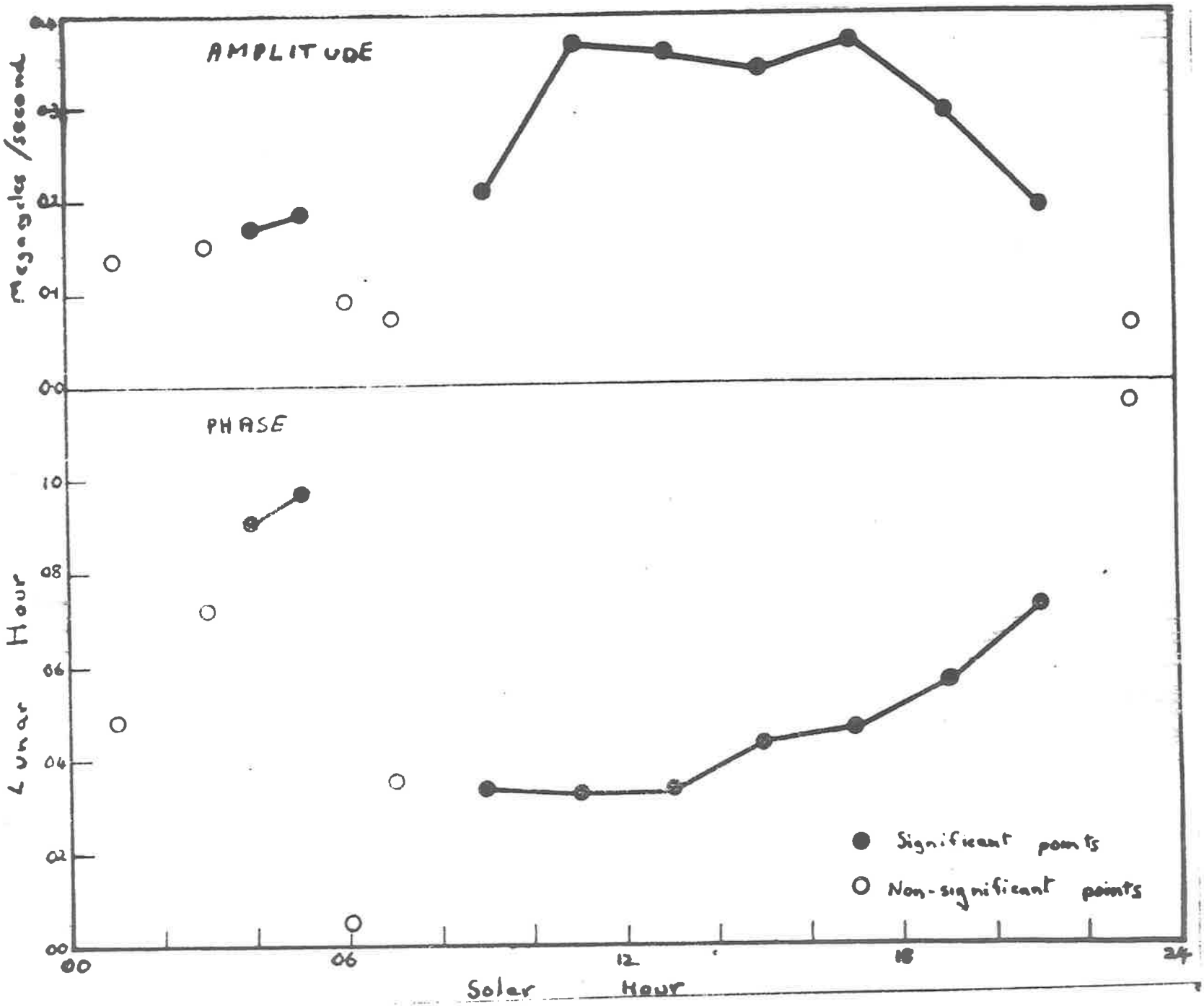
AMPLITUDE
Megacycles/second
0.0
0.1
0.2
0.3
PHASE
Lunar Hour
00
02
04
06
08
10
00
06
12
18
24
Solar Hour
Significant points
Non-significant points

Figure 21

Figure 5

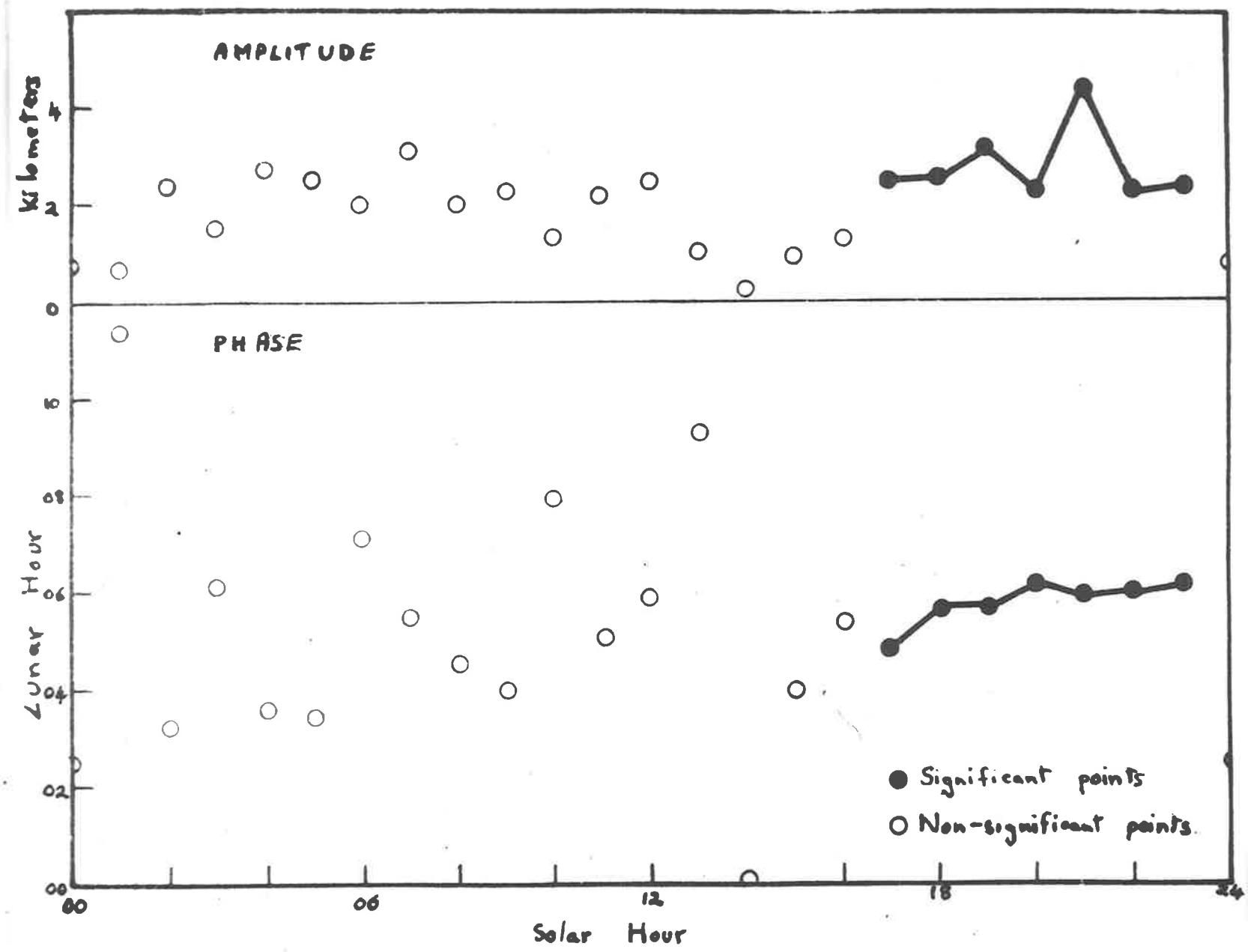

Figure 5

Figure 6

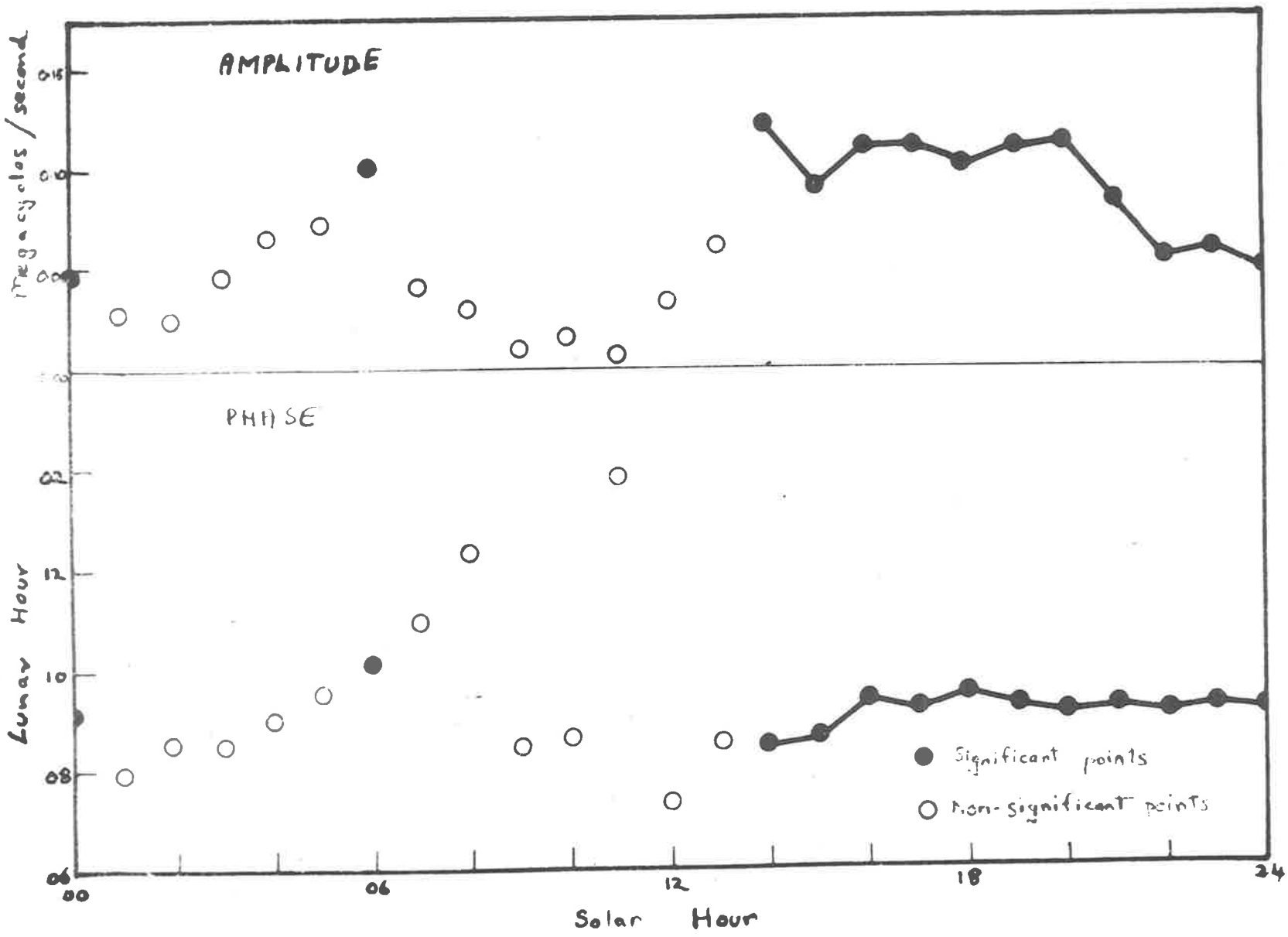

Figure 6

Commonwealth of Australia
COMMONWEALTH SCIENTIFIC AND INDUSTRIAL
RESEARCH ORGANIZATION
Reprinted from *Journal of Geophysical Research*, Vol. 63, No. 3
pp. 491-500, September, 1958

COMPUTATIONS OF ELECTRON DENSITY DISTRIBUTIONS IN THE IONOSPHERE MAKING FULL ALLOWANCE FOR THE GEOMAGNETIC FIELD

By R. A. Duncan

Radio Research Laboratories,
Commonwealth Scientific and Industrial Research Organization,
Camden, N.S.W., Australia

(Received March 19, 1958)

ABSTRACT

Jackson's method of computing electron density distributions from $h'f$ records has been modified slightly and adapted for use on an electronic computer. Reduction of a single $h'f$ record takes about 20 seconds of computer time.

The method makes allowance for the geomagnetic field and is exact save for the uncertainty about the electron density between ionospheric layers which is inherent in the method of pulse sounding from the ground. Rocket measurements (Seddon, *et al.*, 1954) enable a reasonable resolution of this uncertainty.

Some examples of electron density distribution at Brisbane are given. It is shown that the night-time distributions are much closer to the Chapman than the parabolic form. This is to be expected (Martyn, 1956) in a region in which the electron distribution is determined by the opposing processes of downward diffusion under gravity, and a height gradient of electron decay. The effect of geomagnetic disturbance on the day and night electron density profile is illustrated and discussed.

INTRODUCTION

One of the fundamental parameters of the upper atmosphere is the distribution of electron density with height, and many workers have attacked the problem of obtaining this distribution from the great number of $h'f$ records which have been made by ionospheric observatories throughout the world. Yet the number of electron density distributions which have been computed making proper allowance for the geomagnetic field remains very small.

The apparent height of reflection of radio waves from the ionosphere (h') is related to the true height of reflection (h) by the equation

$$h' = \int_0^h n'(f, h)\, \mathrm{d}h \qquad \ldots\ldots(1)$$

where n' is the group refractive index of the medium and f is the sounding frequency. Most workers have seen the problem of computing true heights as that

of inverting this integral to a form like

$$h = \int_0^{f_0} \phi(f_0, f, h')\, df \quad \ldots\ldots (2)$$

In the greatly simplified case where the geomagnetic field is ignored, such an inversion has been performed (Pekeris, 1940).

Analytical inversions of the exact case, which have been suggested to date, are either approximate, invalid, or too complex for routine use (Whale, 1954; Kelso, 1954). Furthermore, all such inversions, and even the numerical inversion made by Budden (1955), fail if the electron density does not increase monotonically with height, so that they cannot be used to analyse daytime records in which there may be a number of electron density maxima. The same limitation applies to the new method recently described by Kelso (1957).

These difficulties were avoided by Jackson (1956), who showed that electron density distributions may be computed directly from $h'f$ records without an integral inversion. Jackson's method is exact, subject to the limitations that

(*a*) It assumes that the geomagnetic field in the region analysed does not vary with height, and has the value extrapolated from the ground intensity.

(*b*) Some assumption must be made about the electron density between ionospheric layers. Jackson assumed that the electron density fell between layers to 90 per cent of its maximum value in the lower layer and showed that this gave results in good agreement with simultaneous measurements of electron density from rockets.

The purpose of this note is to suggest a few simplifications to Jackson's method, to record how the Silliac computer at the University of Sydney has been programmed to do these analyses, and to give results of the reduction of some Brisbane $h'f$ films.

SIMPLIFIED DESCRIPTION OF METHOD

The group refractive index (n') is a complex function of the electron density (N) and the sounding frequency (f), but it may be computed (Whale and Stanley, 1950) and used to obtain the contribution to the apparent height (D') at a frequency f, made by an ionospheric region of thickness (D) in which the electron density varies linearly from N_1 to N_2.

Thus,

$$D' = \int_{h_1}^{h_2} n'(f, N)\, dh \quad \ldots\ldots (3)$$

$$= \int_{N_1}^{N_2} n' \frac{dh}{dN}\, dN \quad \ldots\ldots (4)$$

that is,

$$= \frac{D}{N_2 - N_1} \int_{N_1}^{N_2} n'\, dN \quad \ldots\ldots (5)$$

$$D' = \frac{Q_2 - Q_1}{N_2 - N_1} \quad \text{(6)}$$

where

$$Q(f, N) = \int_0^N n'(f, N)\, dN \quad \text{(7)}$$

This Q function may be computed and tabulated.

Suppose now we have a tabulation, h'_1, f_1; h'_2, f_2; h'_3, f_3, etc.; then, if we assume that the electron density falls linearly to zero with decreasing height at the rate indicated by the first two entries in the $h'f$ table, it can be shown by a simple application of equation (6) that the height of the base of the layer is

$$h_0 = \frac{h'_2 Q_1 - h'_1 Q_2}{Q_1 - Q_2} \quad \text{(8)}$$

where $Q_1 = Q(f_1, N_1)$ and $Q_2 = Q(f_2, N_2)$. Jackson did not derive this expression, but used an equivalent graphical method.

Having found h_0, and again assuming that the electron density changes linearly between each of our tabulated points, we can compute h_1 from the equation,

$$h'_1 = h_0 + \frac{h_1 - h_0}{N_1} Q(f_1, N_1) \quad \text{(9)}$$

Similarly, once both h_0 and h_1 are known, we can proceed to the calculation of h_2, using the equation

$$h'_2 = h_0 + \frac{h_1 - h_0}{N_1} Q(f_2, N_1) + \frac{h_2 - h_1}{N_2 - N_1} [Q(f_2, N_2) - Q(f_2, N_1)] \quad \text{(10)}$$

In this way, we can work through the whole tabulation, for, in general,

$$h'_k = h_0 + \sum_{m=1}^{k} \frac{h_m - h_{m-1}}{N_m - N_{m-1}} [Q(f_k, N_m) - Q(f_k, N_{m-1})] \quad \text{(11)}$$

This involves one summation for each entry in the (h', f) table, work which would be required even if an analytical solution in the form of equation (2) were available.

The method is numerical and makes assumptions such as that the quantities vary linearly between tabulated points, but these are not disadvantages. We are not concerned with analytical functions of h' in f, but with numerical h', f tables; even if an analytical solution were available, it would be necessary to reduce it to a numerical form in order to handle experimental data.

DETAILS OF COMPUTATIONS

In practice, f and N are not convenient variables and the equations actually used are listed below. These are not exactly the same as Jackson's, but they can be derived in an analogous manner. It is believed that their use considerably simplifies the computations, as a differentiation with respect to t is avoided in (15): equation (16) is new, replacing Jackson's graphical method; and the extra variable x used by Jackson has been avoided throughout.

1. *Phase refractive index*

$$n^2 = 1 - \frac{2(1-t^2)t^2}{2t^2 - y^2\sin^2\theta + \sqrt{y^4\sin^4\theta + 4t^2y^2\cos^2\theta}} \quad \text{(Appleton, 1932)} \quad \ldots\ldots(12)$$

where

f_H being the electronic gyro-frequency, and

$$y = f_H/f \quad \ldots\ldots(13)$$

$$t = \sqrt{1 - Ne^2/\pi mf^2} \quad \ldots\ldots(14)$$

N being the electron density, e the electronic charge, m the electronic mass, and f the sounding frequency; θ is the angle between the geomagnetic field and the direction of propagation (in our case, the vertical).

2. *The Q-function*

$$Q(t, y) = 2\int_0^t n't\,dt$$

$$= 2(1-t^2)n + 2\int_0^t \left(3n - y\frac{\partial n}{\partial y}\right)t\,dt \quad \ldots\ldots(15)$$

It should be noted that Q, so defined, is not exactly equivalent to that described in the previous section.

3. *The height of the base of the region*

$$h_0 = \frac{h_2'(f_1)^2Q_1 - h_1'(f_2)^2Q_2}{(f_1)^2Q_1 - (f_2)^2Q_2} \quad \ldots\ldots(16)$$

where $Q_1 = Q(t = 1, y_1)$ and $Q_2 = Q(t = 1, y_2)$.

4. *The analysis formulae*

$$h_k' = h_0 + \sum_{m=1}^{k}(h_m - h_{m-1})\frac{Q(t_m, y_k) - Q(t_{m-1}, y_k)}{(t_m)^2 - (t_{m-1})^2} \quad \ldots\ldots(17)$$

$$N_k = (1.24 \times 10^4)(f_k)^2 \quad \text{(where } f \text{ is in megacycles per second)} \quad \ldots\ldots(18)$$

All quantities in these relations are bounded and the only computational difficulty arises in the second term on the right of equation (12), where both the numerator and denominator go to zero at $t = 0$. However, it was found possible to work down to $t = 0.025$ without serious error and then to instruct the machine to put $n = 0$ for the case $t = 0$. y is bounded because frequencies below the gyro-frequency are not employed.

RESULTS

Electron density distributions derived from some Brisbane $h'f$ films are given in Figures 1 and 2. It will be seen that the machine is not troubled by complex $h'f$ traces, such as those in Figure 1. Readings from these and all other traces were fed into the machine without idealization.

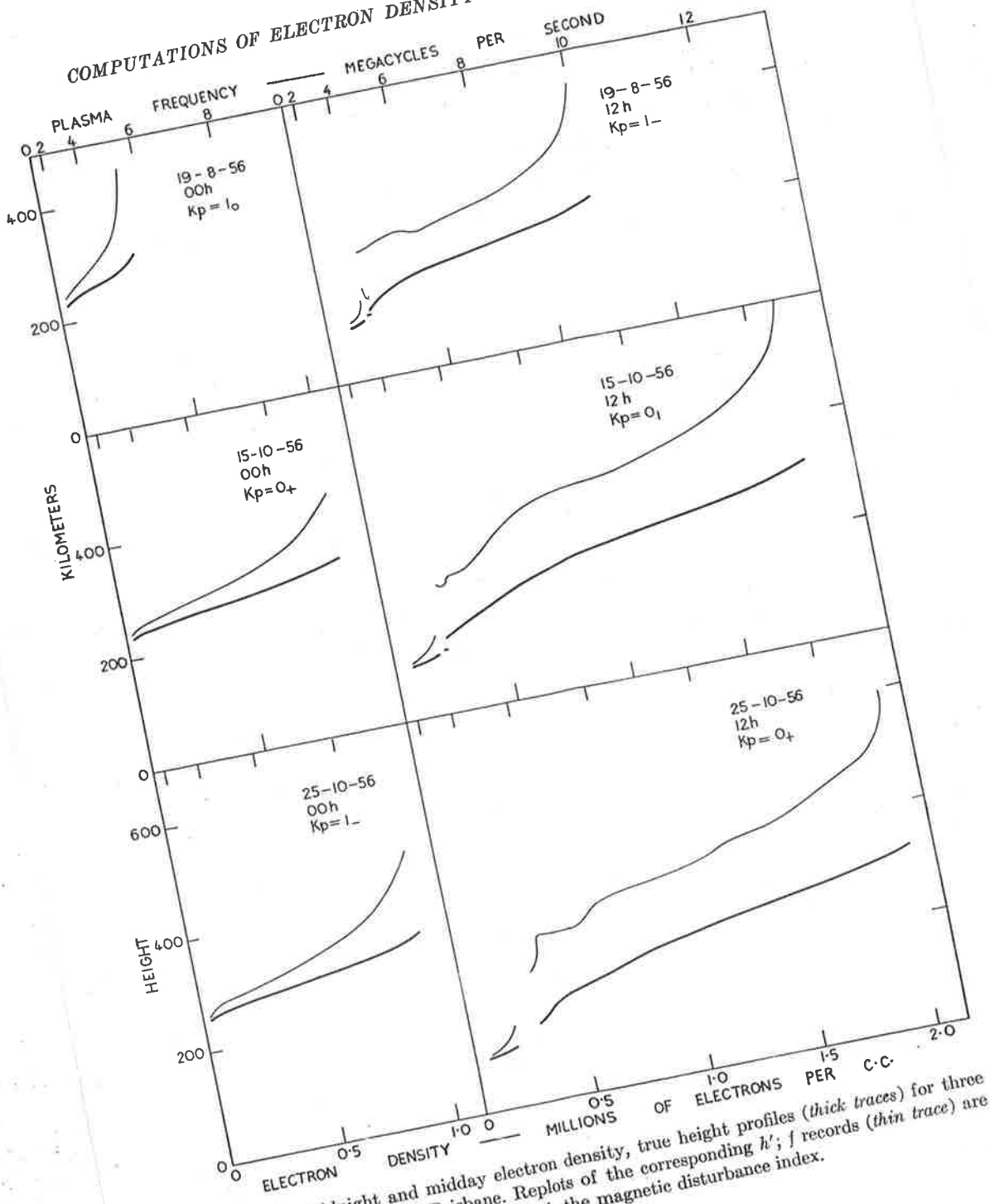

FIG. 1—The midnight and midday electron density, true height profiles (*thick traces*) for three magnetically quiet days at Brisbane. Replots of the corresponding h'; f records (*thin trace*) are given for comparison. Kp is the magnetic disturbance index.

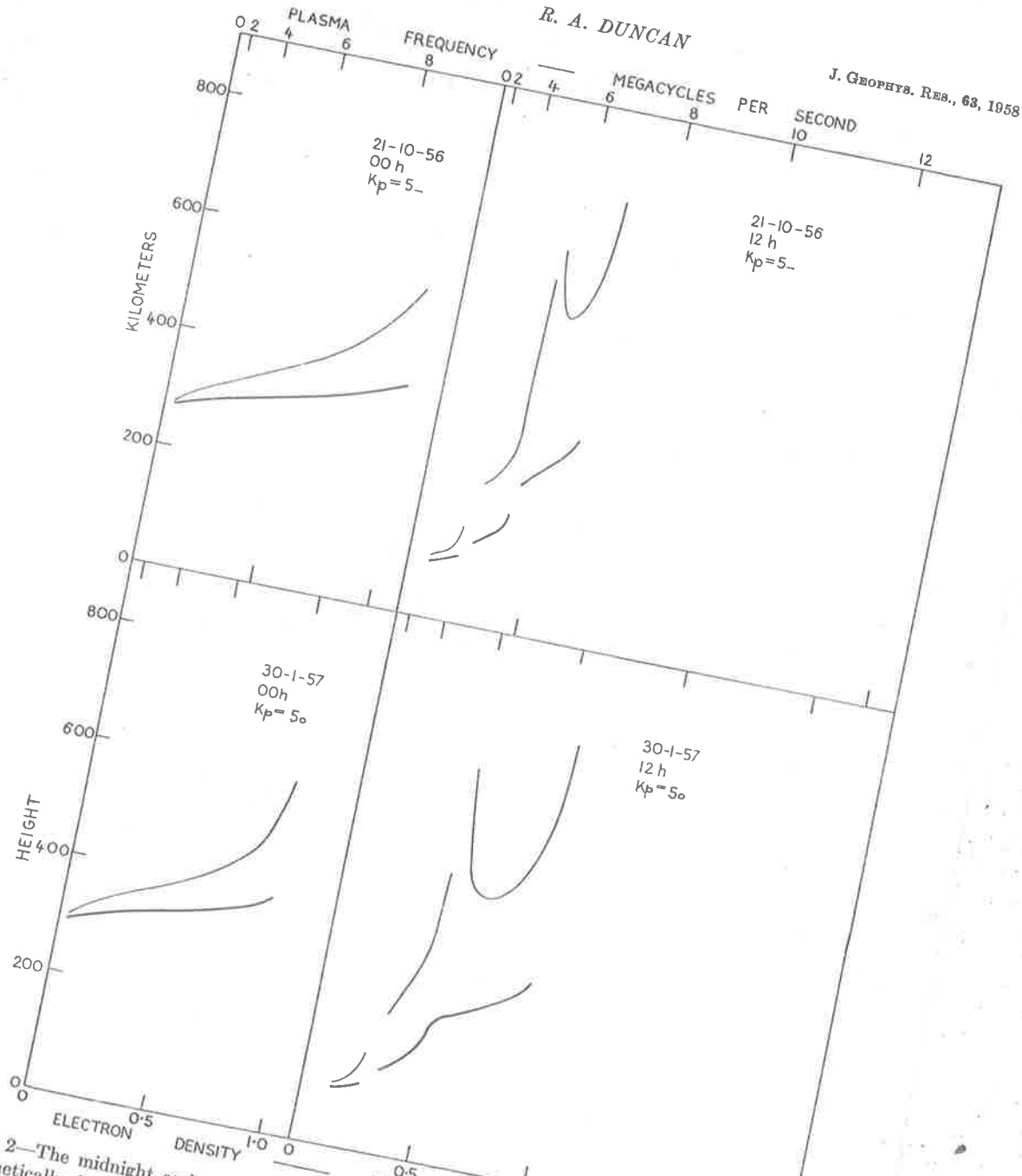

FIG. 2—The midnight and midday electron density, true height profiles (*thick traces*) for two magnetically disturbed days at Brisbane. Replots of the corresponding h'; f records (*thin traces*) are given for comparison. Kp is the magnetic disturbance index.

It would appear from Figure 1 that, although each of the three midday virtual height traces have individual irregularities, the derived true height profiles are quite regular. This impression is not quite correct. For each kink in the virtual height trace, there is a corresponding but much smaller kink in the true height curve, but the latter are often unnoticeable on the scale to which the Figures are drawn.

The night-time electron density distributions are very close to the Chapman form. To illustrate this, some of them have been drawn on a relative scale alongside a calculated Chapman curve in Figure 3. It has long been known that the night-time distribution is parabolic near the electron density maximum (Booker and Seaton, 1940; White and Wachtel, 1949; Ratcliffe, 1951), but the pronounced

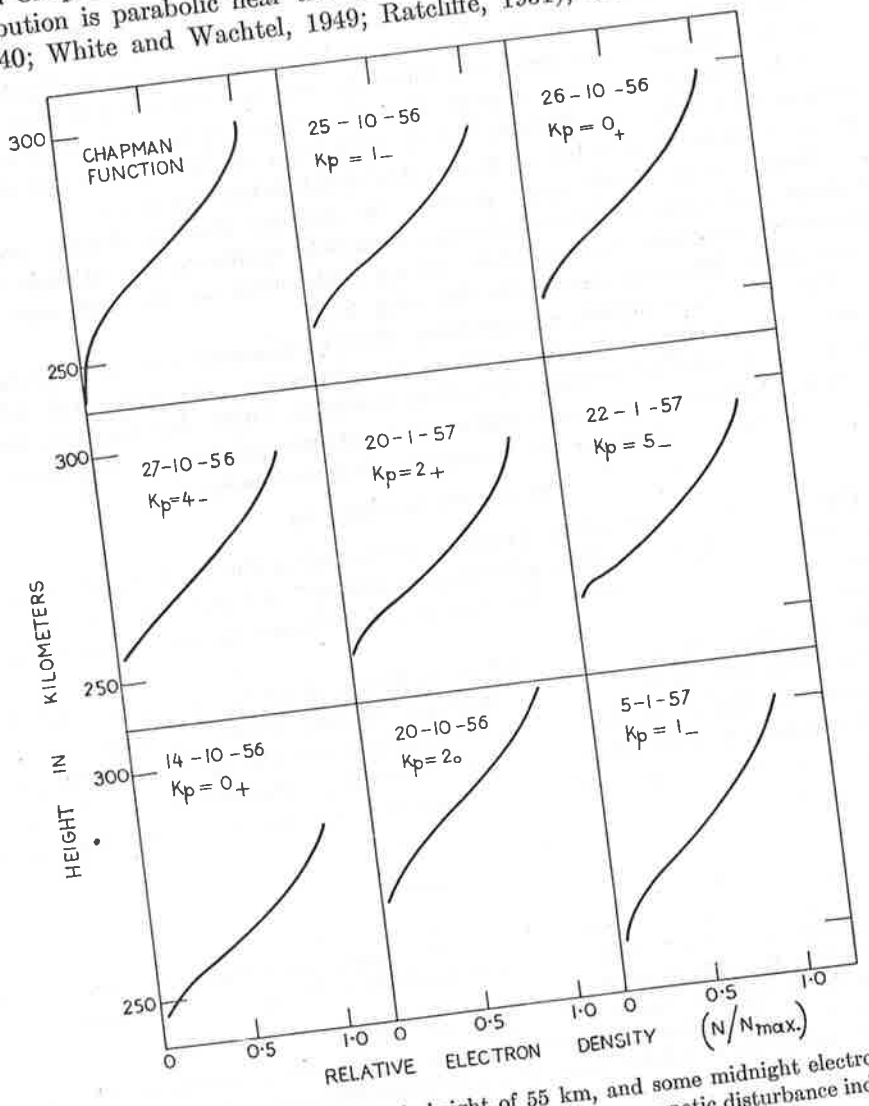

FIG. 3—A Chapman function for a scale height of 55 km, and some midnight electron density profiles at Brisbane drawn to a relative scale. Kp is the magnetic disturbance index.

"tail" at the base of the profile does not appear to have been described in recent literature; however, in what appears to be the earliest paper on this topic, Berkner (1939) produced evidence of it.

Chapman derived his electron density distribution on the basis of equilibrium between electron production by solar radiation and decay by recombination. This can have no application to the night $F2$ region when there is no ionizing radiation and where decay seems to follow an attachment law (Martyn, 1956; Ratcliffe, *et al.*, 1956). However, Martyn (1956), Duncan (1956), Yonezawa (1956), and Dungey (1956) have shown that a Chapman distribution is also to be expected if the controlling processes are diffusion under gravity and a height gradient of electron decay by attachment.

Careful comparison of the observed and theoretical curves in Figure 3 shows that the Chapman fit is very good above 280 km, but that below this the observed electron density falls more rapidly than the Chapman function. This is not surprising, as it is known (Ratcliffe, *et al.*, 1956) that the attachment law of electron decay is replaced by a law of more rapid decay below this level.

During magnetically quiet periods, the daytime electron density profile has a shape and height of electron density maximum similar to that at night (Fig. 1). However, magnetic storms, while having little effect on the night-time profile, cause gross distortion during the day (Fig. 2).

This is to be expected, as a primary effect of magnetic activity is probably to cause vertical electro-dynamic drift of the ionization. At night, drift will shift the F region without causing distortion (Duncan, 1956), but daytime drift, by removing ionization from the region of maximum production, will spread and distort the layer and reduce the maximum electron density.

ACKNOWLEDGMENTS

This work forms part of the program sponsored by the Radio Research Board, and carried out in the Radio Research Laboratories of C.S.I.R.O. I am indebted to the Chief Officer-in-Charge, Dr. Martyn, for discussions on the results of the analyses.

Dr. Jackson very kindly supplied extra details of his computations and these, together with the information in his paper, greatly facilitated programming of the computor. Thanks are also due to Dr. Chartres and Dr. Bennett, of the Adolph Basser Computing Laboratories of the University of Sydney, for advice on the use of the computor. The $h'f$ records were lent by the Australian Ionospheric Prediction Service.

References

Appleton, E. V. (1932); J. Inst. Elec. Eng., 71, 642.
Berkner, L. V. (1940); International Union of Geodesy and Geophysics, Association of Terrestrial Magnetism and Electricity, Transactions of Washington meeting, September 4–15, 1939, Bull. No. 11, p. 417.
Booker, H. G., and S. L. Seaton (1940); Phys. Rev., 40, 87.
Budden, K. G. (1955); Report of the Physical Society Conference on the Physics of the Ionosphere held at the Cavendish Laboratory, Cambridge, September 1954, p. 332.
Duncan, R. A. (1956); Aust. J. Phys., 9, 436.
Dungey, J. W. (1956); J. Atmos. Terr. Phys., 9, 90.

Jackson, J. E. (1956); J. Geophys. Res., **61**, 107.
Kelso, J. M. (1954); J. Atmos. Terr. Phys., **5**, 11.
——— (1957); J. Atmos. Terr. Phys., **10**, 103.
Martyn, D. F. (1956); Aust. J. Phys., **9**, 161.
Pekeris, C. L. (1940); Terr. Mag., **45**, 205.
Ratcliffe, J. A. (1951); J. Geophys. Res., **56**, 463.
——— E. R. Schmerling, G. S. G. R. Setty, and J. O. Thomas (1956); Phil. Trans., A, **248**, 621.
Seddon, J. C., A. D. Pickar, and J. E. Jackson (1954); J. Geophys. Res., **59**, 513.
Whale, H. A. (1954); J. Atmos. Terr. Phys., **5**, 351.
——— and J. P. Stanley (1950); J. Atmos. Terr. Phys., **1**, 82.
White, G. R., and I. S. Wachtel (1949); J. Geophys. Res , **54**, 239.
Yonezawa, T. (1956); J. Radio Res. Lab. Japan, **3**, 1.

Short Communication reprinted from the Australian Journal of Physics, Volume 12, Number 2, pp. 197–198, 1959

PHOTOMETRIC OBSERVATIONS OF SUBVISUAL RED AURORAL ARCS AT MIDDLE LATITUDES*

By R. A. DUNCAN†

A photometer (Roach *et al.* 1958) sensitive to the red oxygen emission at 6300 Å has been in operation at Camden, near Sydney (geomagnetic latitude 42°), since July 1958. In this period three bright aurorae have been seen in southern Australia; on July 8–9, September 4–5, and September 25–26. Following the first two the photometer detected a subvisual stable red arc the next night. On the night after the third aurora, observation was prevented by cloud.

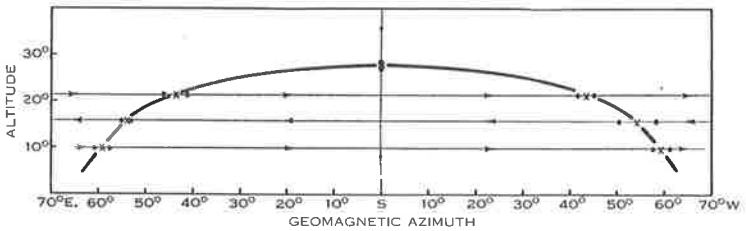

Fig. 1.—Shape of auroral arc observed between 1930^h and 2330^h September 5, 1958. The photometer scanned the sky along the paths indicated by the fine arrowed lines. A complete sky scan was completed once every 5 min. The crosses show the mean positions at which the arc was intercepted. The dots are the quartile points.

These arcs had the following characteristics:

(1) They occurred on the night following a bright visual aurora. By this time the magnetic disturbance index (K) at Watheroo had fallen to 5 or less.

(2) Periodic checks on the 5577 Å emission showed no departure from the quiet airglow pattern. Indeed, during the previous 15 months 5577 Å emission was intensively studied and auroral activity was never detected at this wavelength unless the disturbance index (K) equalled or exceeded 6.

(3) The arcs were centred (to within 1 or 2°) on geomagnetic south, and maintained these positions for some hours. The arc seen on September 5–6 is shown in Figure 1. It maintained this position from 1938 till 2330 E.S.T. After this it began to sink slowly, being 5° lower by 0245.

(4) The intensities of the arcs varied steadily with time (Fig. 2) in marked contrast to the rapid fluctuations which we usually observe during visual aurorae.

* Manuscript received December 15, 1958.

† Upper Atmosphere Section, C.S.I.R.O., Camden, N.S.W.

Using a photometer at Haute Provence (geomagnetic latitude 45·7°) Barbier (1957) found a red arc on January 21, 1957, but this was during a great magnetic storm ($Kp=9$). Störmer (1955) states that only four visual red arcs were observed in southern Norway in the 40 years ending 1955.

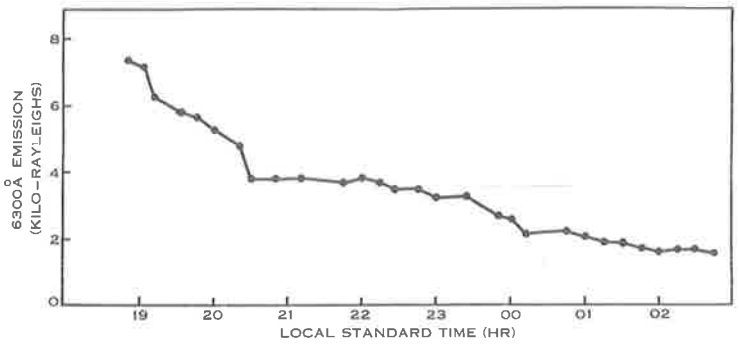

Fig. 2.—Time variation of the brightness of the red auroral arc observed on September 5–6, 1958. The brightness plotted here is that of a point on the eastern limb 15·7° above the horizon (see Fig. 1) but is representative of all parts of the arc.

The existence of auroral arcs at middle latitudes during times of only moderate geomagnetic disturbance does not appear to have been previously reported.

This work forms part of the research programme of the Upper Atmosphere Section of the Commonwealth Scientific and Industrial Research Organization. The photometer was lent by the United States National Bureau of Standards as an I.G.Y. contribution.

The author has to thank Mr. R. O. Errey for help in the observations.

References

Barbier, D. (1957).—*C.R. Acad. Sci., Paris* **244**: 1945.
Roach et al. (1958).—*J. Atmos. Terr. Phys.* **50**: 171.
Störmer, C. (1955).—"The Polar Aurora." (Clarendon Press: Oxford.)

Extrait des ANNALES DE GÉOPHYSIQUE
Tome 18. N° 4, — Octobre-Décembre 1962.

OBSERVATION OF A 6300 Å ARC IN FRANCE, THE UNITED STATES AND AUSTRALIA

by F. E. Roach (1), D. Barbier (2), R. A. Duncan (3)

Résumé. — *Entre le 8 juillet 1958 à 21 h TU et le 9 juillet 1958 à 15 h TU, des arcs aurorаux rouges (6300 Å) ont été observés successivement à l'Observatoire de Haute Provence, au Fritz Peak (U. S. A.) et à Camden (Australie). Les arcs observés à partir de ces trois stations se trouvaient à des latitudes magnétiques constantes (déduites du paramètre L pour la couche de McIlwain) de 44°8 ; 46°6 et 49°6 respectivement. On suggère que les trois arcs faisaient partie d'un phénomène unique.*

Abstract. — *Between 21 UT, 8 July 1958 and 15 UT, 9 July 1958, red (6300 Å) auroral arcs were observed successively at Haute Provence Observatory in France, Fritz Peak in the United States, and Camden in Australia. The arcs observed from the three stations were at invariant magnetic latitudes (deduced from McIlwain's sheet parameter L) of 44°8, 46°6, and 49°6, respectively. It is suggested that all three arcs were part of a single phenomenon.*

Резюме. — Между 8 июлем 1958 года в 21 ч. всемирного времени и 9 июлем 1958 года в 15 ч. всемирного времени красные дуги полярных сияний (6300 Å) наблюдались последовательно в обсерватории Высокой Прованс, в Фритц Пик (С.Ш.А.) и в Камдене (Австралия). Дуги наблюдавшиеся из этих трех станций находились на постоянных магнитных широтах, выведенных из параметра L (для слоя Мак Илвайна) в 44°8 ; 46°6 и 49°6 соответственно. Подается предположение что эти три дуги составляли части единого явления.

During the I. G. Y. a new type of aurora was discovered ; photoelectric photometers, at middle latitudes, revealed stable red arcs with [OI], 6300 A, the predominant, and probably the only emission [1, 2, 3, 4]. The arcs reoriented approximately parallel to magnetic latitude and have been traced continuously over 40° of longitude [5], and with a gap over the Atlantic Ocean, between France and America, 110° of longitude [3]. They maintain themselves with little change for many hours.

The simultaneous observation of these arcs at magnetically conjugate points in the Northern and Southern Hemispheres would be of great interest, but unfortunately conjugate pairs of observing stations do not exist. The three stations operated by the authors (Table 1) differ so greatly in longitude that they do not have coincident darkness. Nevertheless, the great longitudinal extent of the arcs and their stability make a comparison of observations between these three stations useful. We can be reasonably confident that observations on the same day, though separated by many degrees of longitude and a few hours in time, refer to a single phenomenon.

A search of our records shows that there has been one day, 8 July, 1958, on which observations have been made in both the Northern and Southern Hemispheres and on which a red arc was observed. On this day arcs were seen at all three stations, not simultaneously, but within a period of a few hours.

Table 1 and Figure 1 summarize the results. We have calculated the positions of the arcs, seen from each station, from the observed zenith distances, and an assumed height of 400 km. Triangulation on other

TABLE 1

Summary of observations

Station	Coordinates of stations: Geographic Latitude	Geographic Longitude (East)	Magnetic (invariant) (h = 400 km, r = 1.063) L	Magnetic (invariant) Latitude	Time interval of Observations of Arcs (Universal Time)	Position of arcs (h = 400 km, r = 1.063) With respect to station (km)	Magnetic invariant L	Magnetic invariant Latitude
Haute Provence	43°55′	5°43′	1.79	39°35′	8 July 2143 — 2257	340 N	2.11	44°47′
Fritz Peak	39°54′	254°31′	2.41	48°23′	9 July 0454 — 0654	160 S	2.25	46°35′
Camden	— 34°04′	150°38′	1.96	42°36′	9 July 0957 — 1432	676 S	2.53	49°36′

(1) Boulder Laboratories, National Bureau of Standards, United States.
(2) Institut d'Astrophysique, Paris, France.
(3) C. S. I. R. O., Camden, Australia.

arcs (November 27/28, 1959 ; April 1/2, 1960) [5, 6] gave such a height. Because of evidence [7] that red arcs are caused by trapped particles we have used the

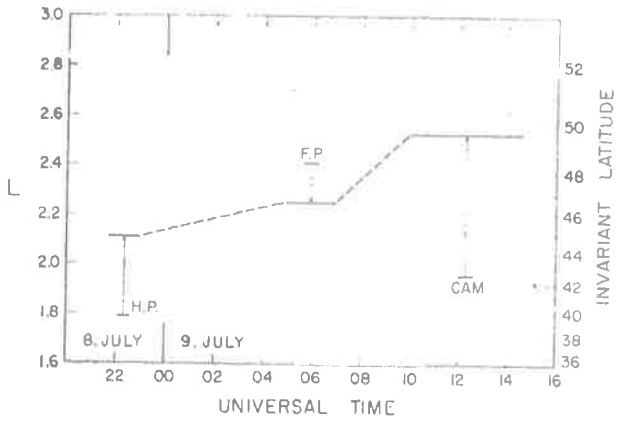

FIG. 1.

sheet parameter L introduced by McILWAIN [8] to describe the arc's position ; L may be approximately described as the equatorial distance to the intersection of the magnetic line of force (in earth radii) of the locus of the trapped particles. The corresponding magnetic latitude (λ) may be derived from L by the relation

$$\frac{r}{L} = \cos^2 \lambda,$$

where r is the distance to the arc (in earth radii) from the centre of the earth. It can be seen from Table 1 and Figure 1 that, to within about 5°, the arcs in the Northern and Southern Hemispheres were at the same magnetic latitude. It seems reasonable to assume that they were conjugate phenomena. The accuracy with which arc positions can be estimated is about $\pm$ 1° so the steady progression of the arcs toward higher latitudes is probably real.

We may connect this conclusion with that to be drawn from observations of visual auroras. Some studies [9, 10] indicate a general correlation between the appearance of auroras in the Northern and Southern Hemispheres, while another [11] indicates close relationships in the intensity, motion, and character of auroral forms at nearly exact conjugate points.

Manuscrit reçu le 10 *octobre* 1962.

REFERENCES

[1] BARBIER D., 1958, *Ann. Geophys.*, **14**, 334.
[2] BARBIER D., 1960, *Ann. Geophys.*, **16**, 544.
[3] ROACH F. E. and MAROVICH E., 1959, *J. of Research of the NBS*, **63D**, 297.
[4] DUNCAN R. A., 1959, *Australian J. Phys.*, 197.
[5] ROACH F. E., MOORE J. G., BRUNER E. C., Jr., CRONIN H. and SILVERMAN S. M., 1960, *J. Geophys. Research*, **65**, 3575.
[6] MOORE J. G and KIRK ODENCRANTZ F., 1961, *J. Geophys. Research*, **66**, No. 7, 2101.
[7] O'BRIEN B. J., VAN ALLEN J. A., ROACH F. E. and GARTLEIN C. W., 1960, *J. Geophys. Research*, **65**, 2759.
[8] McILWAIN C. E., 1961, *J. Geophys. Research*, **66**, 3681.
[9] FILLIUS R. W., 1960, *I. G. Y. General Report Number*, **12**, 8.
[10] JACKA F., 1961, *Ann. I. G. Y.*, XI, 145.
[11] DEWITT R., 1962, *J. Geophys. Research.*, **67**, No. 4, 1347.

Imprimerie TAFFIN-LEFORT, à Lille (France). — *Published in France.*

Imprimerie TAFFIN-LEFORT, à Lille (France). — *Published in France.*

COMMONWEALTH OF AUSTRALIA
COMMONWEALTH SCIENTIFIC AND INDUSTRIAL RESEARCH ORGANIZATION

(*Reprinted from Nature, Vol.* 183, *pp.* 1618–1619, *June* 6, 1959)

Simultaneous Occurrence of Sub-Visual Auroræ and Radio Noise Bursts on 4·6 kc./s.

Since July 1958 the red oxygen (6300 A.) airglow has been recorded at Camden, near Sydney (geomagnetic latitude 42° S.), with a sky-scanning photometer. This instrument has been described by St. Amand[1]. These observations frequently detected greatly enhanced emission towards the south, and less often structures such as arcs and rays. We interpret these as auroræ, usually sub-visual, though on seven nights auroræ were seen.

Table 1. Occurrence and Absence of Noise on 4·6 kc./s. and Auroræ

		Noise on 4·6 kc./s.	
		Yes	No
Auroræ	Yes	18	2
	No	6	27

During the same period, radio noise on 4·6 kc./s. was continuously recorded by a method[2] which largely eliminates impulsive atmospheric and industrial interference. These observations[3] frequently detected distinct noise bursts, many times stronger than the background and usually lasting a few hours.

A comparison of the radio and nightglow records shows that there is a definite correlation between the two. Of 53 nights of simultaneous observations of noise and airglow between June and December 1958, noise bursts and sub-auroræ were recorded during the same hours on 18 nights. On 27 nights neither noise nor sub-auroræ were recorded; on 6 nights noise was recorded in the absence of any auroral pattern in the airglow, while on two occasions auroræ were recorded without any noise bursts. This is summarized in Table 1.

As might be expected, both phenomena are related to magnetic disturbance. They tend to occur when the disturbance index (K) reaches or exceeds 5.

On a few nights the fluctuations of noise and light intensities have shown a minute-to-minute correspondence (Figs. 1–3). This suggests that they may

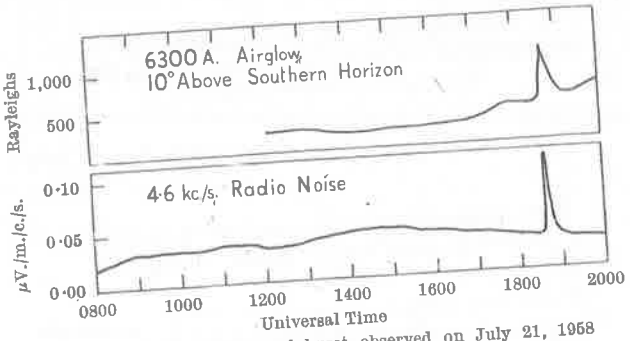

Fig. 1. Noise and auroral burst observed on July 21, 1958

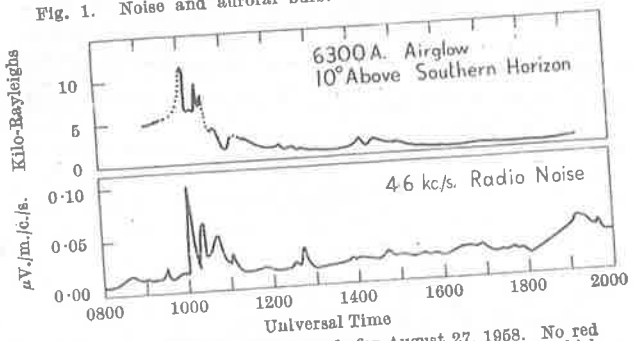

Fig. 2. Airglow and noise records for August 27, 1958. No red airglow observations were made during those periods for which the trace is dotted

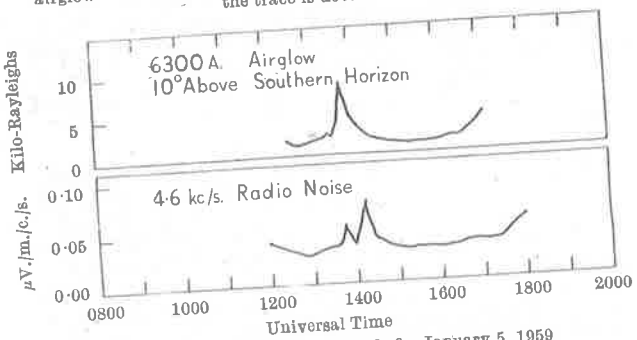

Fig. 3 . Noise and airglow records for January 5, 1959

both be directly generated by the same phenomena, possibly the entry into the atmosphere of proton or electron streams.

However, there is in general no exact correspondence between the two; as Table 1 shows, one is occasionally observed without the other. The radio noise, unlike the auroral light, should be dotectable

even when its apparent source lies below the horizon. This probably accounts for much of the looseness in the association between the two, and for the occasional observations of noise without aurorae. However, the two cases of aurorae without accompanying radio noise cannot be explained in this manner. If the aurorae are caused by proton or electron streams, then it follows that such streams do not always generate radio noise.

This work forms part of the research programme of the Upper Atmosphere Section of the Commonwealth Scientific and Industrial Research Organization.

R. A. Duncan
G. R. Ellis

Upper Atmosphere Section,
Commonwealth Scientific and
Industrial Research Organization,
Camden,
New South Wales.

[1] St. Amand, P., *Ann. de Geophys.*, **11**, 435 (1955).
[2] Reber, G., and Ellis, G. R., *J. Geo. Res.*, **61**, 1 (1956).
[3] Ellis, G. R., "Planetary and Space Science" (in the press).

Printed in Great Britain by Fisher, Knight & Co., Ltd., St. Albans.

Commonwealth of Australia
COMMONWEALTH SCIENTIFIC AND INDUSTRIAL RESEARCH ORGANIZATION
Reprinted from: "Planetary and Space Science"
Vol. 1, No. 2, pp. 112-114, March 1959

POLARIZATION OF THE RED OXYGEN AURORAL LINE

R. A. DUNCAN

Upper Atmosphere Section, Commonwealth Scientific and Industrial Research Organization, Camden, N.S.W., Australia

(*Received* 29 *December* 1958)

Abstract—During an aurora on 8 July 1958 the zenith 6300 Å oxygen emission was found to be about 30 per cent plane polarized with the magnetic vector North-South. It is shown that such polarization would be expected if the aurora was excited by electrons whose predominant motion was gyration about the geomagnetic field lines.

1. OBSERVATIONS AND GENERAL DISCUSSION

During an aurora, observed near Sydney, Australia, (geomagnetic latitude–42°) on 8 July 1958, the zenith red oxygen emission at 6300 Å was found to be about 30 per cent plane polarized with the magnetic vector North-South.

The record showing this is reproduced in Fig. 1. It was obtained by pointing the photometer, which has an inbuilt polaroid, at the zenith and rotating it back and forth about its vertical axis. At the end of each 360° movement a shutter was closed to give a zero level.

There appears to be no mention in the literature of such polarization having been previously observed.

The green airglow (5577 Å) on the same night was unpolarized, and no other examples of polarization have been found in the course of 280 nights' observation of the green (5577 Å) and 30 nights' observation of the red (6300 Å) airglow since March 1957. It therefore seems unlikely that the polarization on 8 July could have been due to some secondary effect such as atmospheric scattering.

It will be shown that the polarization, with the sense observed, would be expected if the aurora were excited by electrons whose predominant motion was gyration about the field lines.

2. THEORY OF AURORAL POLARIZATION

The red (6300 Å) emission on 8 July was about 60 times as intense as the green (5577 Å). Indeed aurorae seen here are always predominantly red, and it is well known that this is the case at all middle and low latitude stations. This fact suggests a low energy excitation process. Middle latitude red aurorae have been discussed by Seaton[1] and Chamberlain[2]. From their work it would seem that they are excited by electric discharges containing electrons with energies less than 10 eV.

Collisions of such low energy electrons with oxygen atoms will produce excited atoms with spin, and hence magnetic moments, about axes lying mainly in planes normal to the collision direction. If therefore the electron velocities are aligned the excited atoms will be largely aligned and the resultant radiations polarized. The effect has been studied experimentally by Skinner[3] and theoretically by Oppenheimer[4] and Bethe[5].

In the upper atmosphere we must consider the geomagnetic field also. Simple aligned electron beams cannot exist except parallel to the field lines; in general the electrons will travel along helical paths. It is always true however that the electron motion, and consequently the distribution of the magnetic dipoles of the collision excited atoms, is axially symmetrical about the field lines.

As the energy level responsible for the red oxygen emission has a half life of 110 sec (Garstand[6]) the excited atoms will precess about the geomagnetic field many thousands of times before radiation occurs. This will further ensure that the distribution of atomic alignments is axially symmetrical about the field lines.

An excited oxygen atom ($1D_2$) radiates at 6300 Å by means of a magnetic dipole transition, and hence the radiation is emitted predominantly in a direction perpendicular to the magnetic dipole of the atom, and with a magnetic vector parallel to this dipole. The distribution of the polarization of photons observed at the ground therefore corresponds to the distribution of the projections of the atomic magnetic dipoles on a plane normal to the line of sight.

It is clear from this, and from what we have said about the axial symmetry of the distribution, that no polarization will be observed on looking directly up the field. On looking perpendicular to the field lines polarization may be detected. We wish to discover where maxima and minima intensities will be observed as a polaroid is rotated about the line of sight.

Let the distribution of the alignments of the emitted photons in the plane normal to the line of sight be represented by the function $f(\theta)$. That is, let the number of photons with magnetic vectors making angles of between θ and $(\theta+d\theta)$ with the geomagnetic field be

$$I=f(\theta)\,d\theta. \tag{1}$$

Polarization measurements do not distinguish between direct and reversed orientations so that θ is restricted to the range $-\pi/2<\theta<\pi/2$.

A polaroid with its "magnetic" axis at an angle ϕ to the geomagnetic field transmits a proportion I' of the photons aligned in the direction θ, where to a good approximation

$$I'=\cos^2(\phi-\theta). \tag{2}$$

The total light transmitted will therefore be

$$I''=\int_{-\pi/2}^{+\pi/2} f(\theta)\cos^2(\phi-\theta)\,d\theta \tag{3}$$

i.e. $$I''=\tfrac{1}{2}\int_{-\pi/2}^{+\pi/2} f(\theta)\,[1+\cos 2(\theta-\phi)]\,d\theta \tag{4}$$

i.e. $$I''=K+\cos 2\phi\int_{-\pi/2}^{\pi/2} f(\theta)\cos 2\theta\,d\theta+ \\ +\sin 2\phi\int_{-\pi/2}^{+\pi/2} f(\theta)\sin 2\theta\,d\theta. \tag{5}$$

Now the distribution of photon alignment must be symmetrical about the field lines and hence can be expressed as a cosine series

$$f(\theta)=A_0+A_1\cos\theta+A_2\cos 2\theta+\ldots \tag{6}$$

and hence from Fourier's Theorem

$$I''=K+\pi/2A_2\cos 2\phi. \tag{7}$$

Hence maximum intensity will be observed, nowhere, or at polaroid orientations $\phi=0$ or $\phi=\pi/2$ as A_2 is zero, positive or negative respectively. That is the light will appear to be unpolarized, polarized parallel to the field, or polarized perpendicular to the field, depending on the actual pattern of atomic alignment.

This conclusion has a simple physical interpretation. The polaroid used in our photometer has transmission characteristics close to that represented by equation (2). It thus selects the second harmonic of the photon alignment distribution and there can therefore be only one maximum intensity observed as the polariod is rotated between $\pm 90°$. The only position for this maximum compatible with the symmetry of the phenomena about the field lines is 0° or 90°.

It should be realized however that this result depends on the characteristic of the analysing polaroid. A more selective polaroid might have a transmission law.

$$I'=\cos^4(\phi-\theta)$$

and in this case two maxima could conceivably be observed, i.e. at both 0° and 90°.

It is clear that along lines of sight which are not perpendicular to the geomagnetic field, the amount of polarization will be less; on looking up the field lines it will be zero; but, assuming again now that equation (2) is correct, the direction of polarization will still be parallel or perpendicular to the projection of the field in the plane normal to the line of sight.

We now relate the sense of the observed polarization, i.e. parallel or perpendicular to the field, to the pattern of electron bombardment. Simple classical arguments will be adequate for present purposes. In general the electrons will move along helical paths up or down the field. If the kinetic energy parallel to

the field is a third of the total kinetic energy we may consider the electron velocities to be unaligned. There are two possible departures from such a pattern. The electron motion may be predominantly longitudinal up or down the field, or it may be predominantly gyration about the field.

If the electron motion is along the field lines, electron collision will produce excited atoms with spin axes and hence magnetic dipoles distributed in a plane normal to the field. The resultant radiation will therefore appear to be polarized with its magnetic vector perpendicular to the field.

In the case of electron gyration about the field lines, collision with unexcited atoms will produce excited atoms with spin axes (and hence magnetic dipoles) half of which will be parallel to the field lines. For random orientation only a third of the spin would be parallel to the field. On looking in a direction perpendicular to the field therefore we will see 50 per cent of the atoms with spin parallel to the field but only 25 per cent with spin perpendicular to the field. The remaining 25 per cent will have spin perpendicular to the field but parallel to the line of sight and hence will be ineffective in producing visible radiation. We should therefore expect at the most 60 per cent polarization with the magnetic vector parallel to the field.

This was the sense of the polarization observed on 8 July so it is concluded that the aurora on this night was excited by electrons gyrating around the magnetic field.

Acknowledgements—This work forms part of the research program of the Upper Atmosphere Section of the Commonwealth Scientific and Industrial Research Organization and was undertaken at the initiative of Dr. D. F. Martyn. The photometer was loaned by the U.S. Bureau of Standards as an I.G.Y. contribution. I am indebted to Drs. S. T. Butler, G. R. Ellis and J. H. Piddington for helpful discussions.

REFERENCES

1. M. J. SEATON, *The Airglow and the Aurorae*, p. 225. Pergamon Press, London (1955).
2. J. W. CHAMBERLAIN, *The Airglow and the Aurorae*, p. 206. Pergamon Press, London (1955).
3. H. W. SKINNER, *Proc. Roy. Soc.* A **112,** 642 (1926).
4. J. R. OPPENHEIMER, *Z. Phys.* **43,** 27 (1927).
5. H. BETHE, *Handb. der Physik*, 24, Part 1, p. 508. Springer, Berlin (1933).
6. R. H. GARSTANG, *Monthly Not. R. Astr. Soc.* **111,** 115 (1951).

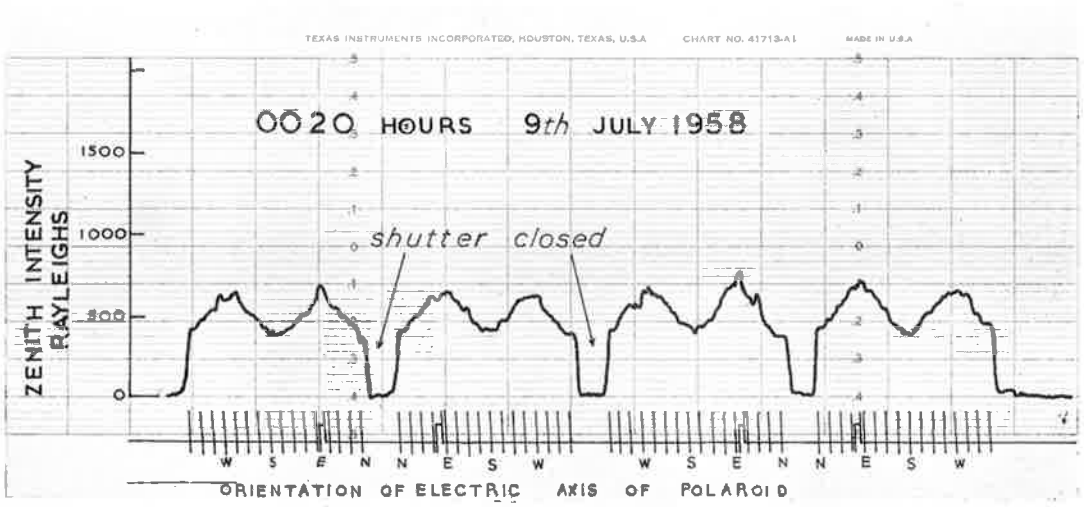

Fig. 1. Record of zenith red (6300Å) airglow intensity. As the photometer with its inbuilt polaroid was rotated a sinusoidal trace was obtained showing that this airglow was plane polarized with the electric vector East-West.

facing p. 114

PHOTOMETRIC OBSERVATIONS OF 5577 Å AND 6300 Å AIRGLOW DURING THE I.G.Y.

By R. A. Duncan*

[*Manuscript received July* 25, 1960]

Summary

Twenty-one months' observation of the airglow from near Sydney, Australia, shows that (*a*) aurorae are detected 10° above the southern horizon at 6300 Å whenever the magnetic disturbance index (*K*) reaches 5 but *K* must reach 7 before detection is certain at 5577 Å; (*b*) the 6300 Å zenith intensity increases rapidly with *K* once this equals or exceeds 4, but the 5577 Å zenith intensity is independent of magnetic disturbance; (*c*) the zenith intensity of 5577 Å tends to be a maximum at 03 hr local time; (*d*) the zenith intensity of 6300 Å drops rapidly from dusk till 01 hr and then rises till dawn.

I. Introduction

As part of the I.G.Y. programme a nightglow photometer, lent by the American National Bureau of Standards, has been operated at Camden, near Sydney (geographic lat. 34° S., geomagnetic lat. 42° S.), since March 1957.

The intensity of the green oxygen emission at 5577 Å was monitored on 280 clear nights from March 1957 till July 1958. After July 1958 attention was concentrated mainly on the red oxygen emission at 6300 Å. Sixty-six clear nights' observation of the red nightglow were obtained to the end of 1958.

In the present paper these observations are studied for dependence on magnetic and ionospheric parameters and for nocturnal behaviour. The results are compared with those of similar studies in the northern hemisphere.

II. The Instrument

The photometer has been described by St. Amand (1955). It has high spectral purity, successfully eliminating the continuous background even during bright moonlight. It scans the sky in a series of horizontal circles at successive zenith distances of 80, 75, 70, 60, 40, and 0°, a complete sky scan taking about four minutes, and usually being repeated each quarter hour.

The photometer sensitivity was calibrated by Roach (1958) against a portable standard photometer, thus permitting comparison with nightglow photometric observations in other parts of the world.

III. Photometric Observations of Auroras

Auroras show clearly on the photometric records as pronounced brightening to the south or as structures such as arcs and rays (Duncan 1959). Figure 1 shows the probability of detecting an auroral form, as a function of the magnetic

* Upper Atmosphere Section, C.S.I.R.O., Camden, N.S.W.

disturbance index (K). It will be seen that the red line is much more prone to auroral excitation than the green. Auroras are always detected at 6300 Å when the magnetic index K reaches 5 but K must reach 7 before we can be sure of detecting an aurora at 5577 Å. This accords with the common observation (e.g. Seaton 1956) that middle latitude auroras are predominantly red.

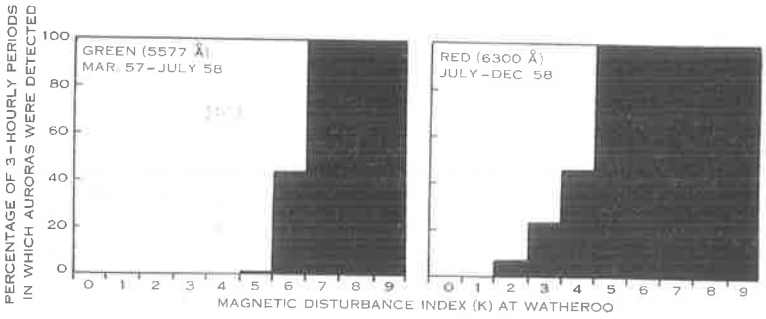

Fig. 1.—The percentage of 3-hourly observing periods during which auroral forms were detected by the photometer against the magnetic disturbance index (K) at Watheroo.

IV. Airglow and Magnetic Disturbance

It may be asked whether auroras make an appreciable contribution to the zenith airglow intensity. A study of the relation between airglow and the magnetic disturbance index K probably has some bearing on this problem.

It will be seen from Figure 2 that, except for the sporadic effect of a few great auroras, the zenith green airglow intensity is independent of the magnetic disturbance index K.

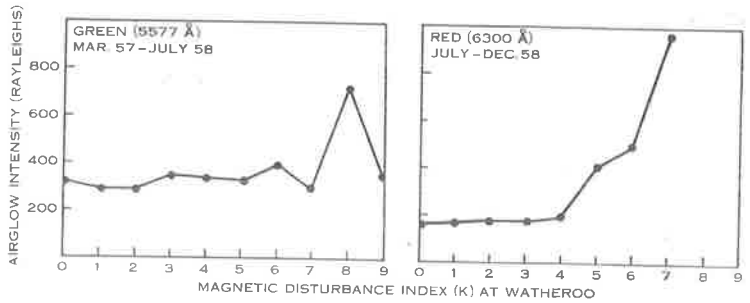

Fig. 2.—The mean zenith airglow intensity against the magnetic disturbance index (K) at Watheroo.

The zenith red airglow intensity, on the other hand, while independent of the magnetic disturbance index K so long as this is less than 4, increases rapidly with larger K. It would seem that the red airglow has a basic non-auroral level of about 175 rayleighs, plus a substantial auroral component on magnetically disturbed nights.

Recently, Roach (1960) has shown that, although the mean intensity at 5577 Å is not significantly increased, there is a tendency for sporadic high 5577 Å

TABLE 1
LOCAL TIMES OF MAXIMUM 5577 Å EMISSION

Station	Latitude	Time of Maximum	Observers
Haute Provence, France ..	44° N.	23·7	Barbier, Dufay, and Williams (1951)
Mt. Elbrus, Russia ..	43° N.	01·6	Rodionov, Pavlova, and Rdultoskava (1949)
Cactus Peak, U.S.A. ..	36° N.	00·2	Roach, Williams, and Pettit (1953)
Flagstaff, U.S.A.	35° N.	01·5	McLennon, McLeod, and Ireton (1928)
Camden, Australia ..	34° S.	03	Duncan
Sacramento Peak, U.S.A...	33° N.	23–01	Manring and Pettit (1958)
Poona, India	18° N.	Minimum 01	Karandikar (1934)

intensities to occur at times of high K-index. Camden data support this conclusion. McCaulley, Roach, and Matsushita (1960) have shown that the lack of correlation between 5577 intensities and magnetic disturbance index K is largely due to the imprecise nature of the K-index. They found a good correlation between 5577 intensities and the horizontal component of the geomagnetic field measured on a nearby magnetometer.

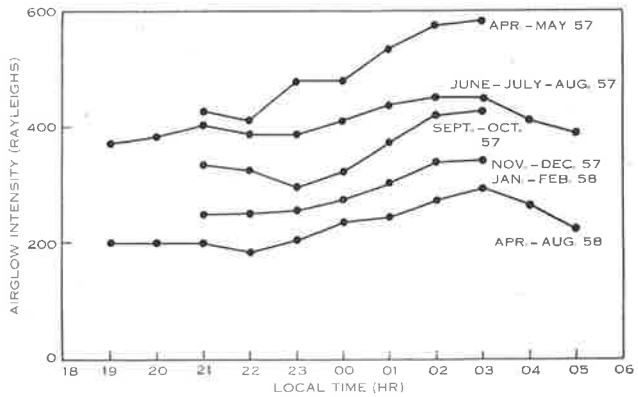

Fig. 3.—Mean nocturnal variation of the zenith green (5577 Å) airglow.

V. NOCTURNAL VARIATION OF THE GREEN (5577 Å) AIRGLOW

The nocturnal variation of the zenith green airglow has been studied by a number of workers. Their results are summarized in Table 1. Observations at Camden confirm previous reports that the diurnal variation varies greatly from night to night. The mean nocturnal variations for each season, however, show a consistent pattern (Fig. 3). In winter a maximum is found at 03 hr. In summer observations run only from 21 to 03 hr, but within this time interval the nocturnal behaviour seems similar to that found in winter.

Observers at middle latitudes in the northern hemisphere (Table 1) have found maxima between 23 and 01 hr.

VI. Nocturnal Variation of the Red (6300 Å) Airglow

The zenith red (6300 Å) airglow shows a far more pronounced and consistent nocturnal variation than the green (Fig. 4). Earlier workers (Elvey and Farnsworth 1942 ; Barbier 1957*a*) have described a dusk and dawn enhancement of the red airglow, but as a transient effect superimposed upon, and easily distinguishable from, the " true " nightglow. It would appear from Figure 4 that the dawn and dusk enhancements are simply parts of a smooth nocturnal variation. If this variation were to be explained entirely in terms of resonance scattering of sunlight, the terrestrial atmosphere would need to be effective at heights as great as 2000 km, for the winter dawn increase is already apparent at 03 hr. The nocturnal variation (Fig. 4) is not symmetrical about midnight. It is about twice as bright at dusk as at dawn, and the lowest intensity occurs not at midnight

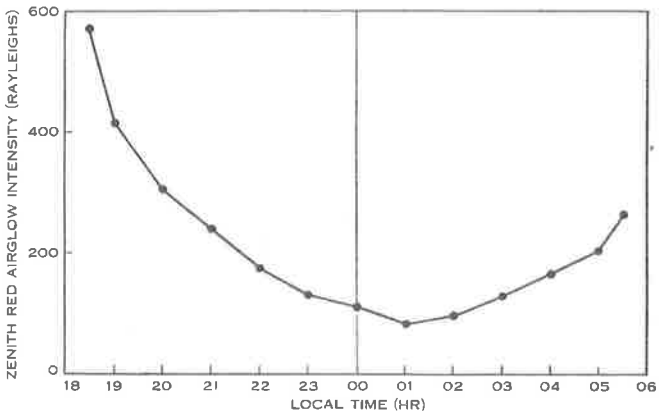

Fig. 4.—The nocturnal variation of the zenith red (6300 Å) airglow intensity. Mean for 20 nights during July and August 1958.

but at 01 hr. This suggests that, in addition to an airglow component dependent on the solar zenith angle, there is a component which decreases steadily from dusk to dawn. Possibly this is due to the dissipation (as airglow) of solar energy absorbed by the upper atmosphere during the day.

Bates and Massey (1946) have suggested that both the red airglow and the decay of the F_2 region could result from the reaction

$$O_2^+ + e \rightarrow O' + O''. \quad \ldots\ldots\ldots\ldots\ldots\ldots \quad (1)$$

In support of this Barbier (1957*b*) found, for the first half of the night, an empirical relation

$$I = (5 \cdot 83 \times 10^6)(f_0)^2 \exp\{(-h' - 200)/88\} \quad \ldots\ldots\ldots \quad (2)$$

between the red airglow intensity I and the ionospheric height h' and critical frequency f_0. A comparison of Camden ionosonde and airglow records gives no support to this finding. Certainly there is support of a kind in the fact that both the red airglow intensity I and f_0F_2 decrease during the first half of the night. However, the airglow intensity at a given hour varies by a factor of 2 or 3 from

night to night and these fluctuations bear no direct relation to ionospheric parameters. Part of the variability is due to magnetic disturbance. As Figure 2 shows, the average red airglow intensity I increases with magnetic disturbance while, as is well known, magnetic storms cause f_0F_2 to decrease and $h'F_2$ to increase. These changes are in opposite directions to those required by equation (2).

Barbier also found that the second half of the night was characterized by an enhanced glow which appeared to the north and gradually spread over the entire sky. This phenomenon has never been seen to the south at Camden.

VII. Acknowledgments

This work formed part of the I.G.Y. programme of the Upper Atmosphere Section of the Commonwealth Scientific and Industrial Research Organization, and was done under the direction of Dr. D. F. Martyn. The photometer was lent by the American National Bureau of Standards.

VIII. References

Barbier, D. (1957*a*).—*C.R. Acad. Sci., Paris* **244**: 1809.
Barbier, D. (1957*b*).—*C.R. Acad. Sci., Paris* **244**: 2077.
Barbier, D., Dufay, J., and Williams, D. R. (1951).—*Ann. Astrophys.* **14**: 399.
Bates, D. R., and Massey, H. S. W. (1946).—*Proc. Roy. Soc.* A **187**: 261.
Duncan, R. A. (1959).—*Aust. J. Phys.* **12**: 197.
Elvey, C. T., and Farnsworth, A. H. (1942).—*Astrophys. J.* **96**: 451.
Karandikar, J. V. (1934).—*Indian J. Phys.* **8**: 547.
McCaulley, J. W., Roach, F. E., and Matsushita, S. (1960).—*J. Geophys. Res.* **65**: 1499.
McLennan, J. C., McLeod, J. H., and Ireton, H. J. C. (1928).—*Trans. Roy. Soc. Can.* **22**: 397.
Manring, E. R., and Pettit, H. B. (1958).—*J. Geophys. Res.* **63**: 39.
Roach, F. E. (1958).—U.S. Nat. Bur. Standards Rep. 5591.
Roach, F. E. (1960).—*J. Geophys. Res.* **65**: 1495.
Roach, F. E., Williams, D. R., and Pettit, M. P. (1953).—*J. Geophys. Res.* **58**: 73.
Rodionov, S. F., Pavlova, E. N., and Rdultoskava, E. V. (1949).—*C.R. Acad. Sci. U.R.S.S* **66**: 55.
St. Amand, P. (1955).—*Ann. Géophys.* **11**: 435.
Seaton, M. J. (1956).—"The Aurorae and the Airglow." Pergamon Press: London.)

Reprinted from the
AUSTRALIAN JOURNAL OF PHYSICS
VOLUME 10, NUMBER 1, PAGES 54-59, 1957

THE MEASUREMENT OF THE DRIFT VELOCITY OF ELECTRONS THROUGH GASES BY THE ELECTRON SHUTTER METHOD

By R. A. DUNCAN

Reprinted from the Australian Journal of Physics, Volume 10, Number 1, pp. 54–59, 1957

THE MEASUREMENT OF THE DRIFT VELOCITY OF ELECTRONS THROUGH GASES BY THE ELECTRON SHUTTER METHOD

By R. A. DUNCAN*

[*Manuscript received August* 27, 1956]

Summary

The behaviour of an electron shutter apparatus such as that used by Neilsen and Bradbury for the measurement of electron velocities is analysed, taking into account the effect of electron diffusion. A relation between shutter frequency and drift velocity, and a relation giving the accuracy obtainable by the method in terms of the chamber length and gas pressure are derived. It is thus shown that neglect of the influence of diffusion can lead to large errors, but that these can be reduced to any desired degree by increasing the chamber length or the gas pressure. Numerical examples are given.

I. INTRODUCTION

An important quantity in the theory of electrical conduction in gases is the drift velocity of electrons through the gas, under the influence of an electric field. Nielsen and Bradbury (1936, 1937) have measured this velocity by using electron shutters. Figure 1 is a schematic diagram of an electron shutter apparatus. Electrons drift from the electrode A to the electrode B under the influence of a uniform electric field. Two shutters S_1 and S_2 are placed in the path of the electrons and these admit electrons only in periodic pulses, the two shutters operating in synchronism. From simple considerations electrode B would be expected to collect a maximum current when the shutter frequency is such that a bunch of electrons admitted by the first shutter (S_1) has just drifted to the second shutter (S_2) by the time the shutters are ready to open again.

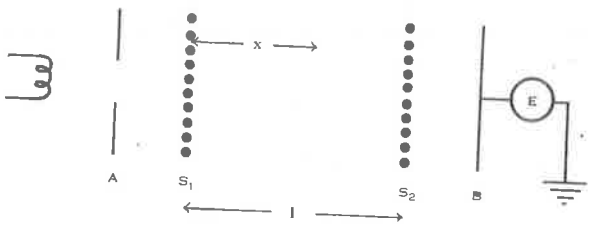

Fig. 1.—An electron shutter apparatus for the measurement of the drift velocity of electrons through a gas.

Thus, if f is the shutter frequency, W is the electron drift velocity, and l is the distance between the shutters, we should expect a maximum current at a frequency f_0 such that

$$W = lf_0, \quad \ldots\ldots\ldots\ldots\ldots\ldots \quad (1)$$

and other maxima at integral multiples of the frequency f_0.

* Radio Research Laboratories, C.S.I.R.O., Camden, N.S.W.

In this paper electron diffusion is considered and it is shown that equation (1) is not strictly accurate. A more precise relation between shutter frequency and drift velocity and an estimate of the accuracy realizable by the method are derived. It is thus shown that the effect of diffusion can be reduced to any desired degree by increasing the chamber length or the gas pressure.

II. An Analysis of the Behaviour of an Electron Shutter Apparatus

The shutter S_1 (Fig. 1) is assumed to admit sharp pulses of electrons at time intervals T or $1/f$ where f is the shutter frequency. These electrons will drift and diffuse down the chamber and an indication of the distribution of electron density n with distance down the chamber, x, at any instant is given in Figure 2. There will be a series of pulses, the centres of which will be a distance W/f apart and, if the first shutter is a point source admitter, the electron density distribution in each pulse will be given by the expression (Carslaw and Jaeger 1947)

$$n=\{N/(4\pi Kt)^{3/2}\}\exp\{-(x-x_0)^2/4Kt\}, \quad \ldots\ldots\ldots \quad (2)$$

where W is the electron drift velocity,
f the shutter frequency,
n the electron density,
N the number of electrons per pulse,
K the electron diffusion constant,
x the distance from the first shutter,
x_0 the position of the pulse centre,
t the age of the pulse.

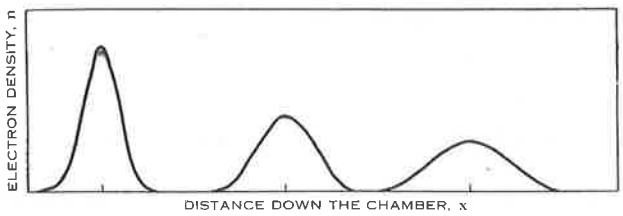

Fig. 2.—The theoretical variation of electron density at some particular instant, with distance down chamber.

Most practical shutters permit electrons to pass for a given fraction of the pulsing period so that the number of electrons in each pulse, N, is inversely proportional to the shutter frequency f,

We may write therefore $N=N_0/f$ and hence

$$n=\frac{N_0}{f(4\pi Kt)^{3/2}}\exp\left\{-\frac{(x-x_0)^2}{4Kt}\right\}. \quad \ldots\ldots\ldots\ldots \quad (3)$$

If the second shutter operates in synchronism with the first, it will admit electrons when the age of the mth pulse in Figure 2 is m/f, and when the coordinate

of the mth pulse centre is mW/f. While the shutter S_2 is transmitting, therefore, the electron density at the shutter will be

$$n=\sum_{m=1}^{\infty}\frac{N_0}{f\{4\pi Km/f\}^{3/2}}\exp\left\{-\frac{(l-mW/f)^2}{4Km/f}\right\},$$

and putting $W=lf_0$ we get

$$n=\sum_{m=1}^{\infty}\frac{N_0f^{\frac{1}{2}}}{(4\pi mK)^{3/2}}\exp\left\{-\frac{l^2}{4K}\,\frac{(f-mf_0)^2}{mf}\right\}. \quad \ldots\ldots\ldots \quad (4)$$

If we treat the second shutter as a mere geometrical plane, the current across it will be

$$i=nW-K\partial n/\partial x.$$

From (3)

$$\frac{\partial n}{\partial x}=-\frac{N_0(x-x_0)}{2f(4\pi Kt)^{3/2}Kt}\exp\left\{-\frac{(x-x_0)^2}{4Kt}\right\},$$

and thus at the second shutter when it opens

$$\frac{\partial n}{\partial x}=\sum_{m=1}^{\infty}-\frac{N_0(l-mW/f)}{2f(4\pi Km/f)^{3/2}Km/f}\exp\left\{-\frac{(l-mW/f)^2}{4Km/f}\right\},$$

that is,

$$\frac{\partial n}{\partial x}=\sum_{m=1}^{\infty}-\frac{N_0lf^{\frac{1}{2}}(f-mf_0)}{2(4\pi)^{3/2}(mK)^{5/2}}\exp\left\{-\frac{l^2}{4K}\,\frac{(f-mf_0)^2}{mf}\right\}. \quad \ldots\ldots \quad (5)$$

Hence

$$i=\sum_{m=1}^{\infty}\left[\frac{N_0f^{\frac{1}{2}}lf_0}{(4\pi mK)^{3/2}}+\frac{N_0lf^{\frac{1}{2}}(f-mf_0)K}{2(4\pi)^{3/2}(mK)^{5/2}}\right]\exp\left\{-\frac{l^2}{4K}\,\frac{(f-mf_0)^2}{mf}\right\}, \quad \ldots \quad (6)$$

or

$$i=\frac{N_0lf^{\frac{1}{2}}}{(4\pi K)^{3/2}}\sum_{m=1}^{\infty}\frac{f+mf_0}{2m^{5/2}}\exp\left\{-\frac{l^2}{4K}\,\frac{(f-mf_0)^2}{mf}\right\}. \quad \ldots\ldots \quad (7)$$

This relation gives the instantaneous current through the second shutter during the time it is open. If this shutter is open for a given fraction of the pulsing period, the average current collected by the electrode B will be proportional to the instantaneous current and we do not need to involve the shutter frequency further.

Now, we are not interested in the absolute magnitude of the current but in its variation with shutter frequency so that it is convenient to multiply equation (7) by the constant factor $(4\pi K)^{3/2}/N_0lf_0^{3/2}$ and thus reduce it to the form

$$i=\sum_{m=1}^{\infty}\left(\frac{f+mf_0}{2m^2f_0}\right)\left(\frac{f}{mf_0}\right)^{\frac{1}{2}}\exp\left\{-\frac{l^2}{4K}\,\frac{(f-mf_0)^2}{mf}\right\}. \quad \ldots\ldots \quad (8)$$

This, then, is the relation which determines the variation of current with shutter frequency in an electron shutter apparatus.

Equation (8) has been used to plot curves for the following cases :

Hydrogen $Z=5$, $p=5$, (Figs. 3 and 4)
Hydrogen $Z=1$, $p=1$, (Fig. 5)

where Z is the electric field in volts per centimetre and p is the pressure in millimetres of mercury. We have assumed l the distance between the shutters to be 5 cm in each case and we have adopted the coefficients of diffusion and

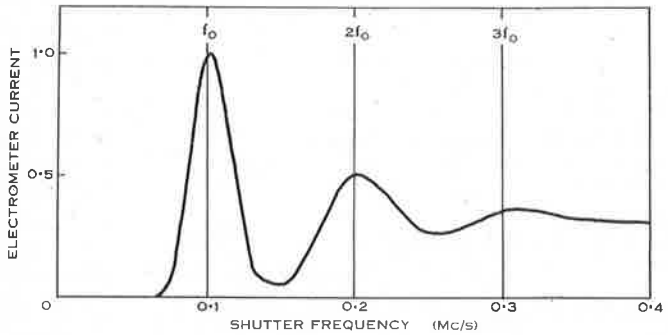

Fig. 3.—The theoretical variation of electrometer current with shutter frequency, for hydrogen at a pressure of 5 mm in a 5 cm chamber and under a field of 5 V/cm.

drift velocities given by Crompton and Sutton (1952) and Nielsen and Bradbury (1936, 1937). It is apparent from these curves that the current maxima are displaced to the right of the positions mf_0.

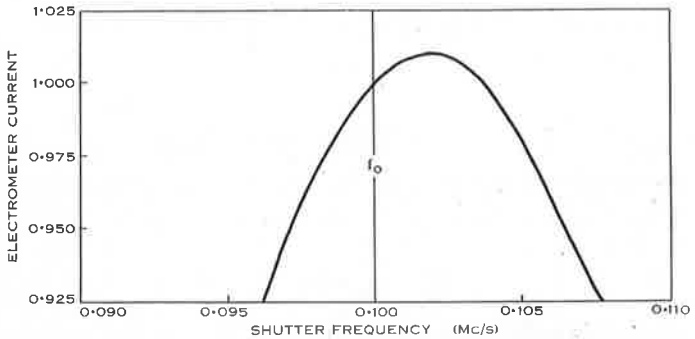

Fig. 4.—The theoretical variation of electrometer current with shutter frequency, for hydrogen at a pressure of 5 mm in a 5 cm chamber and under a field of 5 V/cm.

We can obtain an approximate expression for the difference between the shutter frequency giving maximum current (f_m) and the frequency f_0, if this difference is small. In equation (8) put $2K/l^2=\alpha$ and $(f-f_0)/f_0=\beta$. If α is small we need only consider the first term in the series ; that is, we may assume that at the shutter frequency at which the first current maximum is obtained there is no overlapping of pulses at the second shutter. This is by no means

generally true, but, unless it is true, the difference between the frequency at which maximum current is obtained and the frequency f_0 will not be small.

From (8) then

$$i=\frac{f+f_0}{2f_0}\left(\frac{f}{f_0}\right)^{\frac{1}{2}}\exp\left\{-\frac{(f-f_0)^2}{2\alpha f}\right\}$$
$$\simeq(1+\tfrac{1}{2}\beta)(1+\tfrac{1}{2}\beta)\exp(-f_0\beta^2/2\alpha),$$

hence

$$\partial i/\partial\beta\simeq[1-(\beta f_0/\alpha)(1+\beta)]\exp(-f_0\beta^2/2\alpha).$$

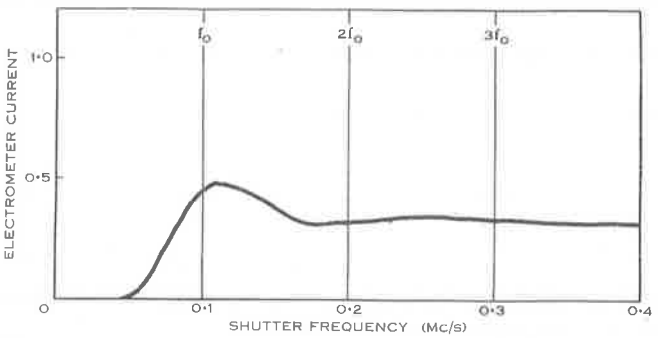

Fig. 5.—The theoretical variation of electrometer current with shutter frequency, for hydrogen at a pressure of 1 mm in a 5 cm chamber and under a field of 1 V/cm.

At the current maximum $\partial i/\partial\beta$ is zero so that

$$1-\beta f_0/\alpha\simeq 0,$$

that is,

$$\beta\simeq\alpha/f_0,$$

that is,

$$f_m-f_0\simeq\alpha\simeq 2K/l^2, \quad \ldots\ldots\ldots\ldots\ldots\ldots \quad (9)$$

where f_m is the frequency at which the first current maximum is obtained. Thus a more accurate relation between shutter frequency for maximum current and electron drift velocity is

$$W=l(f_m-2K/l^2). \quad \ldots\ldots\ldots\ldots\ldots\ldots \quad (10)$$

Even this relation is only useful if $2K/l^2$ is small, and the means of making it small for a given value of drift velocity W is to use a long chamber, high gas pressure (p), and large electric fields (Z) (W is a function of Z/p). A comparison of Figures 3 and 5 illustrates this point.

In our analysis we have ignored the fact that the collection of electrons by the electrode B will perturb the electron density. The error introduced by this simplification is probably not serious, but, if anything, the lowered electron density near the collecting electrode must accelerate diffusion down the chamber and the difference between the shutter frequency for maximum current (f_m) and the frequency f_0 must be greater than we have indicated.

The finite width of the current peaks will limit the accuracy which may be obtained in the measurement of drift velocity by the shutter method under given experimental conditions. This problem may be investigated.

From (8)

$$i \simeq \frac{f+f_0}{2f_0}\left(\frac{f}{f_0}\right)^{\frac{1}{2}} \exp\left\{-\frac{(f-f_0)^2}{2\alpha f}\right\}.$$

The exponential factor in this expression has the greatest influence on the shape of the pulse. Considering this alone we have

$$i \simeq \exp\{-(f-f_0)^2/2\alpha f\} \simeq \exp\{-(f-f_0)^2/2\alpha f_0\}.$$

This is the standard form for the normal distribution. Maximum current occurs in our simplified expression at the shutter frequency f_0, and the current will have fallen by 1 per cent. of its maximum value when

$$f-f_0 = \pm 0 \cdot 14\sqrt{(\alpha f_0)}.$$

If a 1 per cent. drop in current can just be detected, therefore, the possible relative error in the measurement of the frequency for maximum current, and hence in the measurement of the drift velocity W, will be

$$(f-f_0)/f_0 = \pm 0 \cdot 14\sqrt{(\alpha/f_0)} = \pm 0 \cdot 14\sqrt{(2K/lW)}. \quad \ldots\ldots \quad (11)$$

For hydrogen at a pressure of 1 mm Hg, in a 5 cm chamber and under a field of 1 V/cm (the case shown in Fig. 5), this is equal to 4 per cent. It will be noted, however, that diffusion becomes much less important when higher gas pressures and chamber voltages are used, and this fact is of importance in the design of experiments of this nature.

III. Acknowledgments

This work was begun while the author was the holder of a Commonwealth Research Grant at the University of Adelaide, and completed at the Radio Research Board, C.S.I.R.O. The interest taken in the project by Professor Huxley, Dr. Crompton, and Dr. Hall, and the facilities provided by the Board are gratefully acknowledged.

IV. References

Carslaw, H. S., and Jaeger, J. C. (1947).—"The Conduction of Heat in Solids." p. 216. (Clarendon Press: Oxford.)

Crompton, R. W., and Sutton, D. J. (1952).—*Proc. Roy. Soc.* A **215**: 467.

Nielsen, R. A., and Bradbury, N. (1936).—*Phys. Rev.* **49**: 388.

Nielsen, R. A., and Bradbury, N. (1937).—*Phys. Rev.* **51**: 69.

AUSTRALASIAN MEDICAL PUBLISHING CO. LTD.
SEAMER AND ARUNDEL STS., GLEBE, SYDNEY

Commonwealth of Australia
COMMONWEALTH SCIENTIFIC & INDUSTRIAL RESEARCH ORGANIZATION
Reprinted from "Journal of Geophysical Research"
Vol. 66, No. 7, Pages 2087–2094, July 1961

Some Studies of Geomagnetic Micropulsations

R. A. DUNCAN[1]

Upper Atmosphere Section
Commonwealth Scientific and Industrial Research Organization
Camden, N.S.W., Australia

Abstract. Oscillations of the geomagnetic field with periods between 1 second and a few minutes have been studied by means of large ground loops at Hobart, Adelaide, Camden, and Townsville, Australia. Records have been made both on charts and on slowly moving magnetic tape; the tape recordings have been analyzed for frequency components on a 'Sonagraph' sound spectroscope.

The period of the continuous oscillations known as *Pc*'s shows a diurnal variation and a marked dependence on latitude, shorter periods occurring at lower latitudes.

The damped trains of oscillations, occurring predominantly around local midnight, known as *Pt*'s are followed by magnetic bays with an average delay of about 15 minutes.

During storms, 'sweepers'—oscillations with a progressive change of frequency and sometimes with aharmonic overtones—are observed.

INTRODUCTION

Micropulsations, oscillations of the geomagnetic field with periods of a few seconds to a few minutes, were recorded on paper charts by these laboratories at Hobart (geomagnetic latitude 52°), Camden (43°), and Townsville (29°) from September 1959 till May 1960. These records have been described by *Ellis* [1961]. The work has now been extended by recordings at Camden and Adelaide (45°) from August 1960 to February 1961, both on charts as before and on slowly moving magnetic tape. This new work, plus a new study of the old records from Hobart and Townsville, will be presented here. Camden records have been largely neglected because of the high local noise level. The magnetic tapes have been analyzed on a 'Sonagraph' sound spectrograph.

RECORDING METHODS

The micropulsations were picked up on loops buried in the ground; that at Camden had three turns 200 meters in diameter. The signal was amplified 400-fold by a galvanometer-photocell servo system [*Valley and Wallman*, 1948, p. 487] and fed simultaneously onto a recording milliammeter and a magnetic tape, both the chart and tape moving at 6 inches per hour. Full scale deflection of the recorder occurred for a rate of change of field (dH/dt) of 1.3 γ/second, the minimum detectable signal being about 1/25 of this. The response was linear from d-c to 7-second period oscillations but fell off rapidly for periods shorter than this. The apparatus at the other stations was essentially similar.

[1] Address until March 1962: High Altitude Observatory, Boulder, Colorado.

RESULTS

At the middle-latitude stations, in the absence of magnetic storms, the oscillations almost always fell approximately into the usual classes, the persistent irregularly fading sinusoidal oscillations known as *Pc* and the impulsive damped trains of oscillations known as *Pt*.

Occasionally other modes were seen; in the sound spectrogram reproduced in Figure 4, in addition to the dominant *Pc* mode, a mode and associated overtones with a frequency of 8 cycles/minute at 09 hours dropping progressively to 2 cycles/minute at 17 hours can be seen. At Hobart complex records were often observed, and this complexity extended to all stations during severe magnetic storms. The record of Figure 4 was taken on the day following a storm.

Persistent irregularly fading sinusoidal oscillations—Pc. Examples are shown in Figures 1, 2, and 3. These oscillations were almost completely confined to daylight hours, thus conforming to the pattern found by earlier workers [e.g., *Campbell and Nebel*, 1959]. At Adelaide, where the local noise level was particularly low, they were detected on 85 per cent of observing days, the median amplitude of each day's strongest burst being about 2 γ.

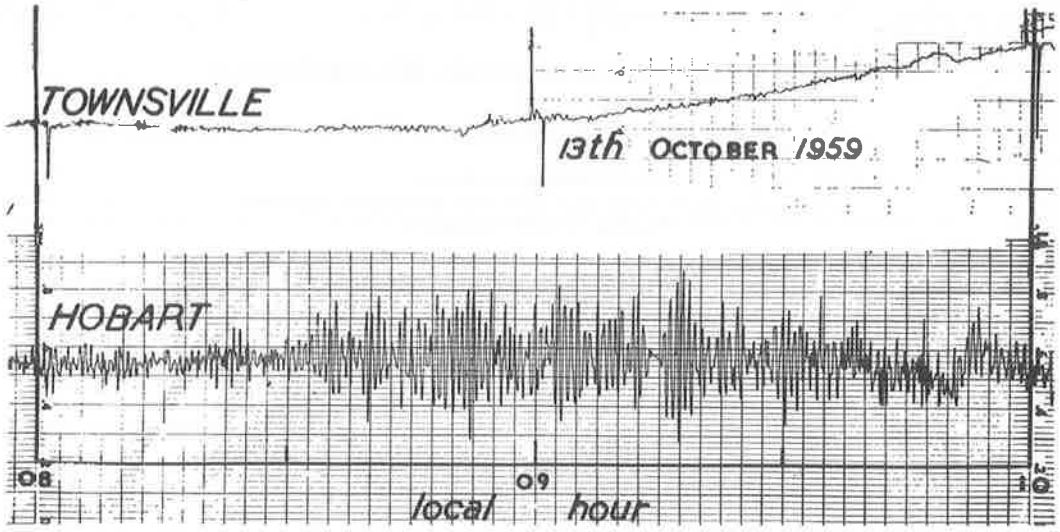

Fig. 1. Simultaneous induction magnetometer records from Hobart and Townsville showing strong *Pc* oscillations at Hobart. The slow drift at Townsville is instrumental.

A diurnal variation of period was found. *Kato and Saito* [1959] found a diurnal variation in the period of the highest frequency oscillations of any type present during each hour. Their variation passed through a maximum of 20 seconds at midday and a minimum of 8 seconds at 03 hours. Such a variation is compatible with the daytime and nighttime *Pc* periods found by *Yanagihara* [1959] and *Maple* [1959]. Some commentators have questioned whether these results refer to a continuous variation, and have suggested instead that they result statistically from the occurrence distribution of discrete classes of oscillations.

The tape recordings made in Australia show that during daylight hours a continuous change of period does occur; such tapes played back at high speeds produce a gliding note, the shorter period oscillations occurring at dawn. Sonagrams of tapes are reproduced in Figures 4 and 5.

Persistent oscillations are rare at night but the eight examples found on the Adelaide charts all had periods greater than 40 seconds, that is, contrary to Yanagihara and Maple, much greater than during the day. The sonagrams suggest a resolution of the conflict. Both the long period component and *Pc* component are found day and night, but at night the long period component is stronger. Nevertheless the period of corresponding modes seems to be shorter.

The only oscillations commonly found at night are impulsive disturbances, or *Pi*'s; the spectra of these, however, seem to correspond to that of the persistent oscillations occurring during the day. An example occurring at 2133 hours September 7, 1960, and illustrating all these points is seen in Figure 5.

Yoshimatsu [1950], *Kato and Watanabe* [1958], and *Maple* [1959] found the periods of *Pc* oscilla-

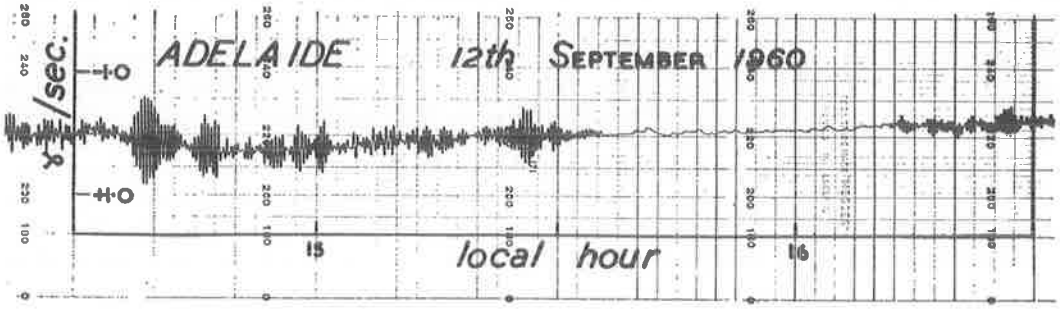

Fig. 2. Induction magnetometer record from Adelaide showing *Pc* oscillations.

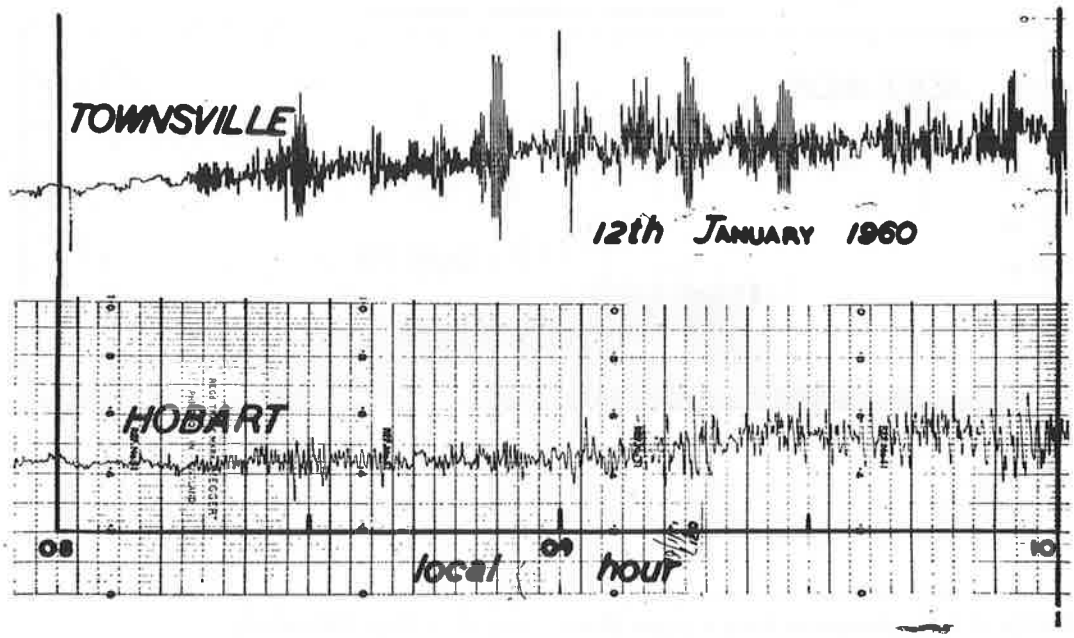

Fig. 3. Simultaneous induction magnetometer records from Hobart and Townsville showing strong *Pc* oscillations at Townsville in the absence of any remarkable behavior at Hobart.

tions to be shortened at times of magnetic disturbance. We have found the situation during magnetic disturbance complex. In the post-storm period, however, typical *Pc* oscillations do appear, with enhanced amplitude and shortened period; the shortening of the period is most pronounced in the morning hours, so that a magnetic disturbance increases the range of the daily variation (Fig. 6).

The distributions of midday periods observed at each station are shown in Figure 7. In compiling these only cases of pure sinusoidal signals lasting at least 2½ minutes were used. This criterion had little effect at Townsville and Adelaide, but it resulted in the rejection of about 60 per cent of the Hobart records. Most of the rejected Hobart records looked like a fundamental oscillation plus overtones and parasitics,

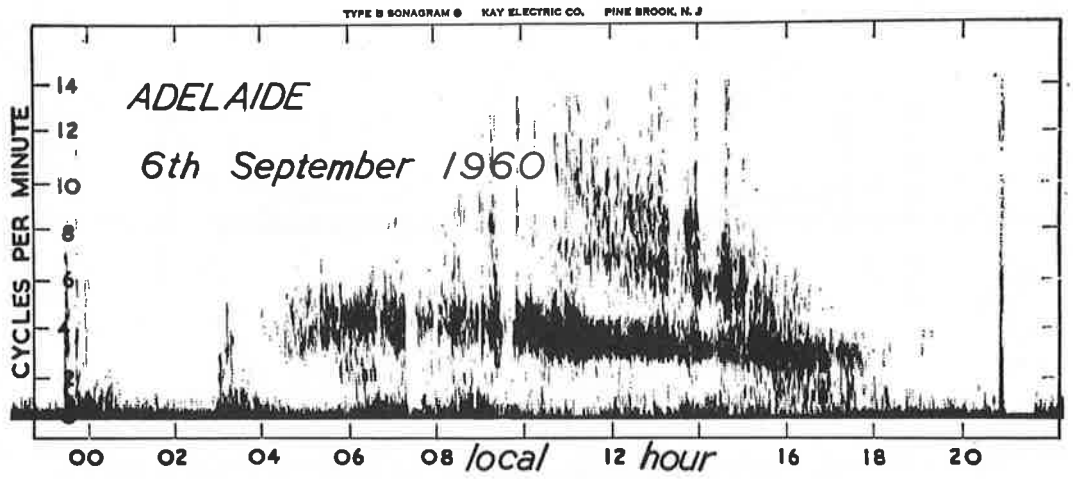

Fig. 4. Sonagram of the Adelaide tape record for September 6, 1960, showing *Pc* oscillations plus an additional mode.

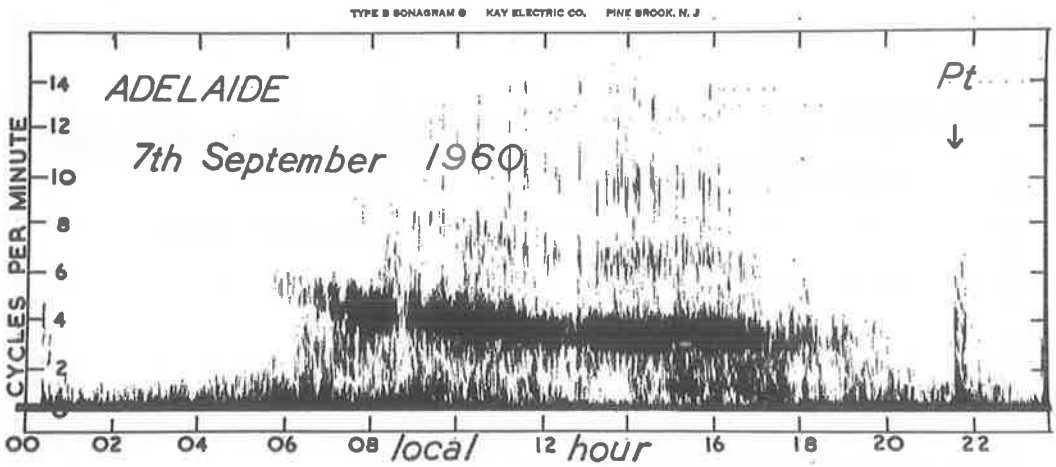

Fig. 5. Sonagram of the Adelaide tape record for September 7, 1960, showing *Pc* oscillations during the day and an impulsive disturbance or *Pt* at 2133 hours. A simultaneous chart recording of this *Pt* is reproduced in figure 8.

but it is very difficult to make quantitative studies of such phenomena from a paper chart; no tape recorder was installed at Hobart.

It will be seen from Figure 7 that the median midday period varies from 19 seconds at Townsville, to 23 seconds at Adelaide, and 27 seconds at Hobart. This result conflicts with the conclusion of *Ellis* [1961] from a study of the same data, but a survey of the literature shows that periods measured by other workers at various stations consistently show the same trend, shorter *Pc* periods at lower latitudes (Table 1). *Jacobs and Sinno* [1960] have noted this; *Obayashi and Jacobs* [1958] found a similar trend for giant micropulsations—storm time oscillations with periods of 50 to 200 seconds.

It has been suggested [*Ellis*, 1961] that the oscillations arise in the auroral zones and propagate to lower latitudes; more effective propagation at shorter periods would then explain the mixed frequencies seen at Hobart and the pure short-period oscillations at Townsville. However this explanation cannot explain much of the observed behavior; strong oscillations were sometimes observed in Townsville in the absence of strong oscillations at Hobart (Fig. 3); good Camden records are few, but we have one example (October 7, 1959) of simultaneous bursts

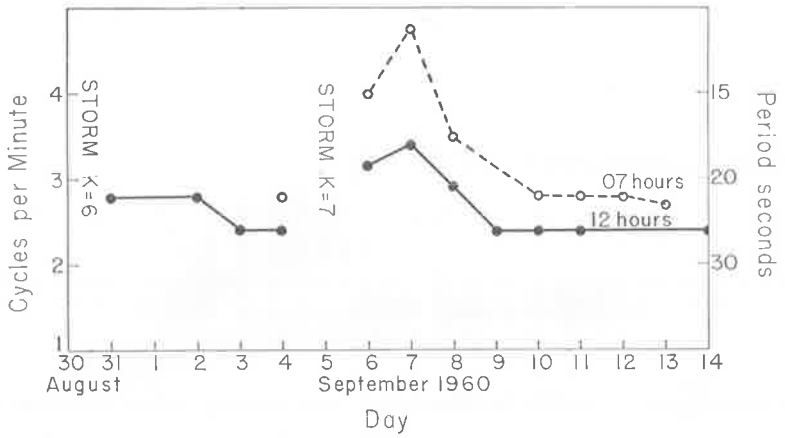

Fig. 6. The secular variation of the midday (solid line) and dawn (broken line) *Pc* period at Adelaide from August 30 to September 14, 1960. Only irregular oscillations with periods, greater than 2 minutes were observed during the moderate storms of August 30 and September 5.

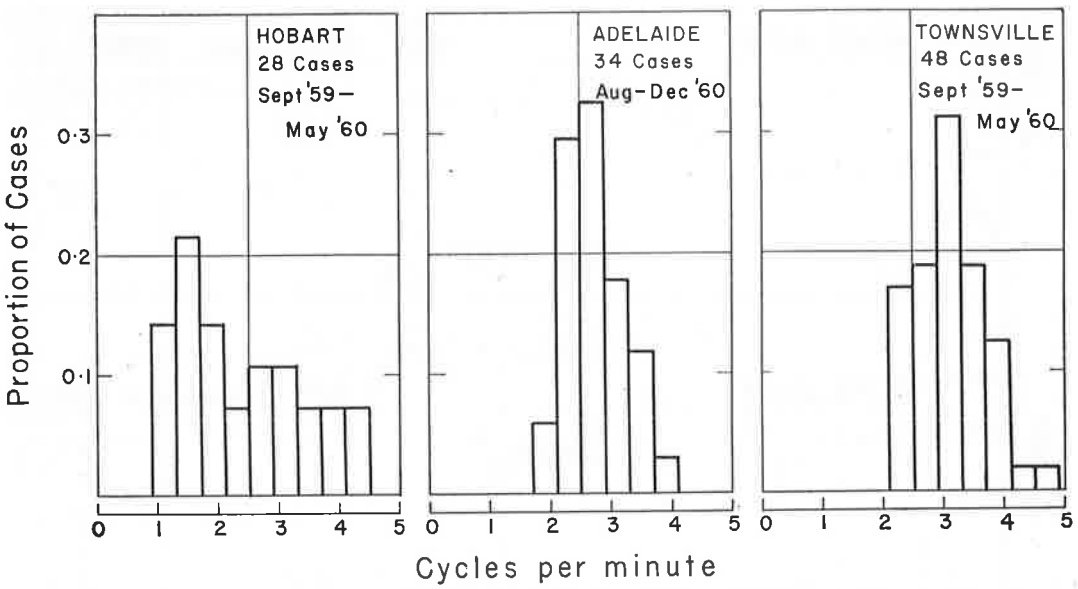

Fig. 7. The distribution of the periods of clean sinusoidal oscillations, lasting at least 2½ minutes and occurring within half an hour of midday, for Hobart, Adelaide, and Townsville, respectively.

of strong oscillations at Hobart, Camden, and Townsville with the same amplitude envelope but a marked latitude gradient of frequency.

Obayashi and Jacobs [1958] suggested that giant micropulsations—storm time oscillations with periods from 50 to 200 seconds—were standing Alfvén waves on the geomagnetic field lines, the vibrating string model. *Pc* oscillations have some properties in accord with this model. The short period at low latitudes where the field lines are short suggests it; the variable period at high latitudes (Fig. 7) could be due to the penetration of high latitude field lines into the disturbed exosphere. We have also the shortening of the daytime period after magnetic disturbance which plausibly could be attributed to the compression of the earth's field by a solar gas stream, and the additional shortening of the period at dawn in the vanguard of the earth's orbital motion through the gas. On this model, however, the field lines on the night side of the earth should be stretched and the nighttime periods long. This does not appear to be the case. As we have said, the little evidence available suggests that the period of corresponding modes is shorter by night than by day.

Impulsive damped trains of oscillations—Pt. Examples are shown in Figure 8, and they appear also on the sonagram (Fig. 5). The sudden commencements observed by the induction magnetometers were always oscillatory, and we have found no clear dividing line between the two phenomena; the oscillations usually termed *Pt* seem to be weak sudden commencements. In agreement with earlier workers [*Meyer*, 1951; *Scholte and Veldkamp*, 1955; *Kato and Wantanabe*, 1958], *Pt*'s were found to have a peak occurrence

TABLE 1. The Variation of *Pc* Period, as Determined by Various Workers, against Geomagnetic Latitude

Observer	Station	Geomagnetic Latitude	Period, sec.
Kato and Saito 1959	Onagawa	28°	20
Duncan	Townsville	29°	19
Campbell 1959	Los Angeles	39°	22
Maple 1959	Tucson	40°	20
Berthold, Harris, and Hope 1960	Arizona	41°	35
Duncan	Adelaide	45°	23
Duncan	Hobart	52°	27
Scholte and Veldkamp 1955	Witteveen	54°	45
Duffus and Shand 1958	Victoria	54°	50

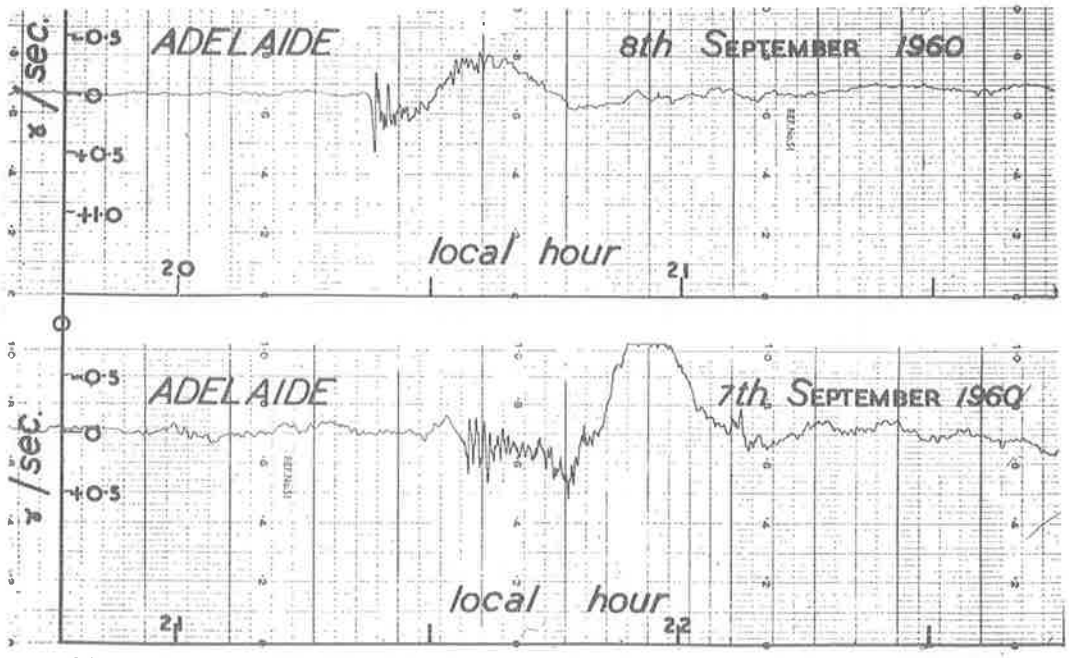

Fig. 8. Two examples of impulsive damped oscillations, or *Pt*, at Adelaide, showing the development of a bay about 15 minutes later. The *Pt* in the lower record is the one seen on the Sonagram reproduced in Figure 5.

at midnight and to precede magnetic bays, the average delay between the onset of oscillations and the peak build-up of the bay being about 15 minutes (see Fig. 8). *Bless, Gartlein, Kimball, and Sprague* [1959], *Bhattacharyya* [1960], and *Stagg and Paton* [1939] found a similar delay between auroral bursts and magnetic bays, suggesting that the two phenomena are closely linked.

Giant pulsations and other storm phenomena. The oscillations observed during magnetic storms have extremely varied and sometimes complex frequency spectra. During moderate storms strong irregular long period oscillations are found, and these seem to supplant shorter period oscillations; on September 5, 1960, for example, oscillations with a period less than 2 minutes were conspicuously absent at Adelaide although the normal *Pc* oscillations with a period of about 20 seconds were strong on the surrounding days (Fig. 6).

At Hobart, and at the lower latitude stations during severe storms, complex frequency spectra are observed, periods ranging from 2 seconds to

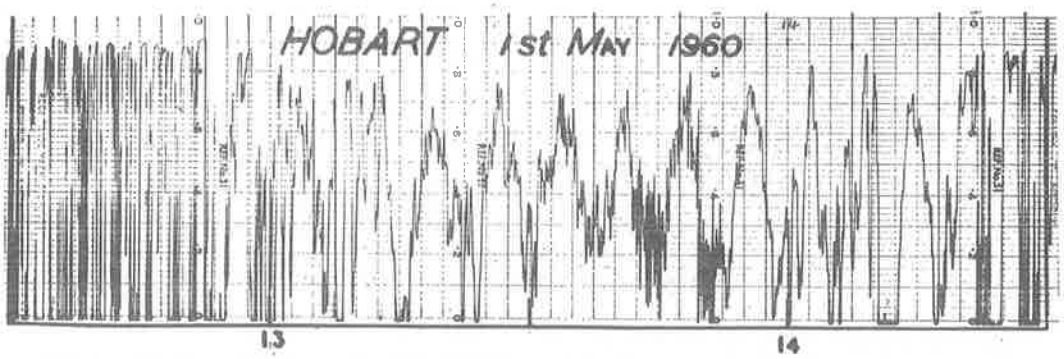

Fig. 9. Storm oscillations at Hobart showing, among other components, giant pulsations with a period of 7 minutes.

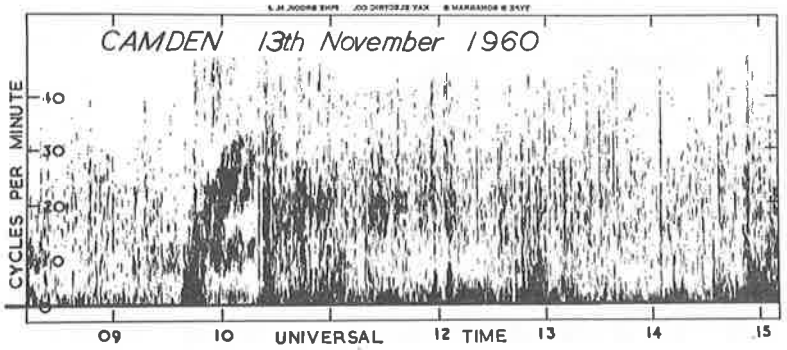

Fig. 10. Sonagram of a 'sweeper' recorded in the course of a storm on November 13, 1960.

10 minutes. It is probable that even shorter period oscillations occur; the recording apparatus, incorporating as it does a galvanometer, loses sensitivity rapidly as periods fall below 7 seconds. In Figure 9 oscillations of period 7 minutes can be seen, together with many higher frequencies. It is only the long period oscillations that are resolved on a normal magnetometer and it is these that are termed 'giant pulsations.' Recording on magnetic tape and subsequent spectral analysis enables us to study the higher frequencies also. *Duffus, Nasmyth, Shand, and Wright* [1958] using this technique discovered a storm oscillation with a progressive change of frequency; they termed it a 'whistler.' We shall give two examples of oscillations recorded at Camden during the great storm which began on November 12, 1960. These differ considerably from each other and from the aforementioned whistler; the phenomena occurring during severe storms are evidently diverse.

Figure 10 is a sonagram of a swept frequency oscillation which began suddenly at 0937 UT on November 13, 1960, and accompanied a very severe bay. As Duffus and his co-workers have remarked in connection with their phenomenon, the tape recording of this phenomenon when played back at high speed sounds similar to the whistlers of the audio frequency spectrum. The frequency swept from less than 2 cycles/minute to 35 cycles/minute in about half an hour. There is also a constant frequency component of about 11 cycles/minute. The sweeper was terminated by a very severe storm sudden commencement at 1022 UT; thereafter the frequency spectrum became more noisy. It will be noticed that many of the impulsive disturbances occurring during the surrounding hours have a discrete spectral structure.

Figure 11 is a sonagram of a storm sudden commencement at 2200 UT on November 15, 1960, following a very severe flare at 0220 hours on the same day. On a tape player this phenomenon sounds like a sharp crack followed by rumbling decaying echoes, such as a lightning stroke followed by thunder, for example. It will be seen (Fig. 11) that the noise begins at low frequencies and then extends to higher fre-

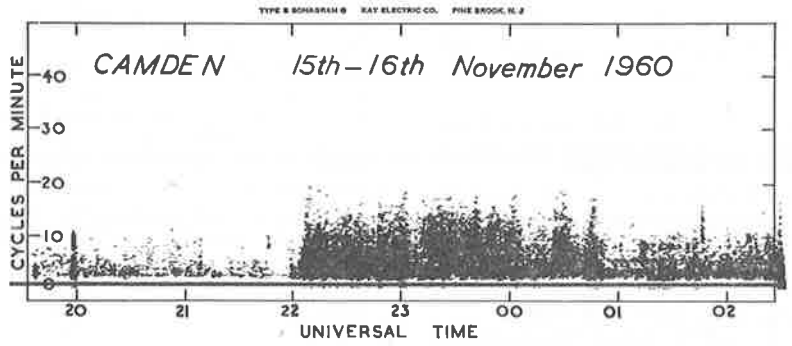

Fig. 11. Sonagram of a storm sudden commencement recorded on November 15–16, 1960, showing noise beginning at low frequencies and extending to high frequencies.

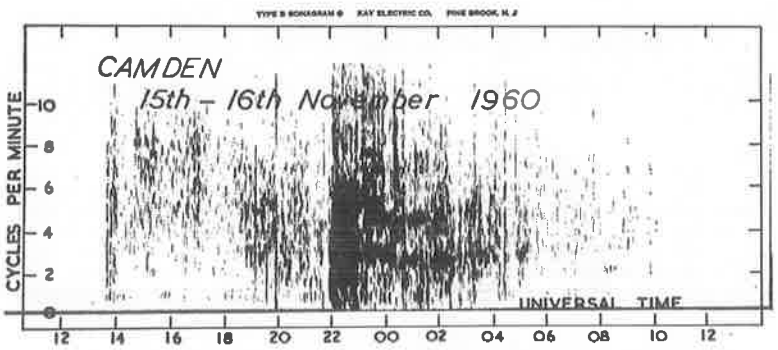

Fig. 12. Sonagram of a storm sudden commencement showing discrete spectral components, which are not harmonically related.

quencies; this is unlikely to be a dispersive effect as theory indicates that the higher frequencies have the greater velocity [*Piddington*, 1959].

In addition to the noise there are discrete frequency components; these do not show well in Figure 11 where we have used high contrast to emphasize the noise, but they may be seen more clearly in Figure 12. The oscillations sweep in frequency, in a manner and through a range similar to that of normal daytime *Pc* oscillations, and perhaps should be regarded as the same phenomenon. The overtones are not harmonically related; this might be anticipated as the upper atmosphere is a dispersive medium.

Acknowledgments. I am greatly indebted to Dr. G. R. Ellis for the suggestion that his earlier work be supplemented by recordings on magnetic tape, to T. W. Davidson for help in this project, and to Dr. D. F. Martyn for careful criticism of the paper. The Townsville recorder was operated by R. Conway of the Australian Ionospheric Prediction Service, and the Adelaide recorder by E. L. Murray of the University of Adelaide, to whom our thanks are due.

References

Berthold, W. K., A. K. Harris, and H. J. Hope, Correlated micropulsations at magnetic sudden commencements, *J. Geophys. Research, 65*, 613–618, 1960.

Bhattacharyya, B. K., Correlation studies of radio aurora, magnetic, and earth-current disturbances, *Canad. J. Phys., 38*, 624–637, 1960.

Bless, R. C., C. W. Gartlein, D. S. Kimball, and G. Sprague, Auroras, magnetic bays and protons, *J. Geophys. Research, 64*, 949–953, 1959.

Campbell, W. H., Studies of magnetic field micropulsations with periods of 5 to 30 seconds, *J. Geophys. Research, 64*, 1819–1826, 1959.

Campbell, W. H., and B. Nebel, Micropulsations measurements in California and Alaska, *Nature, 184*, Suppl. *9*, 628, 1959.

Duffus, H. J., P. W. Nasmyth, J. A. Shand, and C. Wright, Subaudible geomagnetic fluctuations, *Nature, 181*, 1258–1259, 1958.

Duffus, H. J., and J. A. Shand, Some observations of geomagnetic micropulsations, *Canad. J. Phys., 36*, 508–526, 1958.

Ellis, G. R. A., Geomagnetic micropulsations, *Australian J. Phys., 13*, 625–632, 1961.

Jacobs, J. A., and K. Sinno, World-wide characteristics of geomagnetic micropulsations, *Geophys. J. Roy. Astron. Soc., 3*, 333–353, 1960.

Kato, Y., and T. Saito, Preliminary studies on the daily behaviour of rapid pulsations, *J. Geomag. and Geoelect., 10*, 221–225, 1959.

Kato, Y., and T. Watanabe, Studies on geomagnetic storm in relation to geomagnetic pulsations, *J. Geophys. Research, 63*, 741–756, 1958.

Maple, E., Geomagnetic oscillations at middle latitudes, *J. Geophys. Research, 64*, 1395–1404, 1959.

Meyer, O., Über eine besondere Art von erd magnetischen Bay-Störmungen, *Deutche Hydrographische Zeitschrift, 4*, Heft 1/2, 1951.

Obayashi, T., and J. A. Jacobs, Geomagnetic pulsations and the earth's outer atmosphere, *Geophys. J. Roy. Astron. Soc., 1*, 53–63, 1958.

Piddington, J. H., The transmission of geomagnetic disturbances through the atmosphere and interplanetary space, *Geophys. J. Roy. Astron. Soc., 2*, 173–189, 1959.

Scholte, J. G., and J. Veldkamp, Geomagnetic and geoelectric variations, *J. Atmospheric and Terrest. Phys., 6*, 33–45, 1955.

Stagg, J. M., and J. Paton, Aurora and geomagnetic disturbance, *Nature, 143*, 941, 1939.

Valley, G. E., and H. Wallman, *Vacuum Tube Amplifiers*, McGraw-Hill Book Company, p. 743 1948.

Yanagihara, K., Some character of geomagnetic pulsation pt and accompanied oscillation s.p.t., *J. Geomag. Geoelect., 10*, 172–176, 1959.

Yoshimatsu, T., On the frequency of geomagnetic pulsation p.t., *J. Geomag. Geoelect., 11*, 208–213, 1950.

(Manuscript received March 27, 1961; revised April 24, 1961.)